SEISMIC UPGRADE OF DEFICIENT REINFORCED CONCRETE FRAMES USING EXTERNAL SYSTEMS

A THESIS SUBMITTED TO
THE GRADUATE SCHOOL OF NATURAL AND APPLIED SCIENCES
OF
MIDDLE EAST TECHNICAL UNIVERSITY

BY

MUSTAFA EMRE ÖZKÖK

IN PARTIAL FULFILLMENT OF THE REQUIREMENTS
FOR
THE DEGREE OF MASTER OF SCIENCE
IN
CIVIL ENGINEERING

MAY 2010

Approval of the thesis:

SEISMIC UPGRADE OF DEFICIENT REINFORCED CONCRETE FRAMES USING EXTERNAL SYSTEMS

submitted by **MUSTAFA EMRE ÖZKÖK** in partial fulfillment of the requirements for the degree of **Master of Science in Civil Engineering Department, Middle East Technical University** by,

Prof. Dr. Canan Özgen _____________________
Dean, Graduate School of **Natural and Applied Sciences**

Prof. Dr. Güney Özcebe _____________________
Head of Department, **Civil Engineering**

Assoc. Prof. Dr. Barış Binici _____________________
Supervisor, **Civil Engineering Dept., METU**

Examining Committee Members:

Prof. Dr. Güney Özcebe _____________________
Civil Engineering Dept., METU

Assoc. Prof. Dr. Barış Binici _____________________
Civil Engineering Dept., METU

Assoc. Prof. Dr. Erdem Canbay _____________________
Civil Engineering Dept., METU

Assoc. Prof. Dr. Ahmet Yakut _____________________
Civil Engineering Dept., METU

Assoc. Prof. Dr. Özgür Anıl _____________________
Civil Engineering Dept., Gazi Uni.

Date: May 13, 2010

I hereby declare that all information in this document has been obtained and presented in accordance with academic rules and ethical conduct. I also declare that, as required by these rules and conduct, I have fully cited and referenced all material and results that are not original to this work.

Name, Last name: Mustafa Emre Özkök

Signature

ABSTRACT

SEISMIC UPGRADE OF DEFICIENT REINFORCED CONCRETE FRAMES
USING EXTERNAL SYSTEMS

ÖZKÖK, Mustafa Emre

M.Sc., Department of Civil Engineering

Supervisor: Assoc. Prof. Dr. Barış Binici

May 2010, 88 pages

There is a large building stock in seismic regions of Turkey that require seismic upgrades. In order to minimize the disturbance to occupants and not to intervene with the functioning of the building, external strengthening methods can be preferred among different alternatives. This study reports the experimental findings on the upgrading of deficient reinforced concrete frames with external installed structural components. Specimens strengthened with an externally reinforced concrete shear wall, external steel frames, steel plate shear wall and one as-built reference 1/3-scale portal frame specimens were tested under constant gravity load and increasing cyclic displacement excursions. The RC frames had deficiencies those mimic the existing deficient building stock in Turkey. The test results showed that the external upgrading can increase both the lateral stiffness and strength of deficient RC frames considerably. Finite element analyses were conducted to specimen models to investigate the behaviors numerically. Furthermore, corresponding single degree of freedom (SDOF) models of specimens were generated to perform dynamic analysis.

Results show the importance of hysteretic response and enhancement of energy dissipation capability with drift control.

Keywords: Reinforced Concrete Frames, RC Frames, Seismic Strengthening, External Strengthening.

ÖZ

YETERSİZ BETONARME ÇERÇEVELERİN DIŞTAN BAĞLI SİSTEMLER KULLANILARAK SİSMİK GÜÇLENDİRİLMESİ

ÖZKÖK, Mustafa Emre
Yüksek Lisans, İnşaat Mühendisliği Bölümü
Tez Yöneticisi: Doç. Dr. Barış Binici

Mayıs 2010, 88 sayfa

Türkiye'de sismik olarak aktif olan bölgelerde güçlendirmeye gereksinimi olan büyük bir yapı stoğu bulunmaktadır. Bina sakinlerine verilen rahatsızlığı asgari seviyeye getirmek ve binanın işlevine müdahale etmemek için alternatif güçlendirme yöntemleri arasından harici güçlendirme metotları tercih edilebilir. Bu çalışma yetersiz betonarme çerçeveleri dışarıdan bağlanmış yapı bileşenleriyle iyileştirilmesine dair deneysel bulguları vermektedir. Dışarıdan bağlı betonarme perde duvarla, çelik çerçevelerle ve çelik plaka perdeyle güçlendirilmiş numuneler ve bir 1/3 ölçekli referans betonarme çerçeve sabit eksenel yük altında ve artan tersinir deplasman çevrimleriyle test edilmiştir. Betonarme çerçevelerdeki detaylar Türkiye'deki mevcut yapı stoğunda bulunan benzer yetersizliklere sahiptir. Test sonuçları harici iyileştirme yöntemlerinin yetersiz betonarme çerçevelerin yanal rijitliğini ve dayanımını oldukça artırabildiğini göstermiştir. Davranışları sayısal modellemeler ile incelemek amacıyla sonlu elemanlar analizleri gerçekleştirilmiştir. Ayrıca, dinamik analiz yapmak amacıyla numunelere uygun tek serbestlik dereceli modeller oluşturulmuştur. Sonuçlar dış güçlendirme sistemlerinin etkin deformasyon kontrolü sağlayacağına işaret etmektedir.

Anahtar Kelimeler: Betonarme Çerçeveler, Sismik Güçlendirme, Dıştan Güçlendirme.

ACKNOWLEDGMENT

The author wishes to express his deepest gratitude to his supervisor Assoc. Prof. Dr. Barış Binici for his guidance, careful supervision, criticisms, patience and insight throughout the research. The thesis would not have been possible without his support. Besides technical study, I also appreciate very much for his kind of interest on personal problems. I am very grateful to meet with him who has brilliant knowledge and above all, great personality. It will always be an honor for me to study with such a professor.

I would like to extend my greatest thanks to Prof. Dr. Güney Özcebe and Assoc. Prof. Dr. Erdem Canbay for their support.

My special thanks go to Ramazan Özçelik for his assistance and guidance throughout this study. Also, Uğur Akpınar is greatly appreciated for his contribution.

My deepest gratitude goes to my friends Efe G. Kurt, A. Güney Özcebe, İ. Bahadır Önder, Can Karageyik and Emrah Eryaşar for their support, help and friendship.

I would like to convey my thanks to my roommates in K2-105. Everything was great to share with Alper Aldemir, İ. Ozan Demirel, Andaç Lüleç, Taylan Solmaz and E. Erşan Erdoğan.

I thank to the staff of METU - Structural Mechanics Laboratory, Osman Keskin and Hasan Metin for their assistance.

The financial supports from the Scientific and Technical Research Council of Turkey (TUBITAK – 106M493) is gratefully acknowledged

Last, but not least; I would like to exhibit my greatest appreciations to my family who have supported and relied on me for my whole study life.

TABLE OF CONTENTS

LIST OF FIGURES

LIST OF TABLES

Chapter 1

Introduction

1.1 Background

In recent years Turkey and many other countries in active seismic zones suffered greatly from earthquakes causing catastrophic tragedies. It was a well-known reality for the technical community in Turkey that a high percent of the building stock is vulnerable to seismic effects. After the Kocaeli and Düzce (1999) earthquakes, this fact became a sorrow reality showing off the deficiencies in the RC structures clearly.

The existing RC structures mostly have poor ductility and inadequate lateral strength due to deficiencies such as wide spacing of transverse reinforcement, detailing problems at the joints, low longitudinal reinforcement ratio, discontinuity of longitudinal reinforcements and low concrete strength. The difficulties in the structural control mechanism during construction are one of the leading reasons of the seismic vulnerability of the building stock.

For most residential buildings target seismic performance is dictated by the life-safety level according to TEC (2007). In other words, the allowed damage that can be estimated by using engineering demand parameters such as displacements, drift ratios or plastic rotations due to a seismic event should not endanger safety of human lives. The input energy given to the structure by the earthquakes is mostly dissipated at the plastic hinges. Therefore, the member based plastic deformation demands have to be met safely.

The upgrading of existing RC buildings can be a more challenging task than to construct new RC buildings. The objectives of the seismic rehabilitation are;

- bringing the seismic performance of the structure to a target safe perform level,
- meeting the lateral force and ductility demands due to expected scenario earthquakes.

In the case of insufficient expected seismic performance, retrofit of existing buildings may be the only feasible alternative. The performance of the building should be estimated before any strengthening technique is applied. The observed damage types need to be examined correctly in order to implement the most feasible and effective retrofitting system. The retrofit scheme should function so that the structural integrity is maintained. In addition the strengthening technique applied in the structure should not bring out significant application and occupancy problems and preferably should not intervene the functioning of the building.

1.2 Retrofit Methods

In order to define performance of existing structures the deficiencies need to be identified clearly. The assessment of the deficiencies and proposing a convenient retrofit methodology requires the knowledge of both member (local) and system (global) behavior. In member based retrofits the deformation capacities of inadequate individual members is increased to satisfy the target deformation demands (Figure 1.1). FRP or steel jacketing are the most popular examples of member (local) rehabilitation approaches. Global retrofit interventions aim to enhance the strength, stiffness and ductility of the structural system to a desired level (Figure 1.2). Adding structural walls and steel elements are the most common practices of the system (global) level rehabilitation techniques.

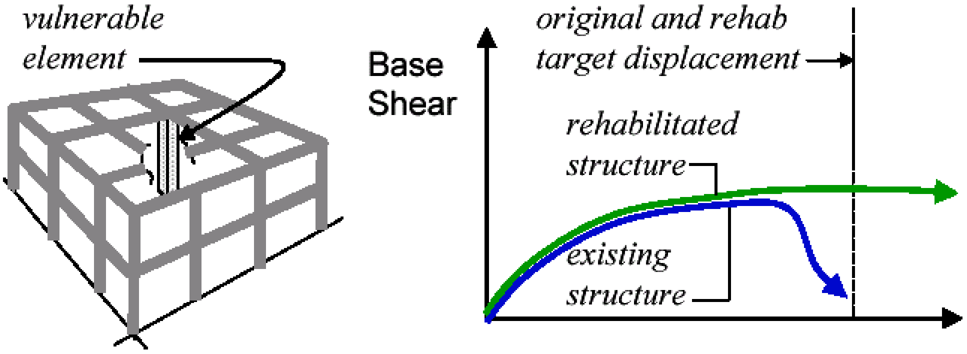

Figure 1.1 *Member (Local) based rehabilitation (Moehle, 2000)*

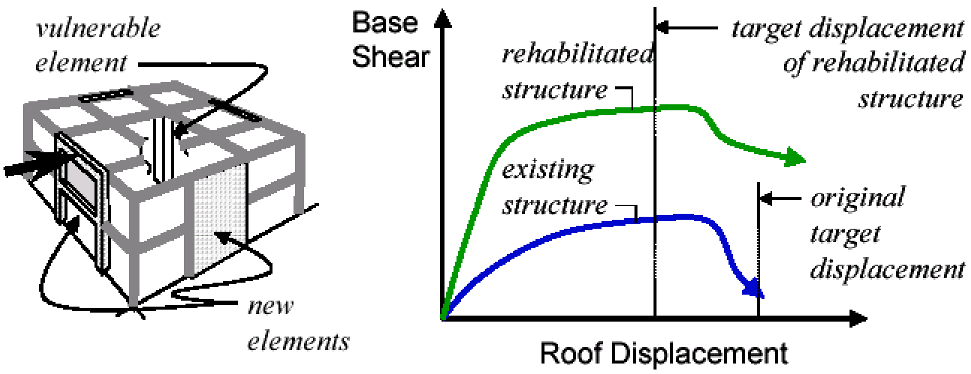

Figure 1.2 *System (Global) based rehabilitation (Moehle, 2000)*

1.2.1 System-Level Retrofit

In order to enhance the lateral stiffness and strength of existing structures for deformation and damage control, global retrofitting methods are commonly employed. Steel braces, Reinforced Concrete (RC) infill walls, and base isolators are the most popular methods. The commonly used techniques are explained below.

The most common upgrading method among the global retrofitting methods is adding RC walls (to the available bays) to increase the stiffness of the structure such that target displacements are controlled. There are numerous studies on post installed RC walls, indicating the important role of them in controlling the deformations of the whole structural system (Aoyama et al. 1984, Pincheira and Jirsa 1995, Ersoy and Uzsoy 1971, Altin et al. 1992, Canbay 2001, Sonuvar 2001, Erdem et al. 2006, Baran 2005).

Retrofitting the existing systems with steel braces is another way to increase the lateral stiffness and strength of the structure in global manner. There are number of researches for steel-brace retrofitting systems (Badoux and Jirsa, 1990; Maheri and Sahebi, 1996; Ozcelik & Binici, 2006) reporting the increase in lateral stiffness and base shear capacity of the systems. However they are also marking the weak points of the system as the connection between the frame and braces. Insufficiency of joint shear strength can result in the failure of the whole system. In other words, the structure can not reach its full capacity if any of the connection elements is not carefully detailed.

1.2.2 Member-Level Retrofit

The member-level retrofitting does not upgrade the whole system's stiffness or lateral capacity but the individual members' deformability is enhanced. Corresponding retrofitting system may be preferable if the member based displacement demands are unsatisfactory. The plastic deformation capacities of members can be improved by confining RC columns and joints using fiber reinforced polymers (FRP), concrete or steel jacketing.

For structures, such as in Turkey, containing many member level deficiencies, upgrade of structural members can be extremely cumbersome and costly. For those cases, system retrofit methods are more appropriate. In this way, deformation control along with lateral strength enhancements can help achieving target performance in a more convenient way.

1.3 External Upgrading Approach

After reviewing some basic concepts about today's retrofitting techniques, alternative global strengthening methods will be investigated throughout this study. The commonly preferred systems used in upgrading the deficient structures are usually connected to the existing frames at certain bays. The system's seismic performance is remarkably enhanced, once those systems are implemented. If there are infill walls made of bricks or parapet like material, they have to be cleared out before the upgrading process. Whenever it is hard to deplete and remove the in-plane materials or to sustain the functioning of the building during the implementation, the property of the retrofitting system need to be well thought. In this sense, avoiding any intervention inside the building and setting up a system on the outer-plane section of the frames is an applicable method that can be used for most of the RC structures. In Japan there are number of buildings that were recently upgraded externally with steel members. The building in Figure 1.3 is owned by the electric and water company of Fukui in Japan. The retrofitting process performed while the building sustained its function.

Figure 1.3
A public building in Japan, retrofitted with external braces

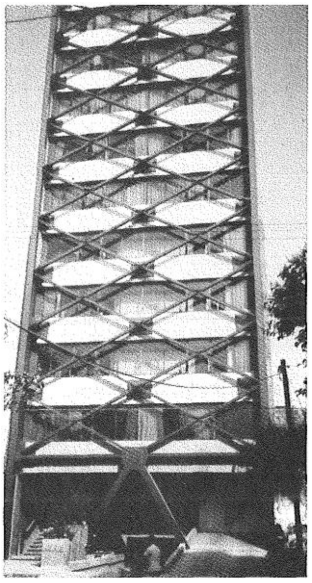

Figure 1.4
A 12 story building in Mexico City, retrofitted just before 1985 EQ

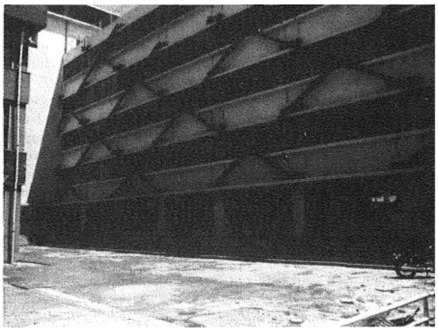

Figure 1.5
School building in Japan, retrofitted after 1978 EQ

The structure in Figure 1.4 in Mexico City also represents an important example for the performance of the retrofitted structure by using external bracing systems. The 12-storey building was retrofitted due to detected deficiencies prior to 1985 Mexico City earthquake. Although the surrounding buildings suffered much from devastating earthquake, the retrofitted structure exhibited remarkably sufficient seismic performance (Badoux and Jirsa, 1990).

Another example from Sendei in Japan was a school building which suffered heavy damage (due to short column effect) after 1978 Miyagi-ken earthquake. The loss of strength and stiffness in the building was restored by the bracing system as shown in Figure 1.5 (Badoux and Jirsa, 1990).

One of the important problems commonly encountered in the Turkish building stock and throughout the world is presence of soft and weak story in the ground level. Considering the retrofitting alternatives, the use of structural steel for this particular problem can be effective solution due to their architectural attractiveness. It is clearly seen in a building in San Francisco that the steel bracing system does not corrupt the architectural aesthetics of the building in addition to the significant stiffness enhancement to the soft story level (Figure 1.6).

Figure 1.6
A Building in San Francisco that had soft story problem retrofitted by steel braces

Aforementioned examples show that use of structural external strengthening systems, especially with structural steel is a promising technique for seismic retrofits. Hence, exploring such methods can help the seismic risk mitigation studies in Turkey.

1.4 Literature Survey

As summarized in previous section; there are many strengthening methods of existing structures. Consequently there are numerous experimental studies conducted for system level retrofitting. Following is a concise review of the examined literature on seismic retrofit methods.

Experimental Studies Conducted in METU:

A review of the major experimental studies conducted in METU is presented in Table 1.1.

Table 1.1 *Major experimental studies conducted in METU*

Researcher	***Retrofit Method***	***Strength & Stiffness Enhancements***	***Remarks***
Ersoy, Uzsoy (1971)	RC infill	~7 times strength ~5 times stiffness	one-bay one-story RC frames
Altin et al.(1992)	RC infill, masonry infill	~7.5 times strength ~45 times stiffness	14 One-bay two-story frames; connection details of panel and frame, type of infill reinforcement, column strength were investigated
Canbay (2001)	RC infill	~5 times strength ~15 times stiffness	three-bay two-story RC frames, infills introduced to damaged frames
Sonuvar (2001)	RC infill	~12-23 times strength ~13-58 times stiffness	one-bay two-story frames, infills introduced to damaged frames
Ozcebe et al. (2003)	CFRP	~1.8-2.1 times strength	one-bay two-story RC frames, proper anchoring was important
Erdem et al. (2006)	RC infill, CFRP	~5 times strength ~10 times stiffness	three-bay two story RC frames
Acun, Sucuoglu (2006)	mesh reinforcement	~2 times strength ~5 times stiffness	one-bay two-story RC frames with unreinforced masonry infill
Baran (2005)	precast panels	~2.7 times strength ~3 times stiffness	one-bay one-story RC frames with masonry infills

The common conclusions of the studies above state the remarkable strength and stiffness enhancement. In their research Altin et al. (1992) mentioned that the effect of RC infills on the enhancement of initial stiffness and strength of the specimens was significant provided that if the connection between the infills and frame was established properly. In his research Canbay (2001) introduced the infill walls after the bare frame was damaged according to an earthquake scenario. It was about 90% of the total lateral load that the infill wall carried just before failure. Sonuvar (2001) tested heavily damaged RC frames strengthened by cast-in-place RC infills. It was concluded that the connecting dowels' anchorage efficiency is dependent on the quality of frame concrete. In their study, Ozcebe et al. (2003) stated that strength of the specimens was enhanced remarkably if the surface of the infill was fully covered with CFRP. Also proper anchoring of CFRP strips to the infills was found to be essential. Erdem et al. (2006) investigated two types of strengthening techniques; the RC frame with CFRP applied on hollow clay block infill wall and with RC infill wall. The initial stiffness of the specimen that was strengthened with RC infill was higher than the CFRP retrofitted specimen. Baran (2005) studied on RC frames with hollow brick masonry infills that were to be strengthened by several types of precast panels. The researcher observed from the tests that, the effective energy dissipation took place as a result of inelastic action of the panels. It was also suggested to rehabilitate the existing frame members before strengthening method was applied.

There are also many experimental rehabilitation studies conducted in Turkey excluding METU. Anil and Altin (2007) studied on one-bay one-story RC partially infilled frames. The infill length to infill height ratio (aspect ratio) and arrangement of the partial infill on the frame were the test parameters. Generally, RC infilled frames exhibited brittle behavior and arrangement of the infills affected the strength of the specimens although the infills had the same aspect ratio. The strengthened RC frames generally showed brittle behavior (Figure 1.7). Karamehmet and Altin (2006) tested one-bay two-story non-ductile RC frames strengthened by partial infills. The best performance was exhibited by the specimens connected to both the beams and the columns of the RC frame. Yuzugullu (1979) studied on one-bay one-story RC frames strengthened with precast panels. With the enhanced lateral capacity and stiffness of the strengthened specimens, author concluded that increasing precast panel number used in the bare frame had not an influence on the failure mode. Turk (1998) conducted study to investigate the performance of one-bay two-story damaged frames strengthened with RC infills. Author's major conclusion was workmanship had a significant factor on the performance of the connecting dowels of RC infills. Also level of damage of the bare frames did not affect the behavior of the infills. Ozden, Akguzel and Ozturan (2003) conducted tests on one-bay two-story RC frames which were strengthened by CFRP strips. They concluded using CFRP strips was ineffective in increasing lateral drift levels at failure loads and initial stiffness of the specimens was not improved with respect to brick only infilled frames.

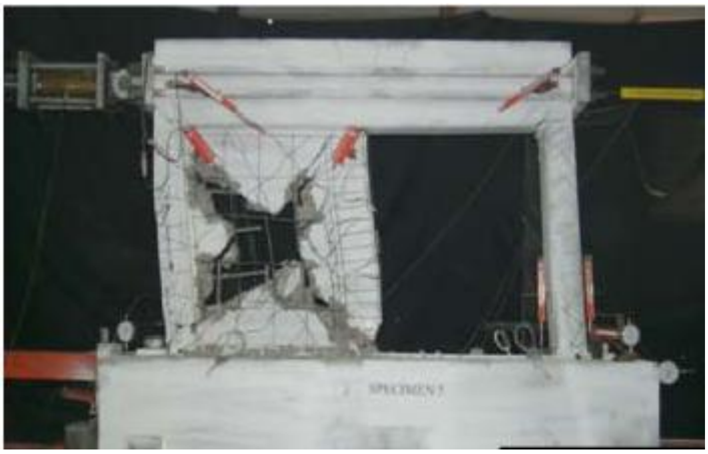

Figure 1.7
Brittle failure of the specimen strengthened by partial infill wall (Anil and Altin, 2007)

External or outer steel retrofitting systems were not studied experimentally in Turkey even if they are believed to be functioning effectively in today's literature. The applications in Turkey are generally based on RC infill walls systems although it is known that installation to the existing structure is hard, expensive and time-consuming process. The study below published recently in Turkey investigates an external approach to strengthen the existing public buildings.

Kaltakci et al. (2007) studied experimentally a new strengthening technique, named as "external RC shear wall". Authors point out deficient school buildings to perform the corresponding method. The most interesting property of the study is that the relevant structure does not need to be evacuated during the construction of new walls. They listed some deficiencies for the existing school buildings in Turkey like compression strength of concrete (as low as 8 MPa) and insufficient plain rebars. The external RC walls are thought to be constructed just out of the exterior frames of a deficient building.

Two bare and two strengthened 1/3 scale specimens were tested under cycling lateral loading. The axial load levels were as high as 50 to 60% of the column capacities. The only parameter for the two strengthened and bare specimens was the longitudinal reinforcement ratio of the columns. The conclusions from the study were as follows:

- External shear wall application is an effective solution for retrofitting existing primary school buildings in Turkey without any internal work in the building.
- The capacity and stiffness of the existing deficient system were increased nearly 4 times of the bare frame with the external RC wall retrofitting method.
- On the strengthened systems there was no significant damages seen on the existing frames at the maximum load levels.

Retrofits using Structural Steel:

Badoux and Jirsa (1990) examined the steel bracing systems for retrofitting the inadequate RC structures. They introduced the steel bracing systems and outlined the retrofitting design as a flowchart. The researchers mentioned the fact that: "In a steel-braced reinforced-concrete frame deforming laterally, the bracing system and the frame can be considered as coupled independent systems. Because of this independence, the flow of forces in the retrofitted structure can be controlled reasonably." Considering that phenomena the design process becomes an easy course of action leading the designers trying few brace parameters to achieve and estimate the best retrofitting system for the existing structure.

The concluding remarks of the study were as follows:

- Steel bracing systems have remarkable advantages over other retrofitting systems especially when it is used as an exterior scheme. Furthermore, the disturbance to the functioning of the building is minimum during the installation of the bracing systems.
- Steel bracing is effective in increasing the lateral strength and stiffness of multistory RC buildings. The strength and stiffness may be adjusted easily and independently by the designer.
- Elastic response should be considered to design steel braces but in case of excess loads they have to be detailed for ductile behavior.
- The major problem is the inelastic buckling of the braces. The slenderness ratio of the braces should be kept as low as possible to limit inelastic buckling.
- Combining the steel bracing with weak-column, strong-beam RC frames can significantly improve the inelastic cyclic behavior of such systems.

Kazunori et al. (1999) developed two strengthening methods for the seismic retrofitting of existing buildings. The first one was installing ultra light-weight precast RC shear panels and the second one was the external steel frame method that upgrades building from outside. The study reported the qualitative findings about the seismic performance and failure properties of corresponding methods and procedure for evaluating the ultimate strengths of integrated systems.

Tsunehisa et al. (1999) studied on seismic strengthening method using braces adjacent to the outer-frame. Shear tests of prestressed joint between steel and concrete and lateral load tests (two directions) of prestressed concrete member were performed. The parameters for shear in the specimen were; normal pressure on joints, friction area and the shape of shear key (with or without cotter). The specimen parameters for lateral loading were the angle of loading and the strength of transverse rebars. The conclusions of this study presented findings about the coefficient of friction of prestressed joint between concrete and steel and behavior of prestressed RC member under lateral loading.

Maheri and Sahebi (1997) carried out a series of tests to investigate the lateral strength enhancements of RC frames that were strengthened by diagonal steel braces. In the test results they stated that steel braces were good alternatives to shear wall retrofits. Following were the brief conclusion of the experimental study:

- The in-plane shear strength of the retrofitted specimens in one diagonal brace increased very significantly up to 2.5 times of the RC frame itself.
- The X-braced systems' in-plane shear strength enhancement was about 4 times of the unbraced frame.
- To utilize the full capacity of the braces, the connection of the braces to the frame was significantly important.
- In the X-braced systems, most of the load was carried by the tension braces. Failure initiated due to the bucking of the compression braces.

Maheri and Hadjipour (2003) conducted an experimental study to investigate the connection of steel braces to the RC frame. Three types of full-scale brace - RC frame connections were tested. Tests showed consistent results with the design strengths. Authors concluded that steel brace – RC frame connection could be designed successfully by implementing the provisions of composite structures.

Maheri, Kousari and Razazan (2003) conducted pushover tests to the 1/3 scale RC frames that were strengthened by X-braced or Knee-braced systems. 2.5 to 3.5 times the lateral strength of the bare frame was achieved in the study for X-braced and Knee-braced systems, respectively. In the braced frames, occurrence of the first plastic hinge on the RC frame was at very large lateral loads leading to the conclusion that steel bracing increased significantly the yielding capacity of RC frames. Authors also concluded:

- Bracing systems can be designed for the desired strength enhancement or drift demands.
- X-bracing was the more effective one of the two bracing types, increasing the lateral stiffness of the ductile frame.

- If ductile behavior was the need of a building that was in a collapse limit, the knee-bracing is more suitable.
- Although it is easy to design connections in new buildings, appropriate connection methods should be developed and their performance needed to be tested for the retrofit of existing structures.

So far general information of several studies for strengthening techniques about infill walls and structural steel were given. Usually steel was employed to construct brace elements or moment resisting frames however, recently there are numerous studies covering relatively new systems; so called the steel plate shear wall behavior (Caccese, Elgaaly and Chen, 1993; Park et al., 2007; Choi and Park, 2008; Choi and Park, 2009). Common conclusions of steel plate shear walls can be summarized below:

- The steel plate shear wall (SPSW) systems enhance initial stiffness and load carrying capacity. For the SPSW employed frames with large aspect ratio and sufficient column shear strength, tension-field action can help to achieve sufficient load carrying capacity and deformability.
- As the ratio of the flexural capacity to the shear capacity increases the total displacement ductility of the steel plate walls increase.
- The failure modes of SPSW are generally in the form of fracture of welded connections at the column base or beam-columns connections.
- The relatively thin steel plate walls exhibit shear-dominant behavior by the moment-frame action whereas the thicker steel plate walls exhibited flexure-dominant behavior by the cantilever action. Better ductility is observed in the shear-dominated walls.
- All of the steel plates exhibited large plastic deformations however the frames with relatively weak columns had smaller energy dissipation capacities.
- The deformation mode is an important factor for determining the ductility and energy dissipation capacity of steel plate walls.
- Although a brace member in a braced frame is directly connected to the beam-column joints, the infill steel plate is connected usually to the entire section of the columns and beams hence bringing a distributed load demand

on neighboring elements. Consequently, the frame members should have sufficient strength to withstand boundary forces.

- Although local buckling occurred at early stages of some tests, the steel plate walls showed sufficient stiffness, strength and ductility due to recovery from post-buckling.
- The strength of the systems was not affected significantly from the local deformation of SPSW. The failures mostly occur in column bases or joints in a well-designed steel plate.
- The load carrying capacity and energy dissipation capacity for steel plate walls can be estimated by using the effective tension field area and the inclination angle of that tension field.
- The load-carrying capacity and energy dissipation capacity of partially connected steel plate infills (welded only to the beams) are less than fully connected solid wall infilled frames however they performed large deformation capacity.

1.5 Objective and Scope

The aim of this study is to investigate new approaches for the global retrofitting techniques of existing deficient buildings. It is not a debate that the number of structures which need rehabilitation can be stated with hundreds of thousands for the RC building stock in Turkey. Considering the facts regarding the economy and time, utilizing rapid strengthening methodologies is extremely important. Hence the fundamental goal of the retrofit design must satisfy the seismic drift control of the structure as well as considering the economy, workmanship and sustainability of construction works with the time.

From this perspective following are the primary objectives of this study:

- to investigate experimentally the performance of external retrofit methods
- to analyze the test specimens by using finite element analysis for a better understanding of force transfer mechanism
- to compare the seismic response of upgraded systems with simple non-linear time-history analysis.

This study is based on the retrofitting experiments conducted at METU – Structural Mechanics Laboratory. One reference (bare) and four strengthened RC specimens were tested. The test setup and the properties of the specimens are explained in Chapter 2. After that, discussions about the test results are presented in the third chapter. Details of the numerical simulations performed for the investigation of behavior for corresponding specimen models are presented in Chapter 4. Chapter 5 presents the major conclusions from the combined experimental and analytical investigation.

Chapter 2

Experimental Studies

2.1 General

A reference RC bare frame and four strengthened specimens were tested in this study. The dimensions and the reinforcement ratios of the RC frame were the same for all specimens. The RC frames were one-bay one-story with a 1/3 scale. The deficiencies of the building stock of Turkey were similar to that of the bare frame that will be discussed in the next section.

The tests were conducted at METU Structural Mechanics Laboratory employing a reaction wall in order to exert lateral displacement excursions to the test specimens. The dial gauges and LVDTs (Linear Variable Differential Transformers) were used for measuring curvatures and displacements respectively. Furthermore, strain gages were employed to check the strains of the critical regions of steel members in the specimens that have been upgraded by using steel sections.

Examining the general performance of the external strengthening methods was the essential objective of this experimental study. The strengthening methods include use of structural steel in three specimens and an external RC shear wall for one specimen. The bare frame test was labeled as **SP1**. Strengthening methods of examined in the course of this study are:

- **SP2**: External Moment Resisting Steel Frame
- **SP3**: External Steel Plate Shear Wall
- **SP4**: External RC Structural Wall

- **SP5**: External Moment Resisting Steel Frame with Post-Tensioned Anchors

2.2 Test Setup & Instrumentation

The test setup was similar to that employed by Ozcelik & Binici (2006) which had a rigid foundation that was used to fix the RC specimens to the test setup (Figure 2.1). The steel surrounding frame was constructed for safety precautions and to prevent out-of-plane deformations. In previous studies that were conducted by Ozcelik & Binici (2006) it was observed in some tests that brittle failures may result in gravity collapse in large drift demands and a support to avoid the undesired dangerous failures may be needed.

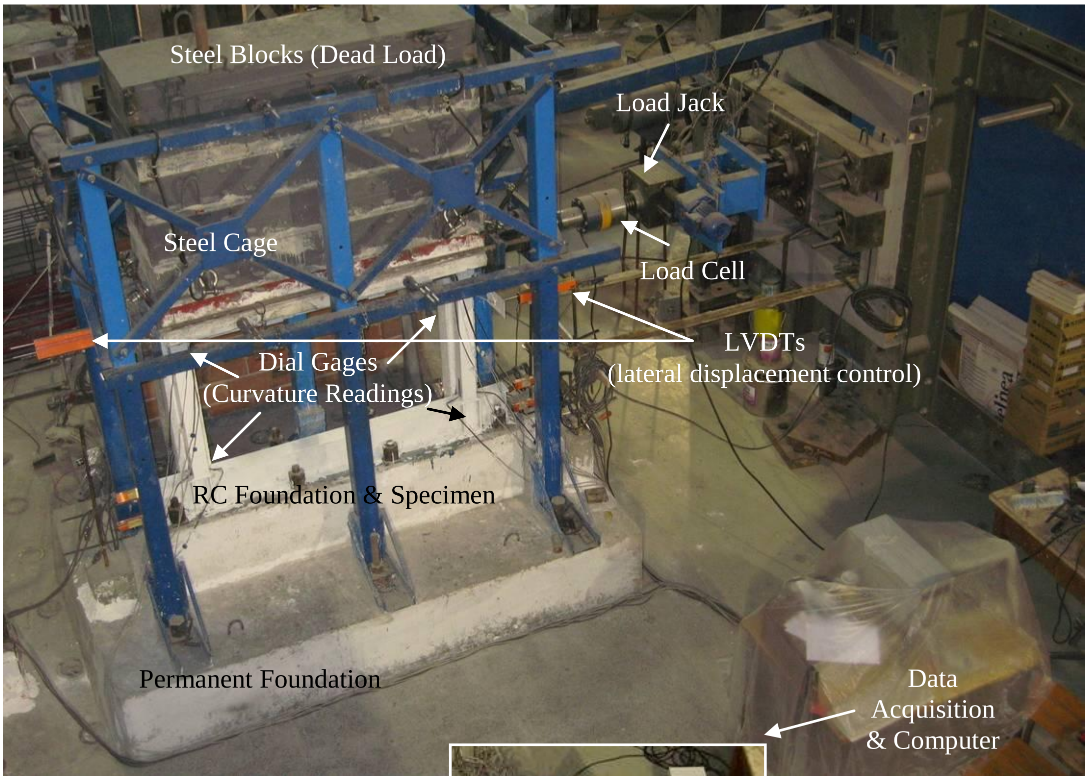

Fig

Displacement controlled loading was employed by the screw jack that was installed with steel attachments. It had a maximum speed of 0.2 mm/sec which was controlled by an electronic inverter. The load cell which had a capacity of 200kN, placed next to the load jack, was used to measure the lateral force on the specimen.

The loading protocol was the same for all specimens. Hysteretic cyclic displacement excursions were given to the specimens in both directions. It was initiated by 0.5% drift ratio followed by 0.5% drift ratio increments up to 2% drift ratio. Further increments were imposed by 1% drift ratio until 5% drift ratio was reached. Each drift ratio increments had 2 cycles for drift ratios smaller than 5%. Afterwards one cycle was imposed to the specimens. That loading protocol is demonstrated in Figure 2.2.

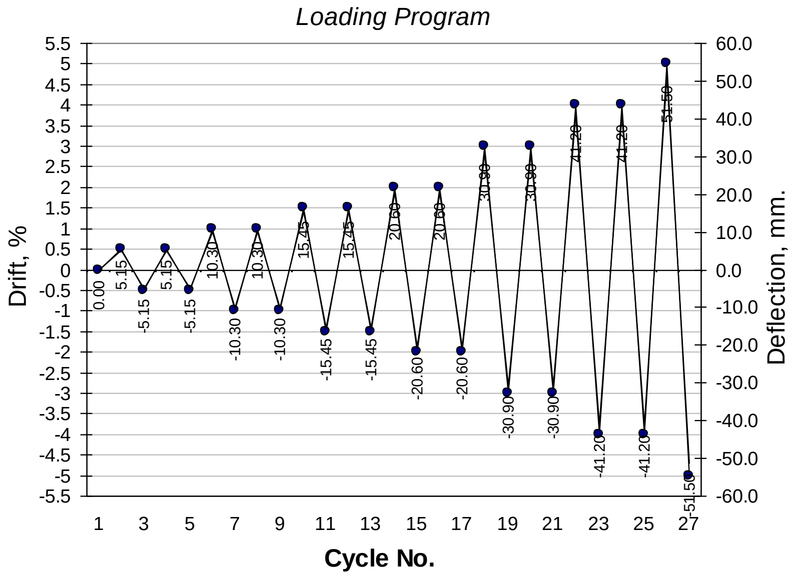

Figure 2.2 *Loading Protocol*

Eight dial gages were used on the test frames to measure column curvatures. The extension and contraction on two opposite symmetric faces of the columns were recorded by means of those gages. The curvatures were estimated with the recorded displacements within the gauge length. Those displacements were converted to strains so that the difference between them could give the average instantaneous curvatures. Dial gages were demonstrated schematically in Figure 2.3. The voltage outputs of these gages were converted into deflections (in mm) and recorded on a computer using a data acquisition system.

The calculation procedure of the curvatures from recorded dial gage data is explained below in Figure 2.4 in which the dial gage calculations were also demonstrated.

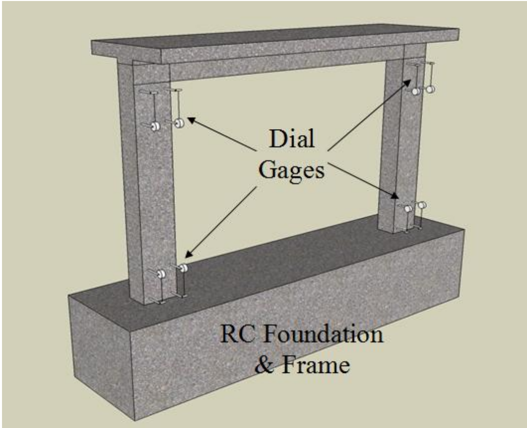

Figure 2.3
3D Representation of the RC frame and dial gages for curvature readings

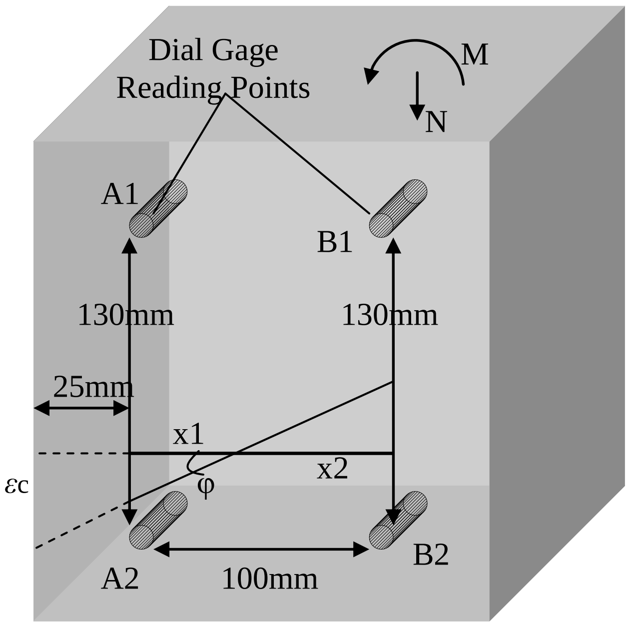

a: Displacement btw. points A1, A2

b: Displacement btw. points B1, B2

$$\varepsilon_a = \frac{a}{130} \qquad \varepsilon_b = \frac{b}{130}$$

$$x1 = \frac{100 \times |\varepsilon_a|}{|\varepsilon_a| + |\varepsilon_b|} \qquad x2 = \frac{100 \times |\varepsilon_b|}{|\varepsilon_a| + |\varepsilon_b|}$$

Strain at Column Face:

$$\varepsilon_C = \frac{\varepsilon_a \times (x1 + 25)}{x1}$$

Curvature: $\phi = \dfrac{\varepsilon_C}{x1 + 25}$

Figure 2.4
Curvature calculations from dial gages

The curvature readings were used to determine the yielding of column plastic hinge regions in order to observe the plastic hinging patterns and specify the yielding points. Besides the dial gauges, four LVDTs with 200 mm stroke were used to measure lateral displacements at story level. At each end of the specimen two of them were placed in order to monitor specimen out of plane movements (Figure 2.5).

Figure 2.5 *Dial gages and LVDTs, respectively*

In order to avoid out-of-plane motions for specimens and dead load during the tests, eight special roller restraints (Figure 2.6) were used on test setup. In each side of the specimens two of them were placed that restrain steel blocks and RC frame. Those fixed rollers were attached to the steel cage frame to minimize the lateral movement of the testing frame. Furthermore, in tests that include steel sections, strain gages were used to check the yielding of steel members.

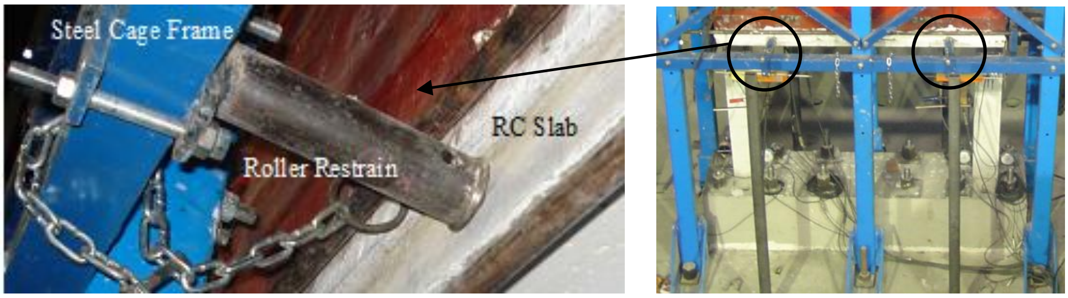

Figure 2.6 *Roller supports: Restraints out-of-plane deflection*

Steel blocks were placed on the slab of the RC frame for distributed dead weight representation. Each has a mass of 550kg, eleven steel blocks was used in the setup that weighs 60kN in total. The axial load ratio on the columns was about 20% of their ultimate axial load carrying capacity as shown in Table 2.1.

Table 2.1 *Experimental Program*

Test Specimen	Property	Strengthening Member	Strengthening Member Dimensions(mm)	Concrete Strength (MPa)	Axial Load Ratio
SP1	Bare	-	-	8.1	0.18
SP2	Strengthened	External Connected Steel Frame	Column: 80x80x4 Beam: 70x70x3	7.8	0.19
SP3	Strengthened	External Connected Steel Plate	1550x1000x0.3	7.6	0.19
SP4	Strengthened	External Connected RC Wall	500x70	8.5	0.18
SP5	Strengthened	External Connected Steel Frame with post t. connection	Column: 80x80x4 Beam: 70x70x3	7.5	0.19

2.3 Materials

The mechanical properties obtained from uniaxial tests for the 8mm reinforcing bars are presented in Figure 2.7. The 4mm diameter transverse and slab reinforcements had 270MPa yield strength and 375MPa ultimate strength. Also, stress-strain responses of coupon specimens are presented in the same figure.

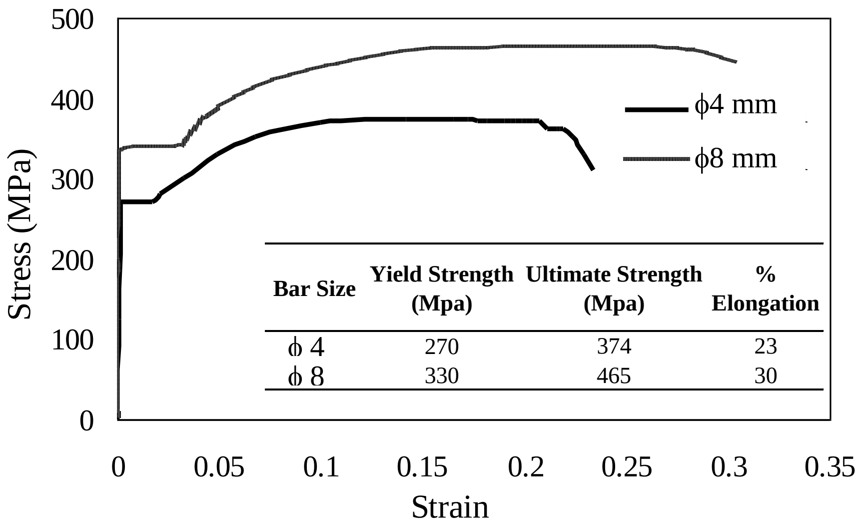

Figure 2.7 *Stress-Strain responses of reinforcements*

In order to have concrete quality that resembles the Turkish building stock, 8 MPa of target compressive strength was used. Maximum aggregate size was 7 mm according to the similitude law of scaling. Table 2.2 presents the mixture proportion of the concrete for the test specimens. The standard uniaxial compression tests on cylinders were conducted for each specimen on the test days. Uniaxial compression strength of concrete on the test day is presented in Table 2.1.

Table 2.2 *Mixture proportion of concrete*

Material	*Weight (kg)*	*(%) of Total Weight*
Cement (PC32.5)	50	11
Aggregate 0-3mm	130	29
Aggregate 3-7mm	220	49
Water	50	11

For the anchor bolts that were used to connect structural steel elements to the RC frame, high strength Mbrace Saturant Epoxy material was employed with its primer MBT-Mbrace. Moreover, in order to facilitate the facial lateral grip of RC frame, Concressive 1406 material was used. The mechanical properties of those chemicals are presented in Table 2.3.

Table 2.3 *Mechanical properties of anchoring chemicals*

Material	*Type*	*Compressive Strength (MPa)*	*Adhesive strength to concrete (MPa)*
MBrace Adesivo Epoxy	High Strength Adhesive	> 60	> 3
MBrace Primer	Epoxy Primer	-	> σ_{tc} (concrete splitting strength)
Concressive 1406	High Strength Mortar	> 75	> 3

All of the bolt anchors were 6 mm diameter high strength bolts with 600 MPa of yield tensile strength. The yield strength of the steel sections 80x80x4 mm and 70x70x3 mm employed for the columns and beams were about 340 MPa (which was the stress at 0.2% strain extension of the stress-strain envelope). In order to connect strengthening elements to RC frame (for the specimens SP2, SP3 and SP4) 6 mm diameter steel bolts were employed. The stress strain response of the coupon test of the corresponding bolt section is presented in Figure 2.8. The stress-strain response of a coupon test of those box sections is presented in Figure 2.9.

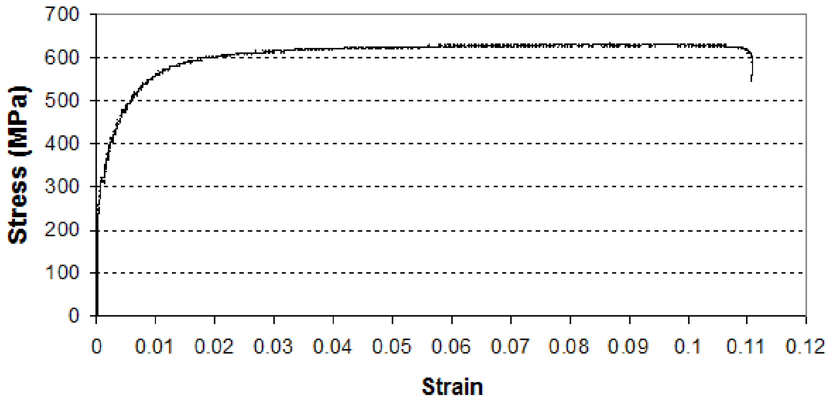

Figure 2.8 *Stress-Strain response of the anchor bolts*

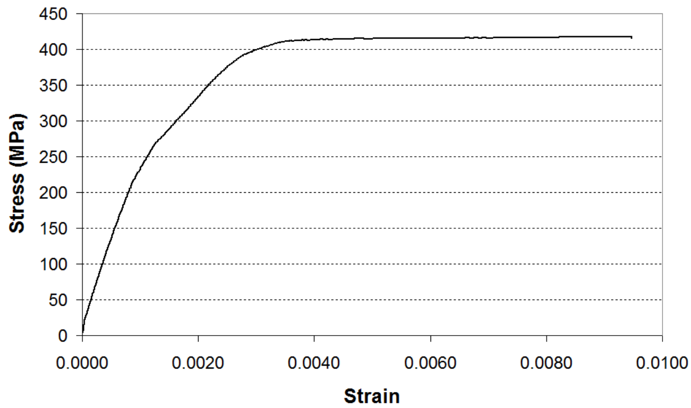

Figure 2.9 *Stress-Strain response of the steel box sections used in SP2 and SP5*

In the conducted coupon tests the ultimate stress of the 0.3 mm plate used in SP3 test was observed as 340 MPa. The mechanical properties of the steel sections which were used in the tests are summarized in Table 2.4.

Table 2.4 *Mechanical properties of steel sections*

	Box Sections (SP2,SP5)	Steel Plate (SP3)	Anchor Bolts (Φ6)	Anchor Bolts (SP5, Φ12)
$\boldsymbol{\sigma_y}$ (MPa)	420	-	400	-
$\boldsymbol{\sigma_u}$ (MPa)	-	340	620	600

where; σ_y and σ_u are the yield and ultimate stress of steel section

2.4 Specimen Preparation and Bare Frame Properties

The RC frame used in each test had the same properties in both dimensions and reinforcement layout. It was cast horizontally using steel forms formwork with a target concrete compressive strength of 8 MPa. The frame had its foundation which was also cast with which is used for attaching the RC frame to the test setup through the permanent foundation. The RC bare frame had the following deficiencies:

- Longitudinal and transverse plain bars in beam and columns (ρ_l=0.013, insufficient lateral reinforcement; A_{sh}=25 mm^2 < 57 mm^2; Turkish Earthquake Code [TEC], 2007)
- Low concrete compressive strength (8 MPa)
- Insufficient lateral reinforcement in columns which had spacing of 100 mm equal to the smaller dimension of the column (required is 33 mm for a 1/3 scale RC frame; TEC, 2007)
- for column stirrups 90˚ hooks were used
- Beam-Column joint had insufficient (with only one) stirrup extending from column into the joint.

The planar dimensions of the frame were 1400x1000 mm and the foundation was 1890x400 mm in plan with a height of 400 mm (Figure 2.10). The columns were 100x150 mm and have four 8mm diameter longitudinal plain bars (Figure 2.11). In order to place dead weight conveniently and represent slab behavior, the beam was designed and cast with a slab thickness of 55 mm having a width of 450 mm.

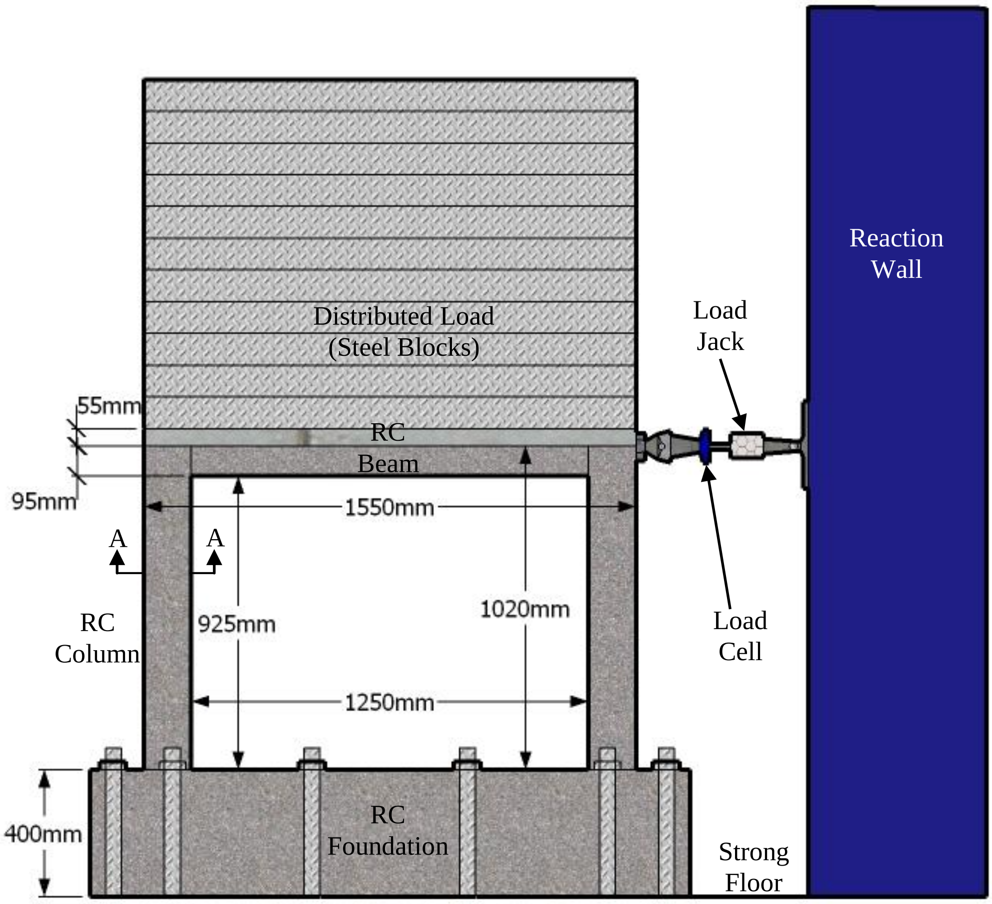

Figure 2.10 *Dimensions of RC Specimen*

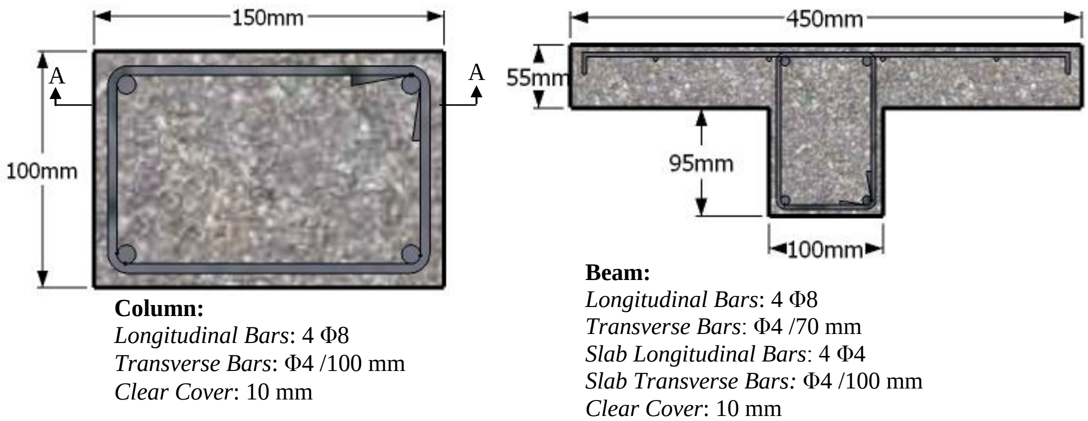

Figure 2.11 *Dimensions of RC column & beam*

The pictures shown in Figures 2.12 demonstrate the reinforcements of column and beams just before placing into the steel formwork. The foundation reinforcements were prepared as it is shown in 2.13. Also the pictures of formworks and the standard test cylinders are presented in the same figure. In Figure 2.14, the RC specimen formworks are demonstrated before and after cast of concrete.

Figure 2.12 *RC column and beam reinforcements*

Figure 2.13 *Preparation of RC foundation reinforcements, steel formworks and standard test cylinders*

Before *After*

Figure 2.14 *Pictures before and just after cast of specimens*

Bare Frame Plastic Design Capacity:

The lateral strength of the bare frame is estimated based on a column hinging plastic mechanism (Figure 2.15) considering the fact that moment capacity of the column is smaller than that of the beams. The Moment – Curvature (M – Φ) response of columns with $0.2N_o$ and beams are shown in Figure 2.16 and Figure 2.17. Equating the external virtual work with internal work, one obtains:

$V_{br} \times \Delta = 4 \times M_p \times \theta$ where $\theta = \dfrac{\Delta}{h}$ and $M_p = 5.4$ kNm

$$V_{br} = \frac{4M_p}{h} = 21.6\ kN$$

$$\Delta N = \frac{21.6}{l} = 15.4\ kN$$

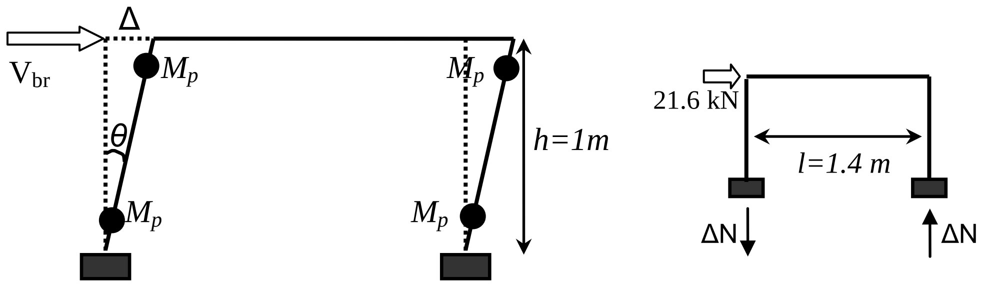

Figure 2.15 *Representation of plastic mechanism in the RC frame and variation of the axial load in the RC columns*

If V_{br} is assumed as 21.6 kN the axial load in the RC columns estimated to be changed between approximately (30 ± 15) 15 and 45 kN during lateral loading and unloading. The variation of the moment capacity of the RC column is shown in the interaction diagram of the RC column (Figure 2.18).

N_o is axial load capacity of RC column section. V_{br} is the lateral load capacity of bare frame, ΔN is the variation of the axial load in the RC columns and M_p or M_{pC} is the plastic moment capacity of RC column section under axial load level of $0.2N_o \approx 30$ kN. M_{pB}^- and M_{pB}^+, in Figure 2.17, are the plastic moment capacities of the RC beam section in negative and positive direction in its major axis, respectively.

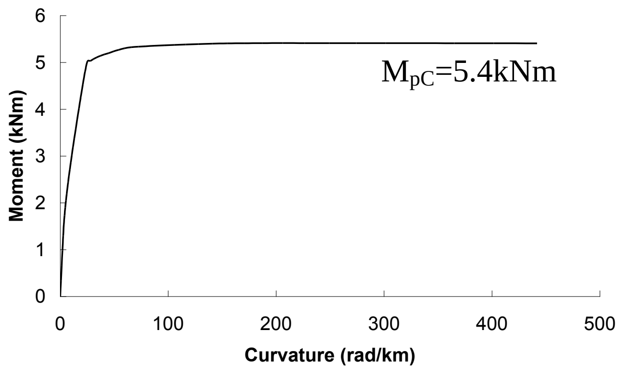

Figure 2.16 *Moment - Curvature relationship of the RC column (0.2N_o)*

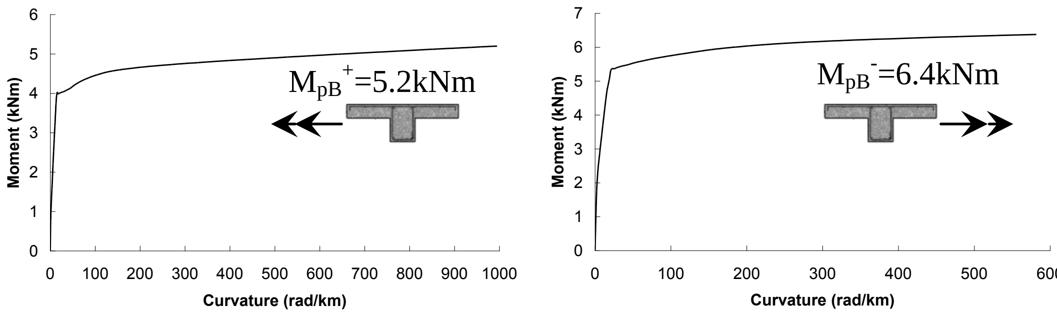

Figure 2.17 *Moment - Curvature relationship of the RC beam*

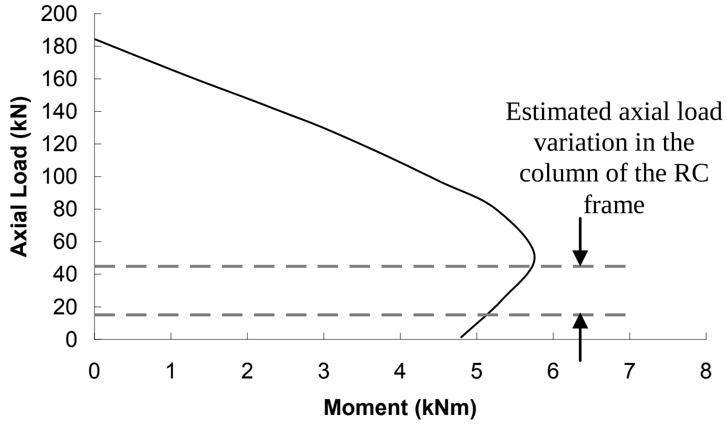

Figure 2.18 *Moment - Axial Load Interaction of the RC column*

Since the mass of the structure is about 6000 kg, the base shear capacity ratio (*V/M*) of the frame is estimated to be about 0.35g. This corresponds to a force reduction of about 3 assuming an elastic base shear demand of 1g for a structure in a seismic zone according to TEC (2007). Given the aforementioned detailing deficiencies the structure is expected to behave in a non-ductile manner without being able to meet the ductility demand corresponding to R=3.

2.5 Strengthening Methods

In actual strengthening implementations, usually the axial load on the columns is not removed during the retrofitting operations. In other words, the dead load on the structure remains while the structure is being retrofitted. In order to consider and simulate this fact, dead load was placed on the RC frames before the strengthening steps were initiated.

For the Steel frame test (SP2) steel box sections were used to construct moment resisting frame that was connected to the bare RC frame at beam-column joints and along beam span. Steel plate test (SP3) involves a thin plate that was connected to the RC frame from columns, beam and foundation. In RC shear wall test (SP4), the wall was cast together with the pre-anchored reinforcements to the existing foundation and with the bolts to the beam. In the last test, steel frame (SP5) with the same dimensions with SP2 was tested using an innovative post-tensioned anchoring method.

The target lateral capacity was set to be approximately 3 to 4 times of the bare frame (in a range 60 – 70 kN). For this target strength, ductility levels, energy dissipation characteristics were aimed to be investigated. In the test series, the strength enhancements of specimens were aimed to be similar in order to compare the ductility and hysteretic properties objectively.

2.5.1 SP2: External Steel Frame Retrofit

In the specimen SP2, the steel moment resisting frame (SMRF) was integrated externally to the bare frame with the anchoring bolts that were provided through the face of the RC beam and joints. For the foundation connection 10 mm thick base plates were employed as welding them to steel column bases.

The lateral load carrying capacity of the added SMRF (V_{SMRF}) was computed based on a beam mechanism (Figure 2.19) and employing plastic design concept.

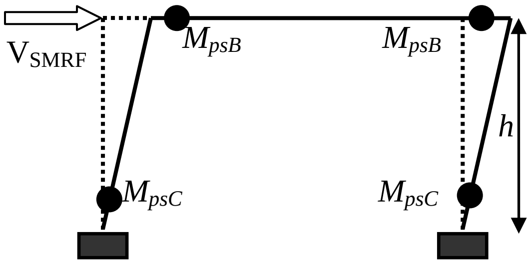

Figure 2.19 *Plastic Mechanism for SP2*

$$V_{SMRF} = \frac{2M_{psB} + 2M_{psC}}{h}$$

where M_{psB}=9 kNm and M_{psC}=13.8 kNm

$$V_{SMRF} = 45.6\ kN$$

M_{psB} and M_{psC} are the plastic moment capacities of beam and column sections of the steel frame, respectively.

Based on this, the estimated capacity of the strengthened system can be computed as:

$$V=V_{br} + V_{SMRF} = 21.6+45.6 =67.2\text{kN}$$

Strengthening was initiated by drilling 8 mm diameter anchor holes for column base plates (190x130 mm). Eight holes were opened up for eight connection bolts followed by the cleaning of those holes with pressurized air for better adherence to the surrounding concrete. After filling holes with epoxy, eight anchoring bolts for each column base were embedded into the concrete and left for curing. Once the epoxy used for anchorages of the base plates was cured concressive material was used on the concrete around the anchor points in order to enhance the adherence between base plates and concrete and fill in little voids under the plates (Figure 2.20).

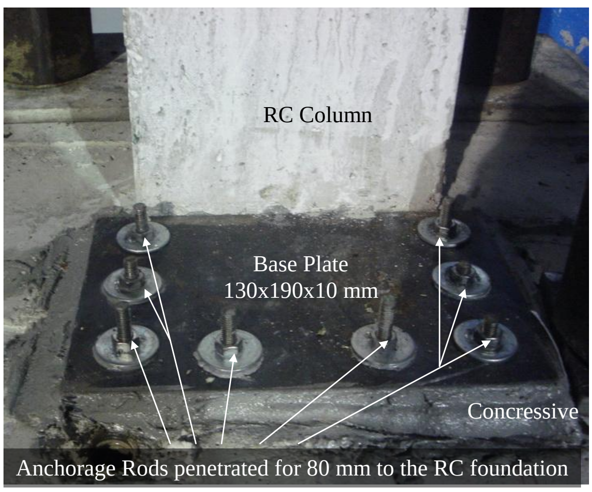

Figure 2.20 *Base plate attached to the RC foundation*

The anchors on the beam and joints were prepared with the same procedure. After the anchorage points were drilled, holes were cleaned up. The embedment depth of the anchors was 80 mm. The lateral load was transferred to the steel frame by a total of 26 anchoring rods; 4 per two joints and 18 for the beam face. They were designed such that the concrete's bearing capacity was not exceeded for an anchor rod and that steel rod was not forced to have shear failure when the system reaches lateral plastic load capacity. The design calculation for the anchors is summarized below:

shear check for steel rods:

σ_y=600MPa for a bolt

shear capacity of a single bolt(Fss)(D=6mm) :

$$\text{Fss}=600\times 0.5\times \frac{6^2\times\pi}{4}=8482N\cong 8.5kN$$

bearing capacity of the concrete (Fbc) for a bolt:

$$Fbc=0.85\times 6\times 80\times 8=3264N\cong 3.26kN$$

$$\text{Fbc}<\text{Fss}$$

$\therefore$ concrete bearing failure was critical

Load transfer capacity (Ftr) of 26 anchors:

$\text{Ftr}=3.26\times 26=84.8kN$ > V_{SMRF} (Factor of safety $\approx$ 2)

In the above calculations single steel bolt's shear capacity was taken approximately as half of its yield strength. The bearing capacity of the concrete surrounding the single bolt was estimated by considering the concrete area of 6x80 mm. Total numbers of 26 anchors were used in the frames that were condensed on the joints and beam ends to avoid failure due to stress concentrations. The faces of the bolted beam and concrete were covered with concressive material. Epoxy was employed to increase the adherence between steel frame and RC frame (Figure 2.21).

Figure 2.21 *Installation of anchorage rods for beam and joints and covering of beam and columns with concressive and epoxy*

The same procedure was conducted for the beam and then the nuts of bolts of both columns and beam were fastened before starting welding of steel members and base plates (Figure 2.22). Since the sections on steel members that were left on the face of RC frame become unavailable for welding, the steel joints were reinforced with suitable angle-sections (Figure 2.23) to assure moment transfer between steel column and beam sections. In Figure 2.24, SP2 specimen details are presented with a picture taken after retrofitting operation.

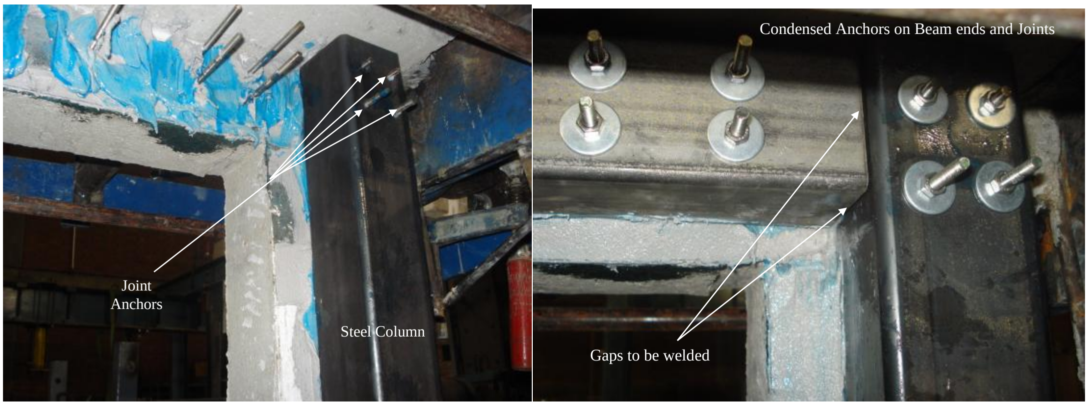

Figure 2.22
Integration of steel beam and steel columns, fastening of bolt caps

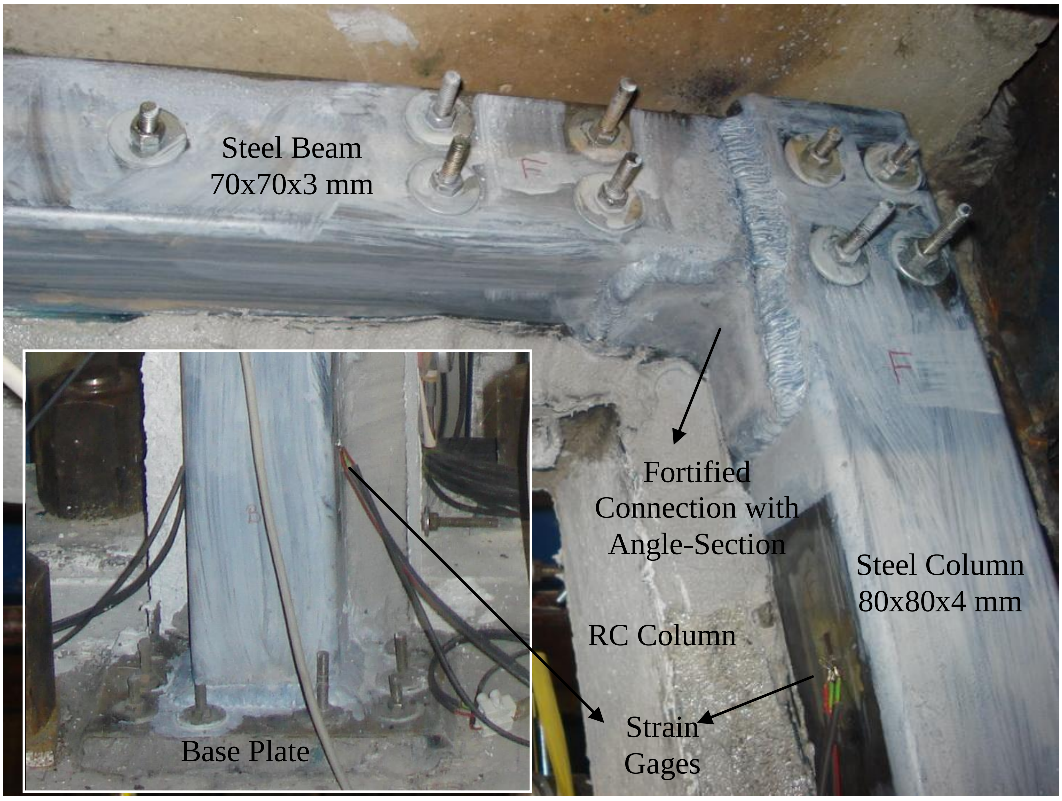

Figure 2.23 *Base plate and beam-column connection after welding*

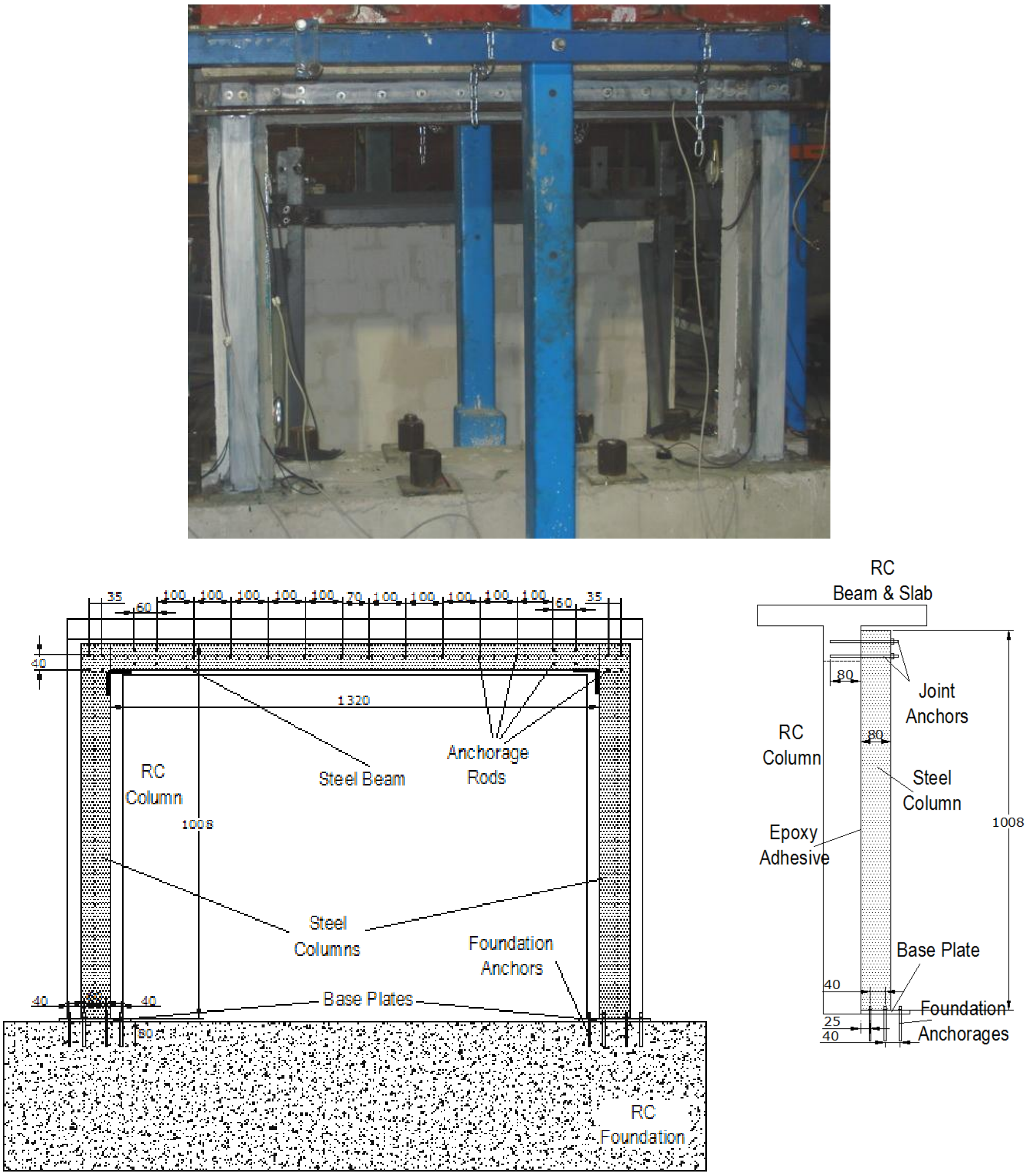

Figure 2.24 *SP2Specimen, external connected steel frame (all units in mm)*

2.5.2 SP3: Steel Plate Shear Wall (SPSW) Retrofit

As an external retrofitting system for the deficient RC frame a thin steel plate was attached externally to the bare frame which was installed through the anchors on both beams and columns. In order to satisfy the boundary fixity steel plate was also connected to the bare frame along the foundation by means of a steel L-Section.

The lateral strength of steel plate shear wall system is controlled by the thickness of the plate. The minimum available steel plate thickness that can be employed in the system was 0.3 mm. The dimension of the prepared plate was 1550x1000 mm which covered the whole RC frame. Assuming the whole section bear shear stress, the lateral capacity of the steel plate (V_{spsw}) after formation of the tension field is found as (Kurban, 2009):

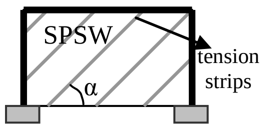

Figure 2.25 *Horizontal angle of tension strips of SPSW*

$$V_{spsw} = 0.5 \times \sigma_{spy} \times L_{spc} \times t_w \times \sin 2\alpha$$

where; α: the angle of the tension field (Figure 2.25, assumed as 45˚),

σ_{spy}: yield stress of the steel plate (the yield stress and ultimate stress of the plate material is very close, taken as 340 MPa),

L_{spc}: clear distance between the vertical boundary elements (1250 mm)

t_w: thickness of steel plate wall (0.3 mm)

The 0.5 coefficient is replaced by 0.42 in the AISC Seismic Provisions (2005) due to the overstrength factor of 1.2 (Kurban, 2009).

$$V_{SPSW} = 0.42 \times 340 \times 1250 \times 0.3 \times 1\ N$$
$$V_{SPSW} = 53.5\ kN$$
$$V = V_{br} + V_{SPSW} = 21.6 + 53.5 \approx 75\ kN$$

The number of anchors was determined similar to the previous specimen. Likewise the plate had to be restrained on every four sides to achieve tension-field action; from columns, beam and the foundation. In addition to the anchors on the beam and joints in the SP2 test, steel plate was anchored along the two columns as well (Figure 2.26). The total number of anchors on the RC frame was 52 and on the L-section that connects the plate to RC foundation was 14.

The implementation of the declared connection method was initiated by the drilling of anchoring holes. Foundation, columns and the beam was drilled with 8mm diameter drilling bit then cleaned similar to the SP2 test. The foundation and the frame anchorage rods were attached to the RC specimen at the same time with epoxy adhesive. The penetration length was 80 mm for the anchors on the boundary frame members and 100 mm for the foundation anchors.

Figure 2.26

SP2 Specimen with the anchors attached on foundation, columns and beam

After the epoxy cured, the face of the RC frame and the region around the foundation anchors (that the L-Section would be placed) were covered with concressive and with epoxy material to obtain a smooth attachment surface (Figure 2.26). The prepared L-Section was attached on the anchorage rods on the foundation and then the bolt caps were fastened. After the L-Section was installed, steel plate was attached to the relevant anchorage points on the RC frame. The arranged bolts for the foundation connection were placed from both L-Section and steel plate. Connection points on the plate were fortified with another steel plate that was also arranged for that operation in order to distribute the concentrated stress on connection nodes of the plate uniformly (Figure 2.27). Finally, the caps of were fastened for all column, beam and foundation anchorage bolts (Figure 2.28). The details of the steel plate shear wall system are presented in Figure 2.29.

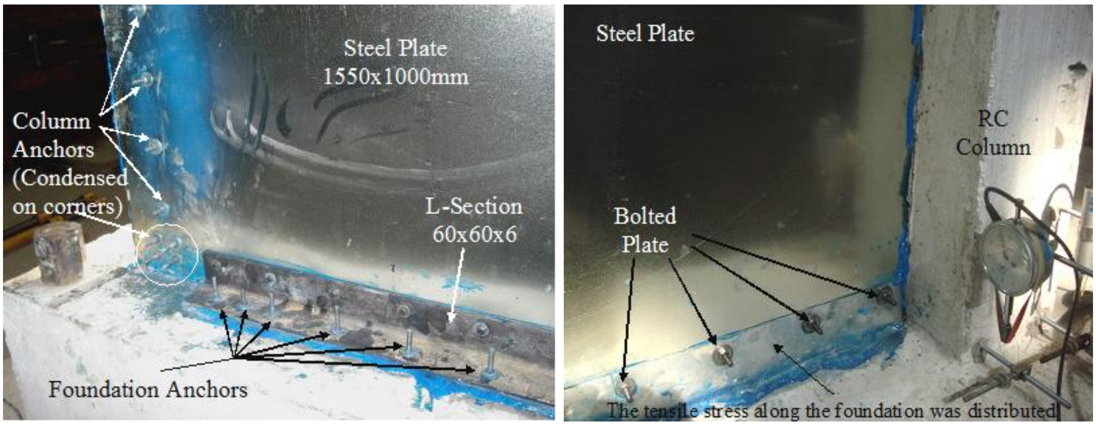

Front View *Back View*

Figure 2.27 *Foundation connections, L-section and connecting bolts*

Figure 2.28 *SP4 Specimen after retrofitting process was finished*

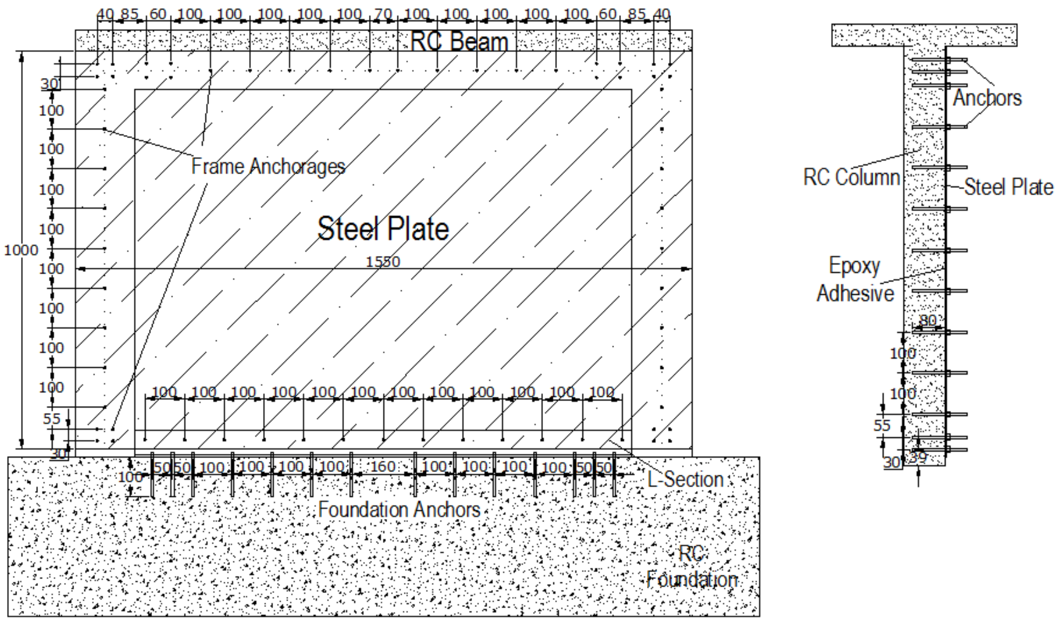

Figure 2.29 *Dimensions of SP3 Specimen (all units in mm)*

2.5.3 SP4: External Structural RC Wall Retrofit

Among today's retrofitting methods, adding RC shear walls are the most preferred alternatives because of its superior performance and established experience. In order to compare its performance with the suggested strengthening methods of this study, RC Shear Wall was integrated to the bare RC frame with anchors on the beam and pre-attached reinforcement dowels in the foundation.

According to TEC (2007), sections with an aspect ratio greater than 7 are considered as structural walls. Considering the minimum scaled thickness (200 mm/3 ≈ 70 mm), the length of the wall is selected as 500 mm. Following the detailing requirements of TEC2007 for structural walls, reinforcement detailing presented in Figure 2.31 is obtained. The external RC shear wall was connected to the bare RC frame from the beam which was aligned on the vertical centerline of the frame.

The M – Φ response of the wall section for zero axial load is shown in Figure 2.30. Based on the expected ultimate moment capacity of the wall, the lateral strength of the specimen with the added structural wall is computed based on Figure 2.31.

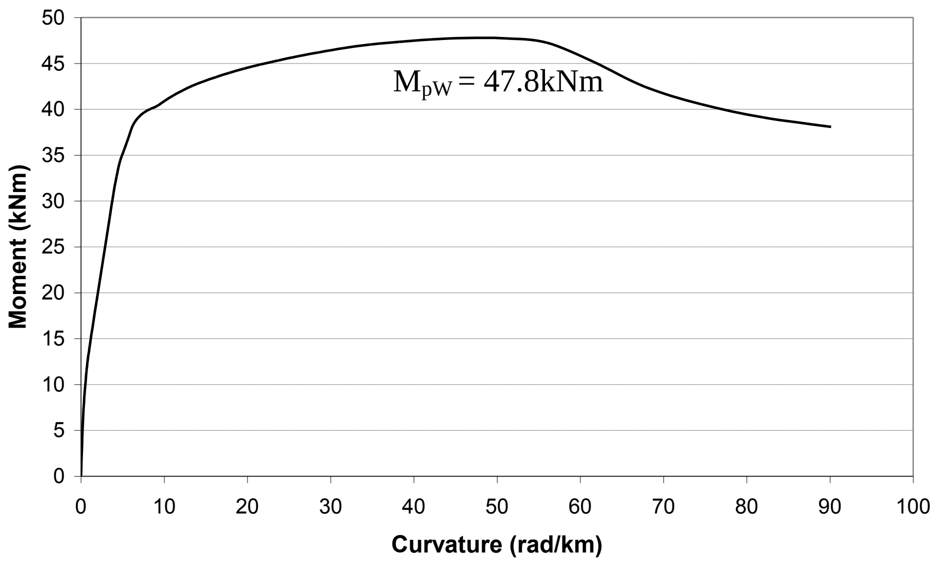

Figure 2.30 *Moment-Curvature relationship of the RC wall (SP4)*

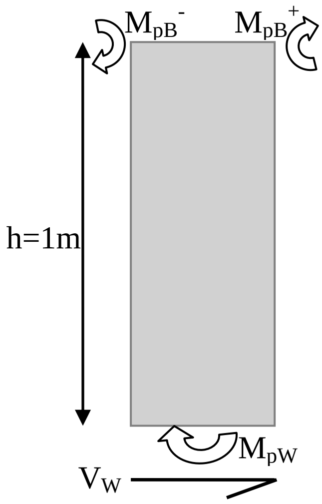

$$V_w = \frac{M_{pW} + M_{pB}^{+} + M_{pB}^{-}}{h}$$

$$V_w = \frac{47.8 + 5.4 + 4.8}{1}$$

$$V_w = 58kN$$

$$V = V_{br} + V_w$$

$$V = 21.6 + 58 = 79.6kN$$

where; V_w is the base shear capacity and
M_{pW} is the plastic moment capacity of RC wall section.

Figure 2.31 *SP4, RC wall plastic mechanism*

Firstly, the anchorage locations were defined on the bare specimen. The foundation anchors consisted of 8 mm diameter reinforcements arranged such that they are lapped with the longitudinal reinforcements of the RC shear wall. The diameter of the holes drilled for foundation anchors was 10 mm. The beam anchorage holes were the same as the previous tests which were drilled with the foundation anchorage holes. After they were cleaned up, the anchor rods for the beam (total of 20 anchors) and the reinforcements for the foundation were attached to the bare specimen with the same procedure explained before.

Concrete for External RC Shear Wall was cast in-place by means of a timber formwork. First, the half of the front face of the wooden formwork left open (Figure 2.32). After the concrete was cast for the first half of the wall, the upper cover of the formwork was closed with a little opening on top so that the concrete was to be placed for the second half of the wall. The compressive strength of the concrete at the testing day was 50 MPa. SP4 specimen details and picture of the retrofitted frame are demonstrated in Figure 2.33 and Figure 2.34, respectively.

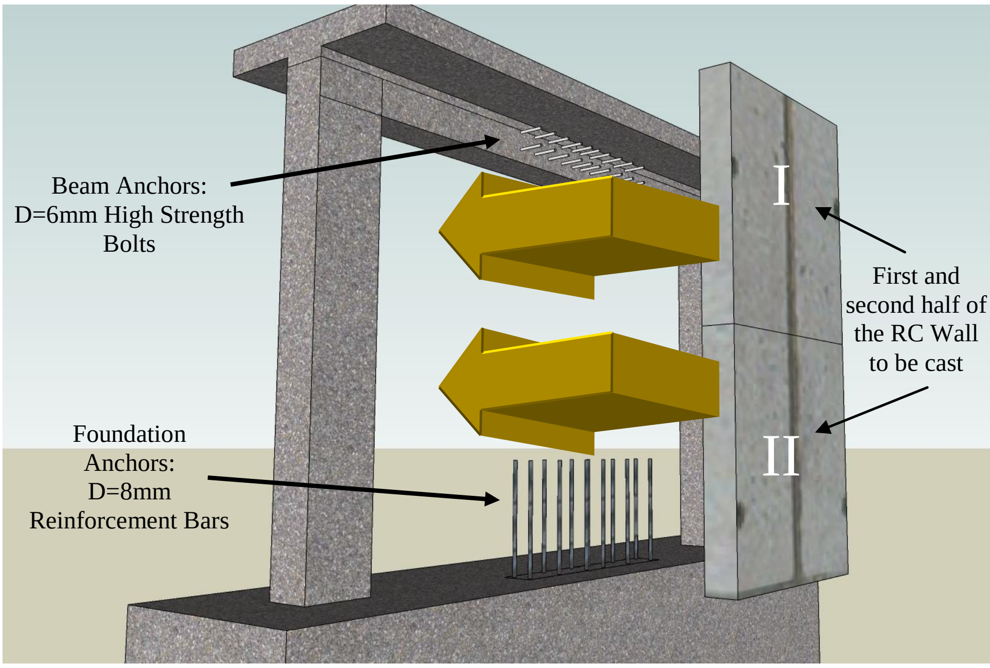

Figure 2.32 *3D Illustration: Integration of ex. RC wall to the bare RC frame*

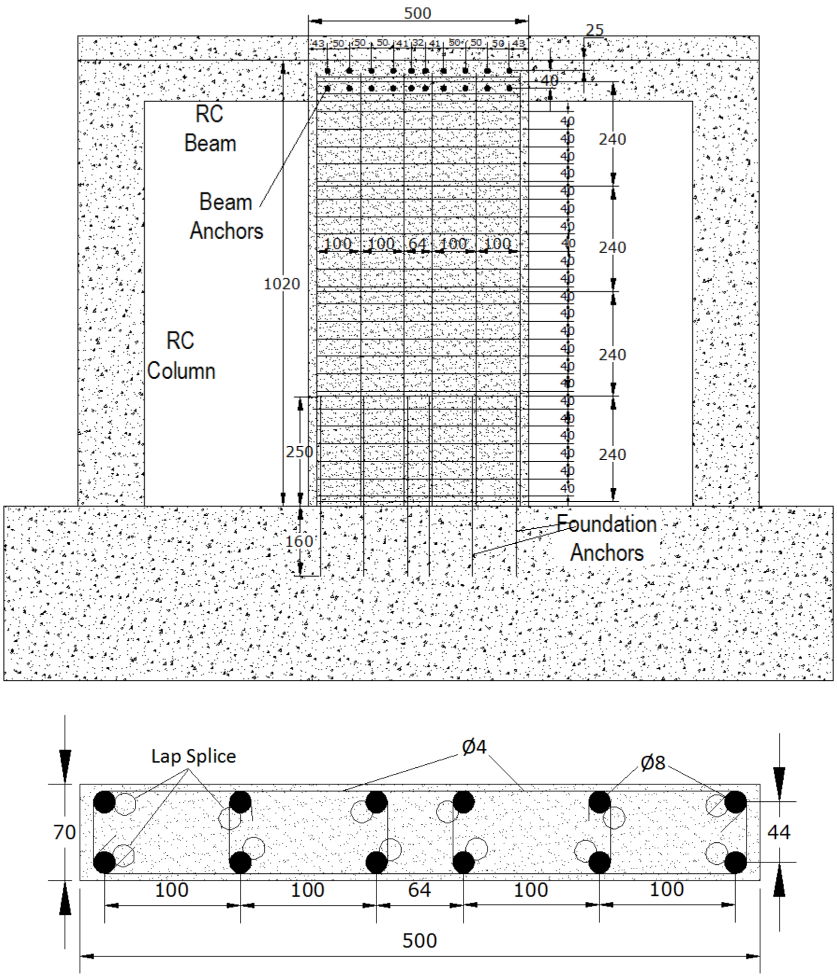

Figure 2.33 *Dimensions of SP4 Specimen (all units in mm)*

Figure 2.34 *Specimen SP4: External connected RC wall*

2.5.4 SP5: External Steel Frame Retrofit (Post-Tensioned Connections)

One of the reasons of the failure modes specified in the test results of SP2 specimen was the anchor failures at base plates that were used to attach column ends to RC foundation as will be explained in the next chapter. In order to achieve the expected plastic mechanism in the external steel frame, a new test specimen with a new foundation connection method and an innovative frame anchoring system was tested. To decrease the number of anchors used for integration of the steel frame, post-tensioned anchoring method was used in this specimen. In SP2 test, specimen was strengthened with a steel frame which was integrated to the bare RC frame in three parts (two columns and a beam). After attaching base plates into the foundation, columns were connected through pre-anchored connection bolts. Last operation was welding of those individual members; beam to column and columns to base plates. L-sections were provided on the beam-column connections to fortify the steel joints because the part of the relevant section that was left on the face of the RC frame could not be welded. (i.e. the face of steel frame that was in touch with RC frame). In order to overcome this issue, instead of integrating steel members one-by-one, steel frame was constructed first. In other words, steel members were welded and that steel frame was produced outside before it was integrated to the RC bare frame. An I-beam was used in order to attach the beam to foundation. Moreover, an I-section was employed to obtain the sufficient force transfer from the specimen to the foundation. The installation process of the foundation beam is presented in Figure 2.35.

Figure 2.35 *I-200 foundation beam during installation*

SP5 specimen also differs from the SP2 specimen with its frame anchoring technique. In order to decrease the number of bolts that were employed to connect the steel members to RC frame, post-tensioned anchoring method was developed. For this implementation, instead of using 6mm diameter anchorage bolts, 12mm bolts were employed. Post-tensioned bolts were used such that those anchors would compress the steel members to RC frame so that the lateral force needed to be transferred shall be carried by the friction force on the surface between steel and concrete. The post-tension anchor holes are presented in Figure 2.36.

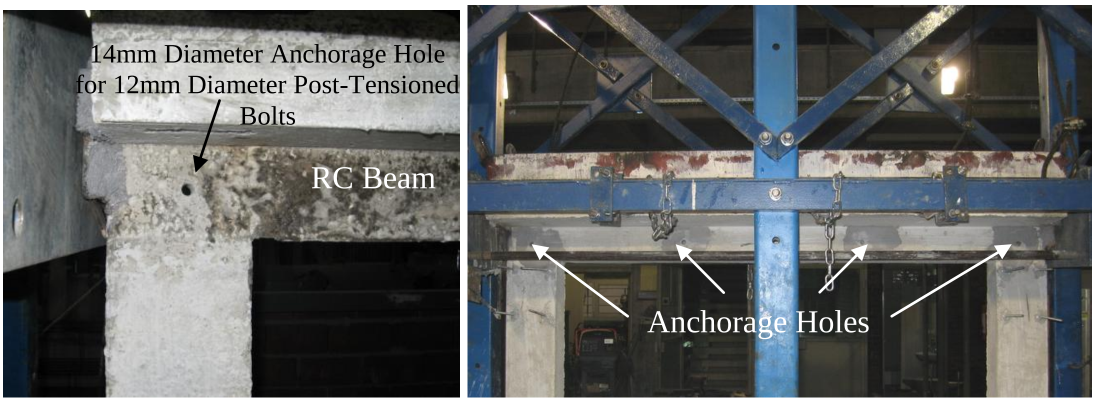

Front View, Joint *Back View*

Figure 2.36 *Connection regions after drilling*

Assuming:

concrete compressive strength f_c=7MPa at the time of installation and concrete shear strength τ_c= 2MPa;

Maximum compression load capacity(N_{max}) on 70x80mm concrete area (A_c):

$$N_{max}=0.85\times f_c\times A_c$$

$$N_{max}=0.85\times 7\times(70\times 80)=33320N$$

Maximum shear force capacity (F_{SCmax}) on 70x80mm concrete area:

$$F_{sCmax}=\tau_c\times A_c$$

$$F_{sCmax}=2\times(70\times 80)=11200N$$

Maximum force could be transferred by friction (F_{sfmax}) with 70x80mm contact area: (coefficient of friction between steel and concrete: μ_c=0.45)

$$F_{sfmax}=N_{max}\times\mu_c$$

$$F_{sfmax}=33320\times 0.45=14994N$$

$$F_{s\ max}=\min\left\{F_{sc\ max}\ ,\ F_{sf\ max}\right\}$$

$$F_{s\ max}=F_{sc\ max}=11200N=11.2kN$$

Four bolts were enough to generate the lateral friction which transfers lateral force to steel frame.

Total transferred force by friction:

$$F_s=4\times 11.2=44.8kN$$

The bolts needed to be tensioned so that the force on the connection (contact) area was <u>33.2 kN</u> and the tension stress on the bolts (σ_b) was;

$$\sigma_b=\frac{33320}{\pi\frac{d^2}{4}}=294MPa\quad<\quad 600Mpa$$

The bolts had to be tensioned by 33.3 kN which was assured by pre-calibrated torque wrench. In order to generate the calculated tension force on the bolts, they were given a torque of 104 Nm (Figure 2.37).

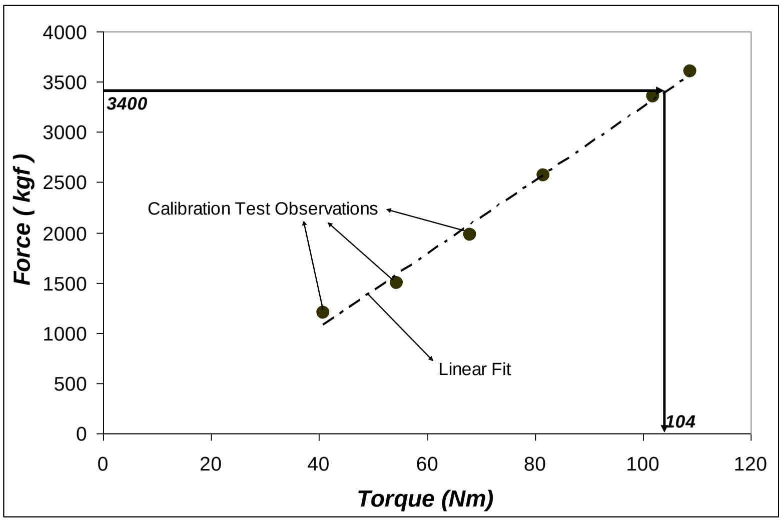

Figure 2.37 *Verification data of torque wrench*

The connection zones of the steel members also needed to be strengthened in order not to bend the sections once the bolts were tightened up and tensioned. Steel plates were provided on the column top ends, they were also strengthened by steel sections (stiffeners) that were welded inside (Figure 2.38).

On both faces of the beam, steel plates were also provided to transfer the stresses to the concrete as uniformly as possible. After the steel column bottom ends were welded to the foundation beam, the bolts were tightened up to the required torque level (104 Nm). Figures 2.38 and 2.39 show the manufacturing of steel elements. The specimen dimensions and a picture from the test setup prior to test SP5 specimen are demonstrated in Figure 2.40.

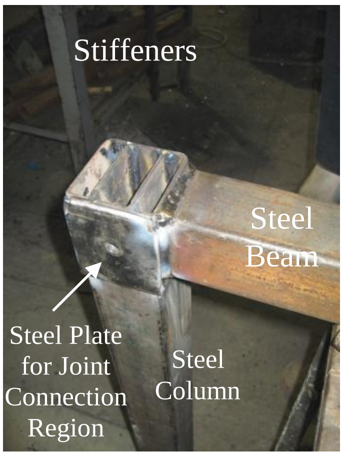

Figure 2.38
Steel Frame was being constructed before integration, steel members

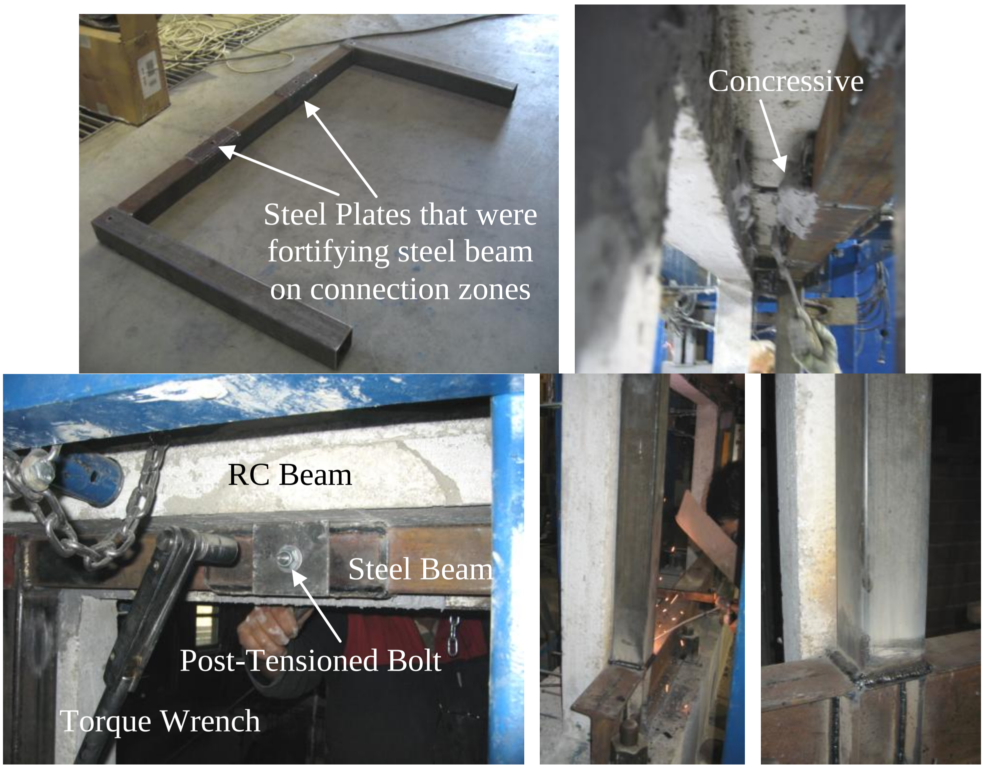

Figure 2.39 *Constructed steel frame, post-tensioning operation and welding of column bases to the foundation beam*

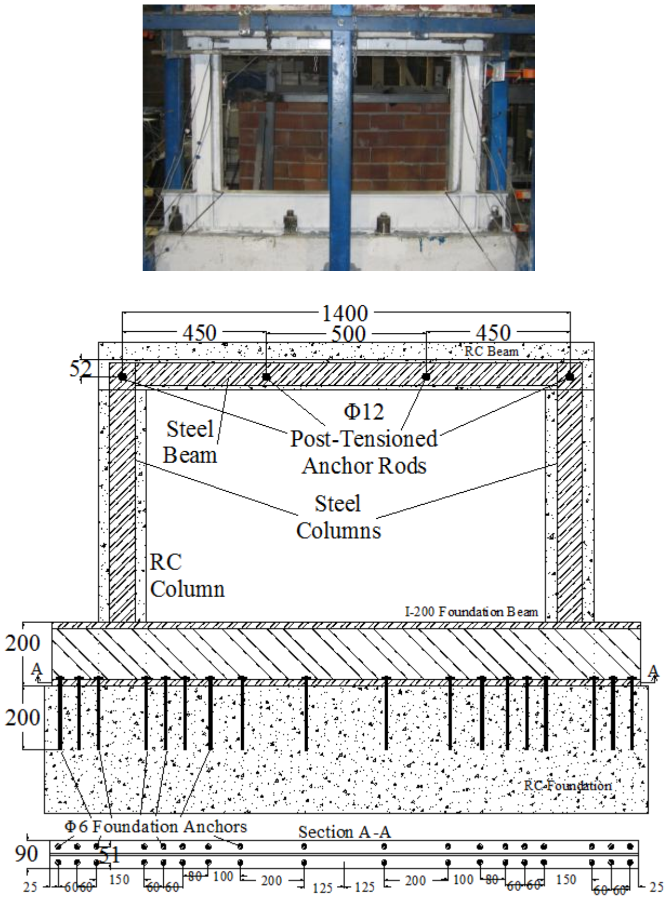

Figure 2.40 *SP5 Specimen and details*

Chapter 3

Test Results and Behavior of Specimens

The test results of the specimens are presented in this chapter. The reversed cyclic displacement controlled load-displacement history was continuously monitored and specimen behavior was observed. In addition, RC frame plastic hinging pattern was also obtained from the measured curvatures. The yielding was defined as the point at which calculated curvatures exceeded the estimated yield curvature values of the sections.

While making comments on the test specimens, the right column refers to the column that was on the reaction wall side whereas; left column refers to the column on the opposite side. For the loading directions, positive direction refers to the displacement excursions away from the reaction wall, and negative displacements are those towards the reaction wall (Figure 3.1). The base shear is equal to the lateral load measured from the load cell.

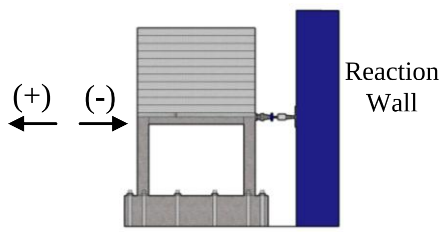

Figure 3.1 *Reference directions*

Initial stiffness of the specimens was defined as the slope of the load-deflection curve at the very first cycle of the test (0.5% D.R.) in both positive and negative directions. The initial stiffness and displacement ductility estimation is represented in Figure 3.2. Interstory drift ratio - which is given in percentages - refers to the ratio of the displacement of the story level (gross centre of the beam) to the height of the effective column length.

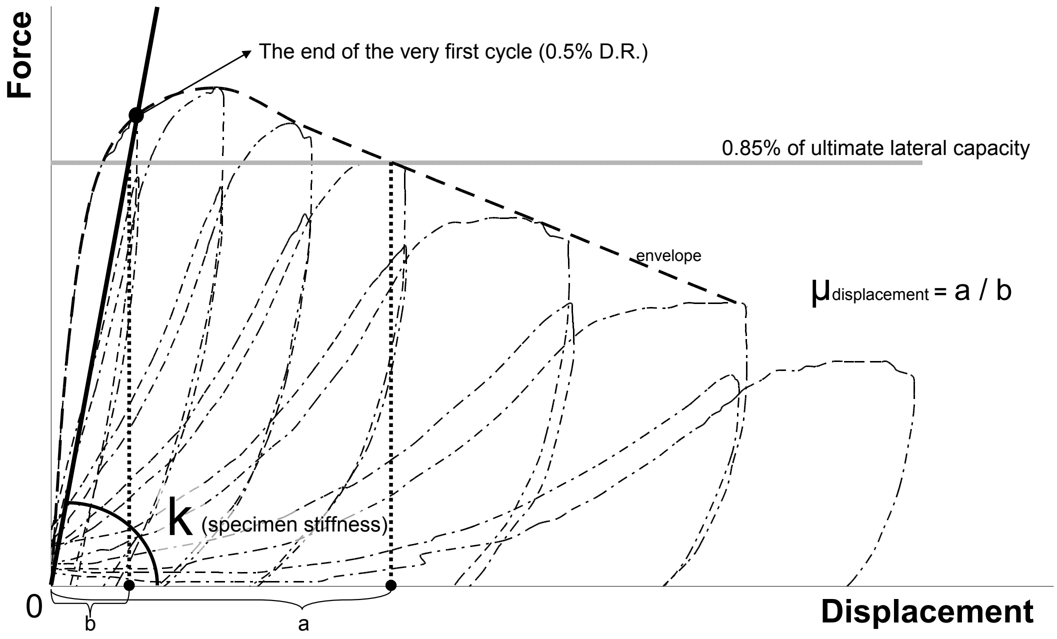

Figure 3.2 *Graphical estimation of initial stiffness and displacement ductility*

In the summary of results table the key properties obtained from the recorded test data of the specimens are presented (Table 3.1). The quantitative values include lateral capacity, lateral rigidity, energy dissipation capacity, ductility and failure modes. Interstory drift ratio at failure is also presented in order to specify a performance (or drift) limit for the tested specimens. The drift ratio that the lateral capacity degraded under 85% of the ultimate capacity was considered while noting the failure modes.

Table 3.1 *Summary of Test Results*

Test Specimen	Lateral Capacity (kN)		Lateral Stiffness (kN/mm)		Energy Dissipation (kN.mm) at 15% Cap. Drop	Interstory Drift Ratio at Failure	Failure Mode	Lateral Capacity Ratio retrofitted / bare		Energy Diss. Ratio retrofitted / bare (15% Cap. Drop)	Lat. Stiff. Ratio retrofitted / bare		Disp. Ductility	
	(+) direction	(-) direction	(+) direction	(-) direction				(+) direction	(-) direction		(+) direction	(-) direction	(+)	(-)
SP1	13.7	12.5	2.5	2.4	993	2%	Column Plastic Mechanism	-	-	-	-	-	4.4	4.6
SP2	31.6	34.7	4.7	4.9	6390	4%	Beam-Column Connection Fracture, Base Plate Pull-Out	2.3	2.8	6.4	1.9	2.0	8.6	7.6
SP3	56.9	60.3	9.4	10.5	5637	3%	Foundation Anchor Pull-Out, Plate fracture	4.2	4.8	5.7	3.8	4.3	5.9	7.0
SP4	93.4	79.5	13.6	12.7	10520	3%	Foundation Pull-Out	6.8	6.4	10.6	5.4	5.2	6.6	7.1
SP5	60.0	59.0	6.6	6.6	11493	3%	Connection Fracture	4.4	4.7	11.6	2.6	2.7	4.4	3.7

3.1 SP1: The Bare Frame

SP1 specimen, which was the reference bare frame, exhibited poor lateral strength and energy dissipation capacity as expected. Significant pinching effect and the lateral stiffness loss with increasing displacement excursions was observed. Base shear ratio (Lateral Force / Weight) was about 0.2 indicating insufficient lateral strength. First column hinging was observed at bottom of the columns followed by the hinging of column tops which describes the plastic story mechanism. The lateral load carrying capacity was 13.7kN and the lateral stiffness was 2.5kN/mm at the very first cycle. In the cycles after 1.5% drift ratio, the lateral load capacity decreased lower than 85% of ultimate. It had a displacement ductility of about 4.5. The cyclic curve of the bare frame is presented in Figure 3.3 and pictures related with the plastic mechanism are demonstrated in Figure 3.4.

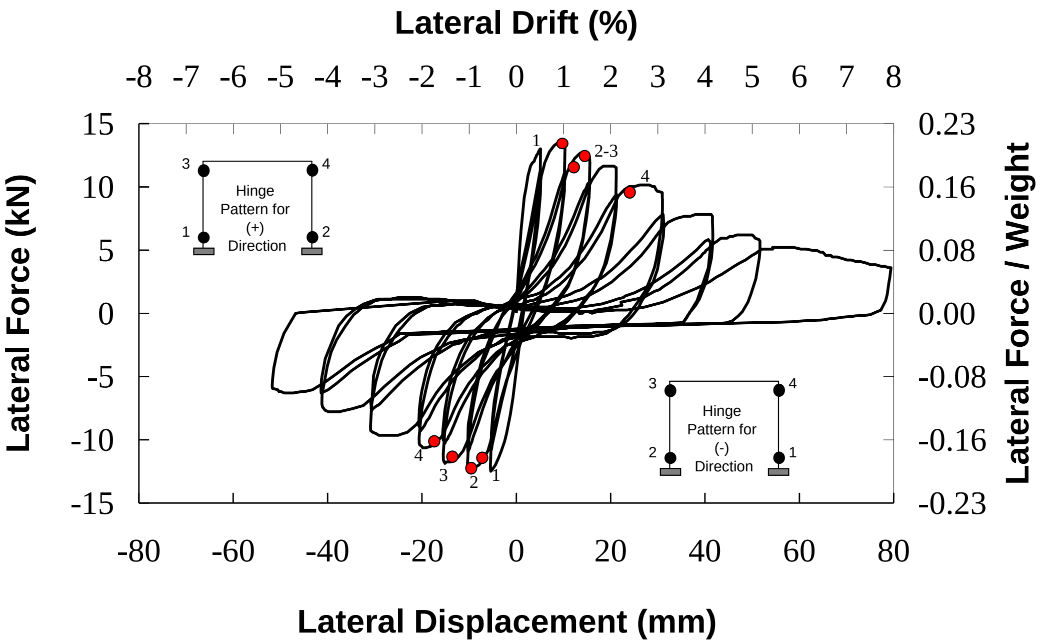

Figure 3.3 *Hysteretic load-displacement response of SP1 Specimen*

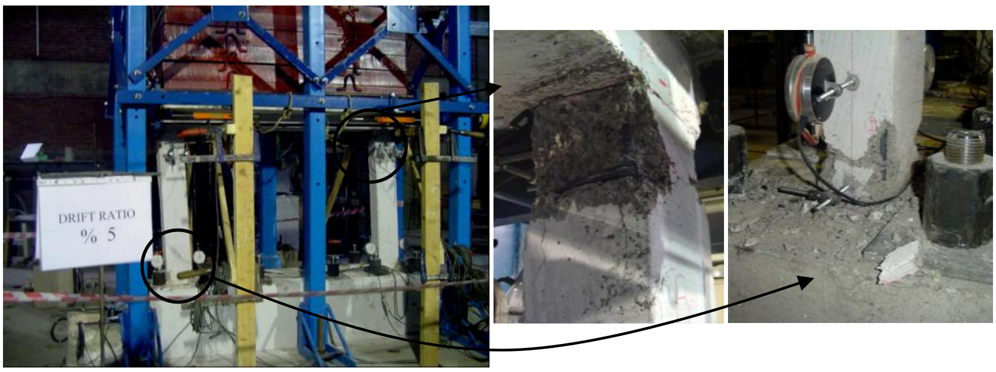

Figure 3.4 *SP1 Specimen in 5% drift ratio*

3.2 SP2: External Connected Steel Frame

SP2 specimen had a lateral load carrying capacity and stiffness of about 2 times the bare frame. The ultimate lateral load was about 35kN which was observed in the negative loading direction. Stiffness of the system was estimated around 4.8kN/mm. The first observed damages were on the column plastic hinge zones similar to that of observed in SP1. All plastic hinges formed at about 3% drift ratio. The decrease in the lateral load capacity first occurred at 4% drift ratio in positive direction and 3% drift ratio in negative loading direction. The estimated displacement ductility was 8.6 and 7.6 for positive and negative loading cycles respectively. Cyclic curve of the specimen and the damages in the RC columns are presented in Figure 3.5 and Figure 3.6, respectively. For the final failure, foundation anchors pulled out that avoided the plastic hinging of the steel column bases and caused a premature failure. Hence expected lateral strength could not be obtained.

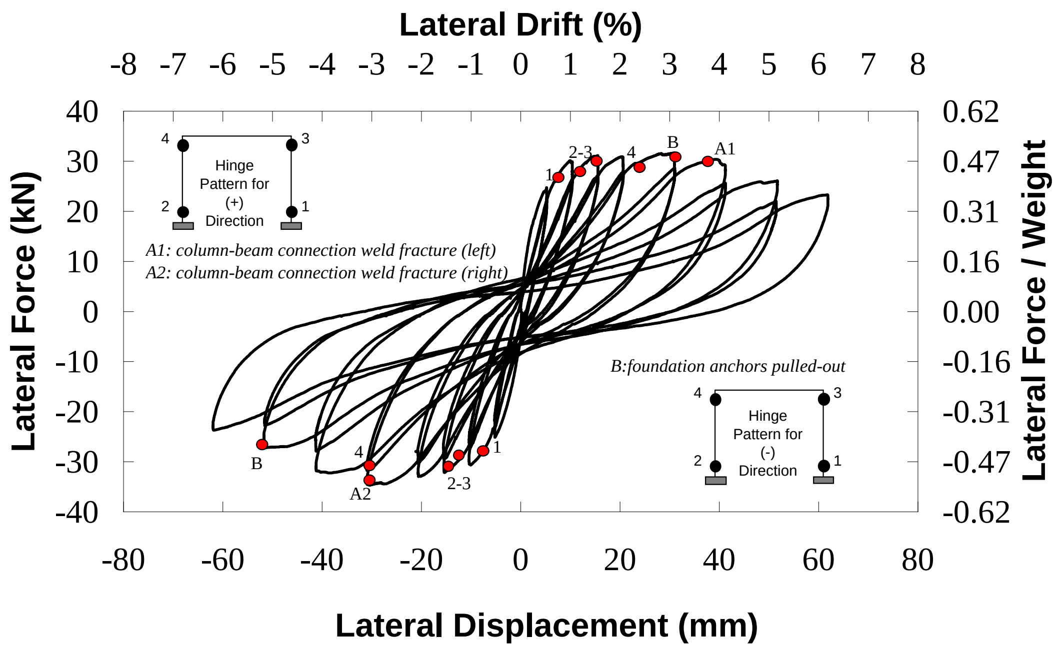

Figure 3.5 *Hysteretic load-displacement response of SP2 Specimen*

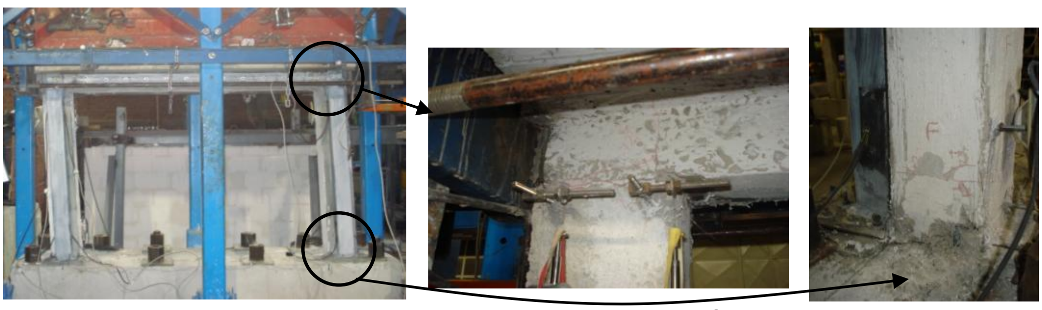

Figure 3.6 *SP2 Specimen in 5% drift ratio*

Cracking of the base plate foundation was the first critical observed damage on the external steel frame, SP2 (Figure 3.7). It was initiated at 3% drift ratio beyond which the further excursions caused significant damage in the foundation. Premature failure of the base plate connection resulted in a smaller lateral load carrying capacity than expected. However this issue led the system to exhibit rocking displacements resulting in sustaining high displacement ductility (8.6). Fracture initiated at beam column connections at 3% drift ratio (Figure 3.8). Both separations of the base-plates and cracking of steel beam on the welding points due to high drift demands caused the lateral strength degrade after 3% drift ratio. The steel column members did not reach their plastic capacity verified with the strain gage readings. Those readings taken from critical zone of the steel column are presented in Figure 3.9. The damages in the RC column were demonstrated in Figure 3.10.

Figure 3.7
Cracking of concrete under base-plates, SP2, 3% D.R.

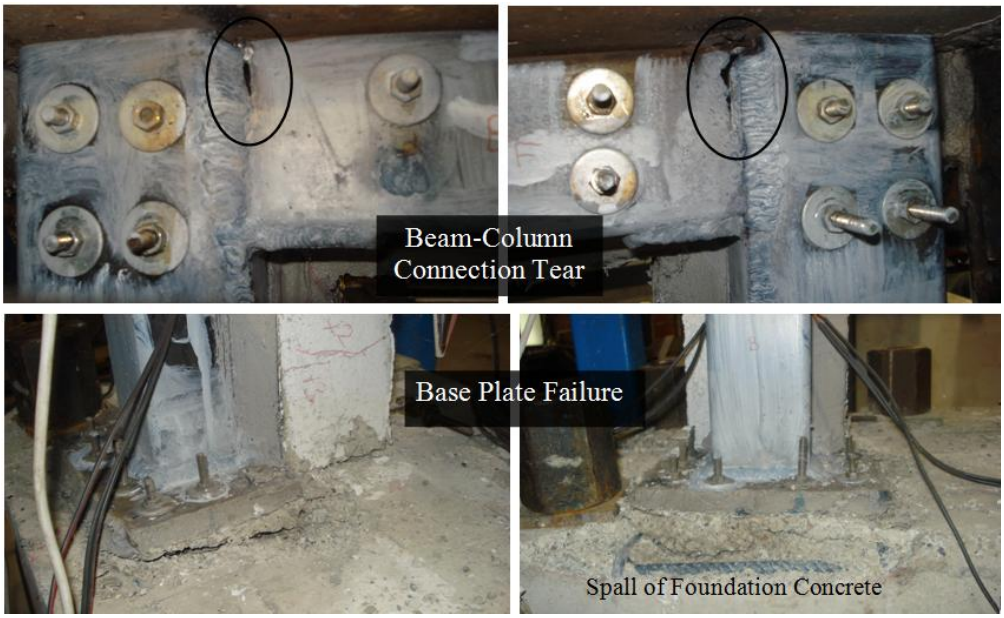

Figure 3.8 *Members of SP2 Specimen, 5%D.R (Failure Modes)*

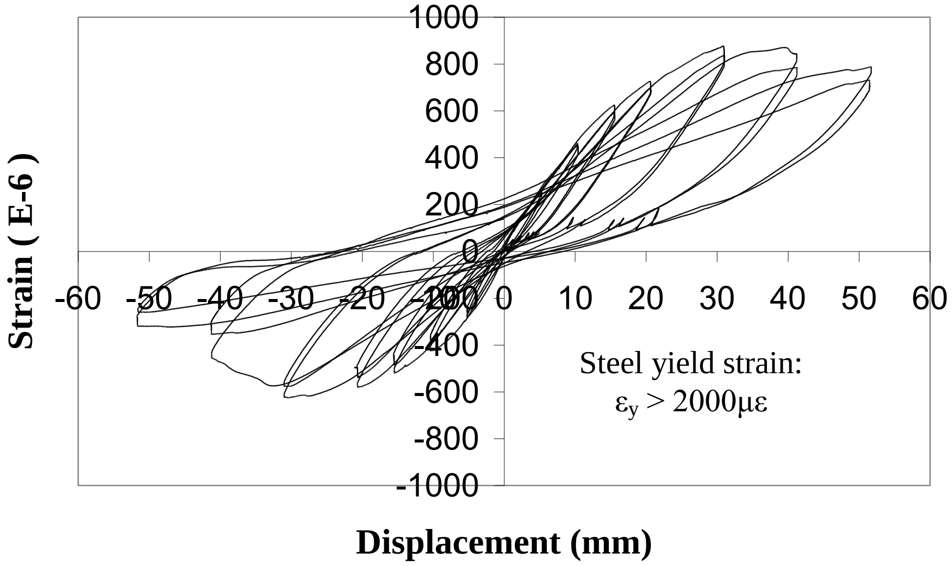

Figure 3.9 *Strain gage readings (SP2, bottom of right steel column)*

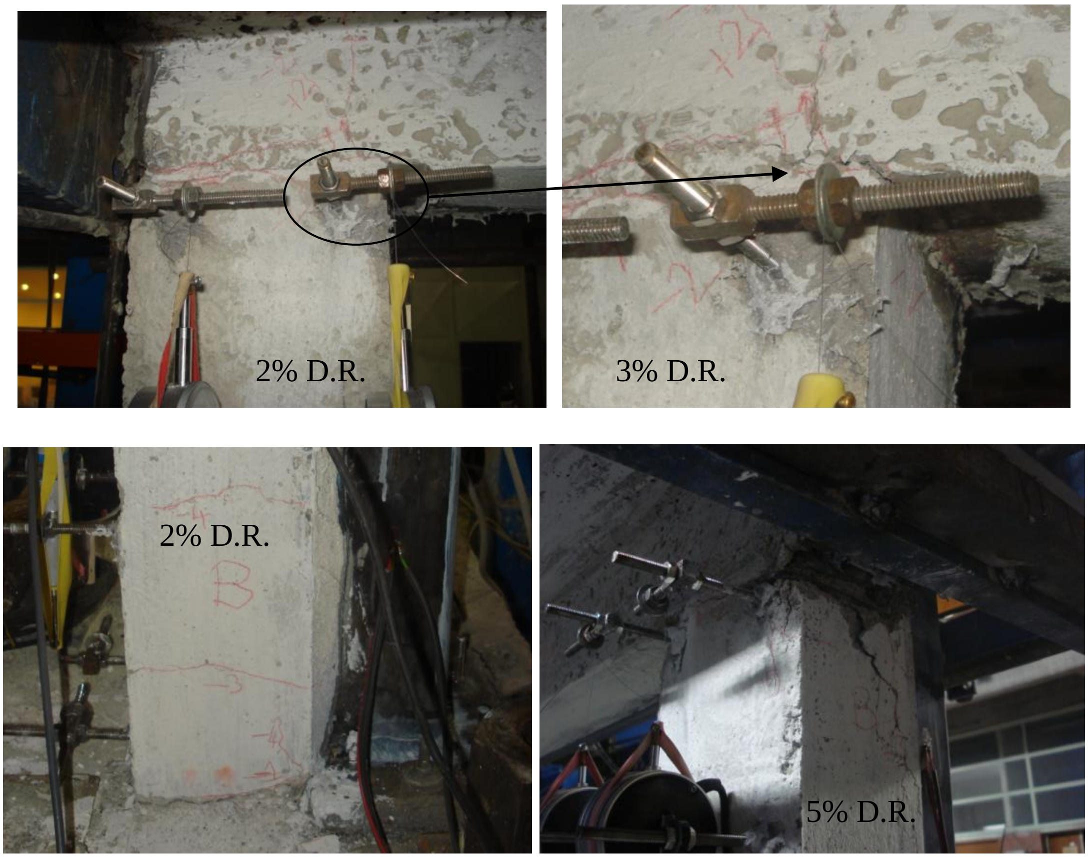

Figure 3.10 *Damage in SP2 Specimen RC columns*

3.3 SP3: External Connected Steel Plate

SP3 specimen exhibited load carrying capacity and stiffness about four times the bare frame specimen, SP1. The maximum load recorded from the load cell was 60kN that was in the negative loading cycle. The stiffness of the system was about 10kN/mm. The displacement ductility was 5.9 and 7.0 for positive and negative loading cycles, respectively. In the cyclic response (Figure 3.11), it can be inspected visually that the system was subjected to severe pinching of the load-deformation curve. The initial damage in the specimen was at the bottom column ends similar to SP1 whereas there was no hinging at the top of the columns (Figure 3.12). Plastic hinges occurred starting from 1% drift ratio. The decrease in the lateral load capacity occurred at 2% drift ratio. Failure occurred as a result of combined plate fracture and foundation uplift at L-section connection.

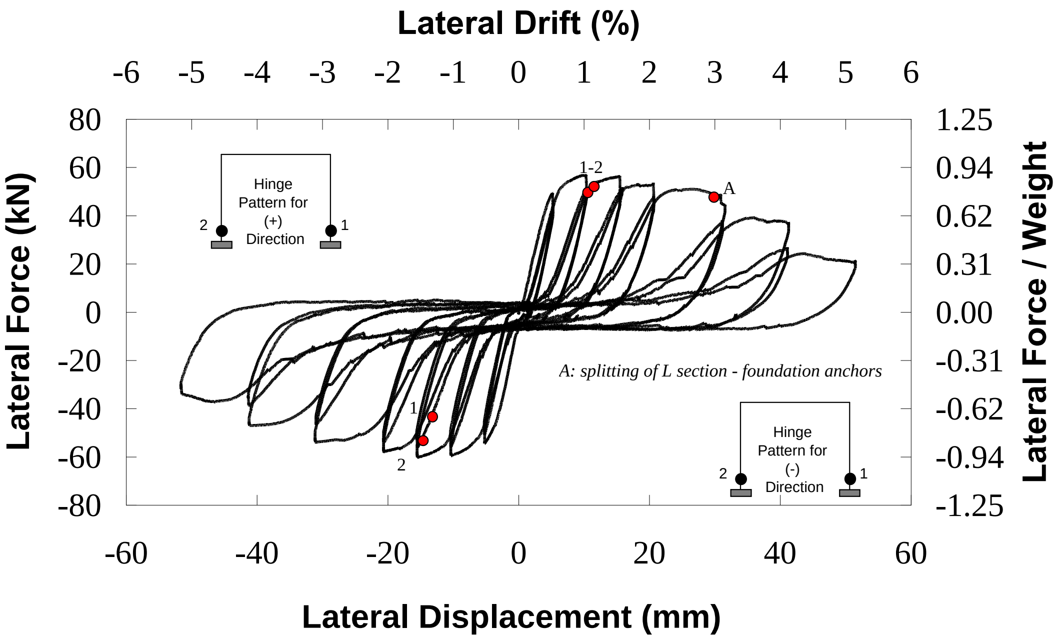

Figure 3.11 *Hysteretic load-displacement response of SP3 Specimen*

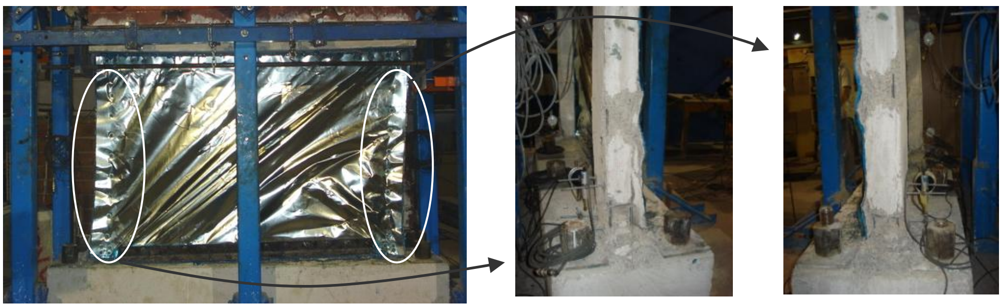

Figure 3.12 *SP3 Specimen in 5% drift ratio*

The lateral strength enhancement in SP3 was mainly provided by means of the tension-field action (Figure 3.13) of the steel plate in the loading stage of cycles. During a typical loading cycle, the compression zone immediately buckled and strength was provided in the tension field diagonal. Once the displacement excursion direction was reversed, the buckled zone recovered and became tension zone. The reason of the pinching behavior in SP3 (like as SP1) was the buckle-recover-tension field response of the steel plate. In other words, recovery from post-buckled shape (Figure 3.14) while forming the tension field caused pinching of the load-deformation response. It should be noted that all the reversed displacement excursions resulted in a high volume audible sound. The plastic hinges did not form on the top of the RC columns for SP3, although they formed at 1.5% drift ratio on the column bases. Discrete anchor connections on the columns caused formation of plastic hinges at 4% D.R. near the middle of columns as can be observed in Figure 3.15. Since the boundary elements (especially RC columns) of SPSW were not rigid enough to provide full fixity for the steel plate, the system did not reach its full design plastic capacity. The failure in SP3 occurred with the local tearing of plate and splitting of anchorages in the L-section that establishes the connection between plate and foundation (Figure 3.16). In Figure 3.17 the damages in the RC column are shown for 1.5% and 4% D.R. and in Figure 3.18 the shape of the steel plate is demonstrated for every 1% D.R. increment during loading cycle of 5% D.R.

Figure 3.13
Tension field action for SP3
(5% D.R.)

Figure 3.14
Post-buckled shape of SP3
(unloading cycle, 5% D.R.)

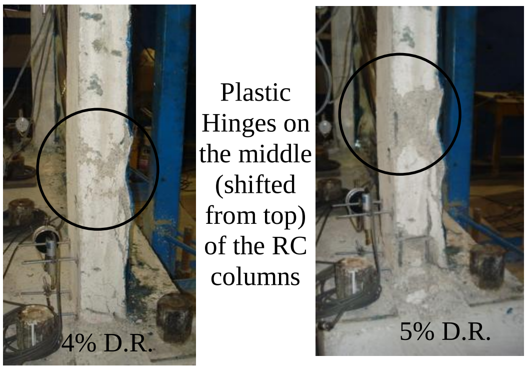

Figure 3.15 *Plastic hinges on RC columns of SP3*

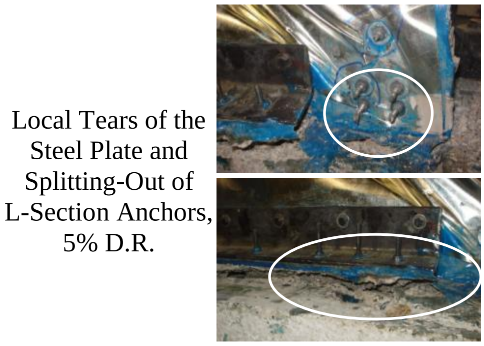

Figure 3.16 *Local failures, SP3*

Figure 3.17 *Damage in SP3 Specimen RC columns*

Figure 3.18 *SP3 Specimen in the loading cycle of 5% D.R. with 1% D.R. increments*

3.4 SP4: External Connected RC Wall

SP4 specimen had a lateral load capacity and stiffness slightly more than 6.5 times of the bare frame. The maximum load recorded was 93.4 kN in the positive loading direction. The stiffness of the system was about 13kN/mm. The estimated displacement ductility was about 7.0. Despite all of the plastic hinges were observed at 2% drift ratio, the decrease in the lateral load capacity was first observed at about 3% drift ratio as it can be seen in specimen's cyclic response (Figure 3.19). Nevertheless, there was not vital damage on the RC columns even at high drift demands (Figure 3.20). Strength of the test frame decreased as a result of pull-out of the foundation anchors resulting in foundation splitting.

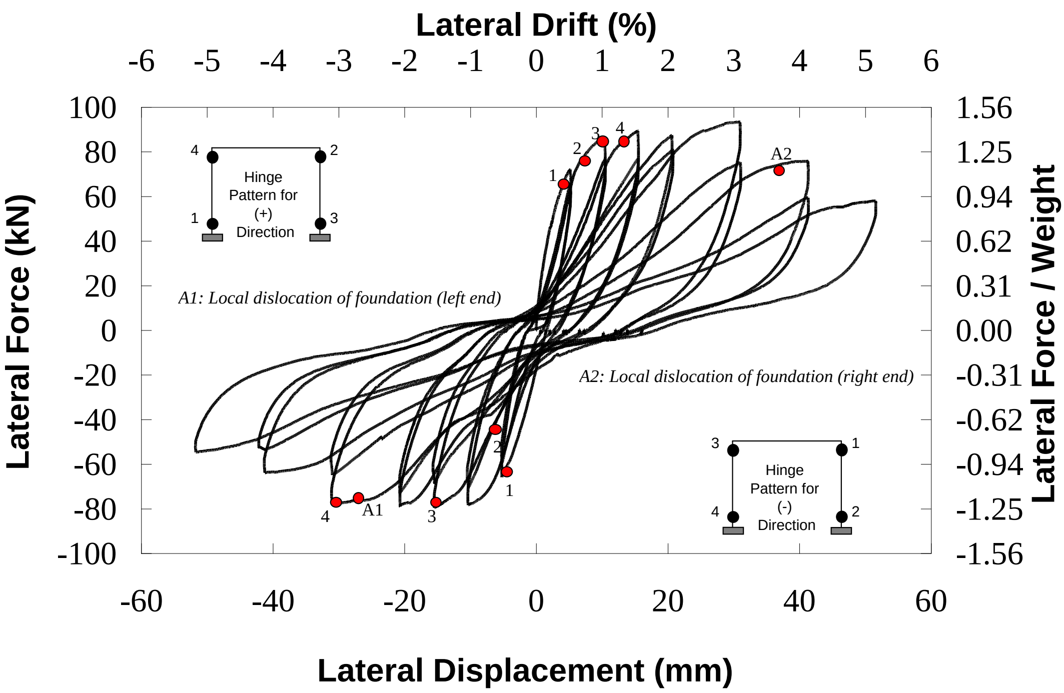

Figure 3.19 *Hysteretic load-displacement response of SP4 Specimen*

Figure 3.20 *SP4 Specimen in 5% drift ratio*

The damages in the SP4 specimen observed firstly on the wall with some bending cracks at 1% drift ratio. However those cracks did not become wider in further drift demands. With the increasing cyclic excursions, the cover concrete spalled of on the bottom face of the beam along the wall-beam connection and the shear reinforcements of the beam were pushed out (Figure 3.21). In addition, bending cracks were observed on the RC beam due to the moment transfer from post-installed wall to RC beam (Figure 3.22). After 3% drift ratio, the decrease in the capacity was due to extensive damage and pull-out failure of the foundation anchors as it is demonstrated in Figure 3.23.

Figure 3.21 *RC Beam stirrups forced out of the beam, SP4*

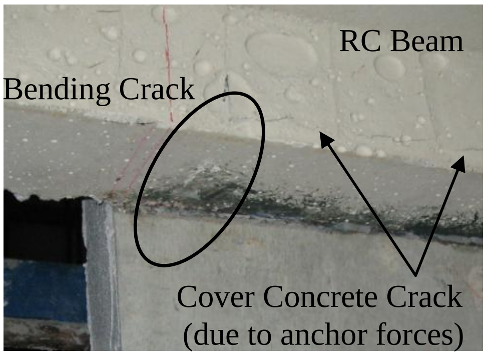

Figure 3.22 *Some cracks along the RC beam, SP4 (1.5% D.R.)*

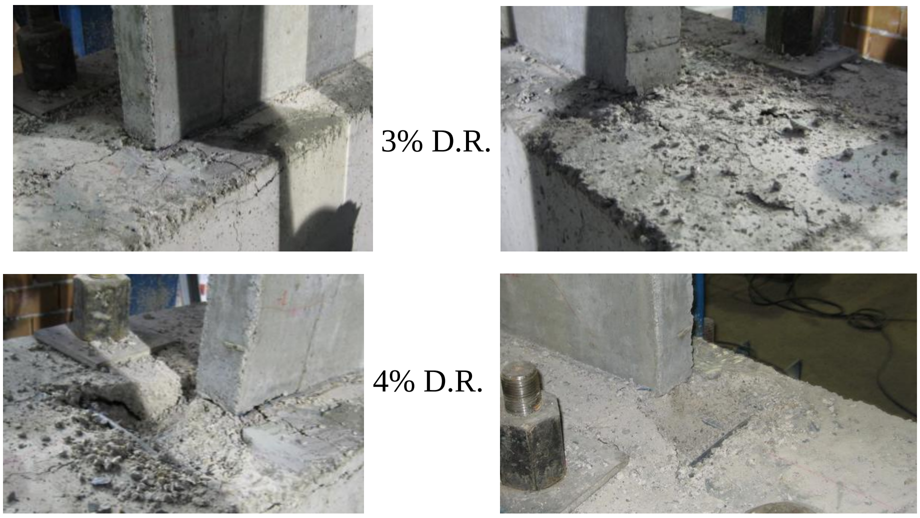

Figure 3.23 *Existing RC foundation, SP4*

3.5 SP5: External Connected Steel Frame with Post-Tensioned Anchors

SP5 specimen had about four times the lateral capacity of the bare frame. The recorded maximum load was in positive direction with 60kN. The estimated stiffness was 6.6kN/mm which was about 2.5 times greater than that of the reference frame. The decrease in the lateral capacity initiated after 3% drift ratio in positive direction and after 2% drift ratio in negative direction as it can be observed in the cyclic response of the specimen (Figure 3.24). Calculated displacement ductility was 4.4 for positive direction which seems to be similar to that of the bare frame. The damages in the RC columns were similar to that of bare frame had (Figure 3.25). The failure was due to the fractures at the welded regions of the steel sections.

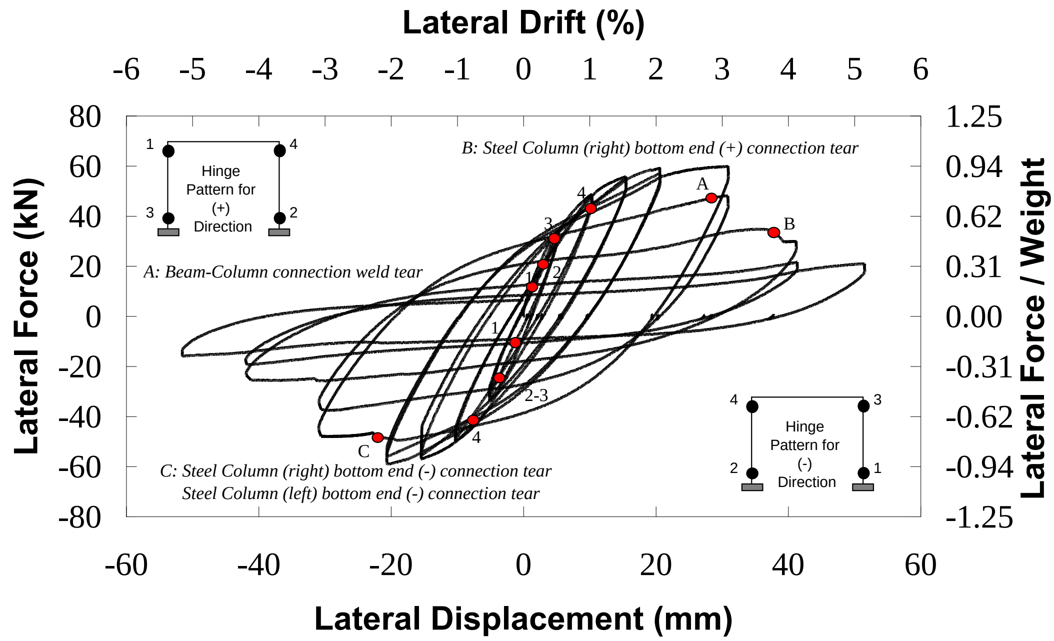

Figure 3.24 *Hysteretic load-displacement response of SP5 Specimen*

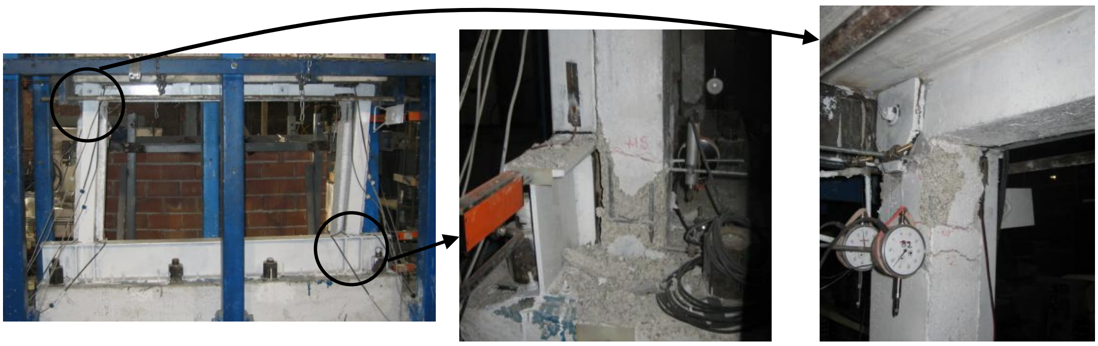

Figure 3.25 *SP5 Specimen in 5% drift ratio*

In the first cycles of SP5 specimen, there were cracks observed on the RC beam in the direction of the post-tensioned anchors (Figure 3.26). Fortunately, those cracks did not get wider in further excursions. At 3% drift ratio, the RC joints experienced some cracking due to the post-tensioned post - tensioned anchors. During the loading to the negative direction in the cycle of 3% drift ratio, just prior to the end of the excursions, there was a local failure observed on the steel column (right) with an audible sound. The bottom of the column fractured just from the adjoint of the weld and the steel section (Figure 3.27). As it can be visualized from the cyclic response of SP5 specimen, this led the system to loose its lateral capacity in the negative direction during 3% drift ratio. This failure mode was the consequence of the relatively brittle, cold-formed box section that was employed in the system demonstrated in Figure 3.28.

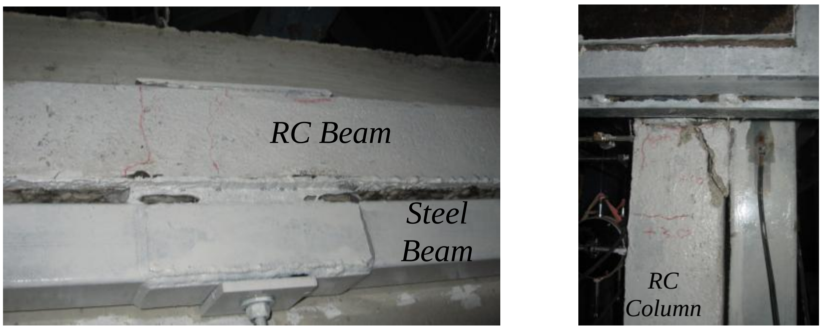

Figure 3.26 *Cracked RC beam and joint due to anchor forces, SP5 (1% D.R.)*

Figure 3.27 *Fracture initiated on the steel column bottom ends, SP5 (3% D.R.)*

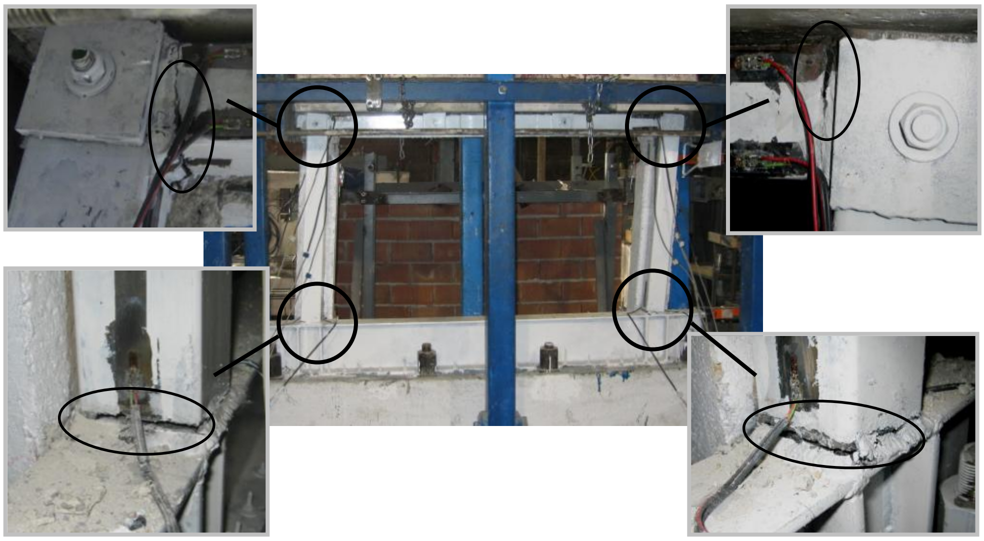

Figure 3.28 *SP5 Specimen in 5% D.R. and the fractures in the steel members on their welding zones*

The strain gage reading from the bottom of the right steel column is demonstrated in Figure 3.29. In that curve strain was plotted against lateral displacement of the specimen that the yield strain of the steel was described over 0.002 (2000E-6 = 2000με). The curve shows the plastic capacity of the steel frame was achieved in 1.5% drift ratio (column was yielded after 12mm lateral displacement) which is consistent with the lateral cyclic response of the system. Furthermore the tearing of the box section could be observed clearly at 4% drift ratio (or after 30mm displacement) which the consistency of the readings was lost afterwards.

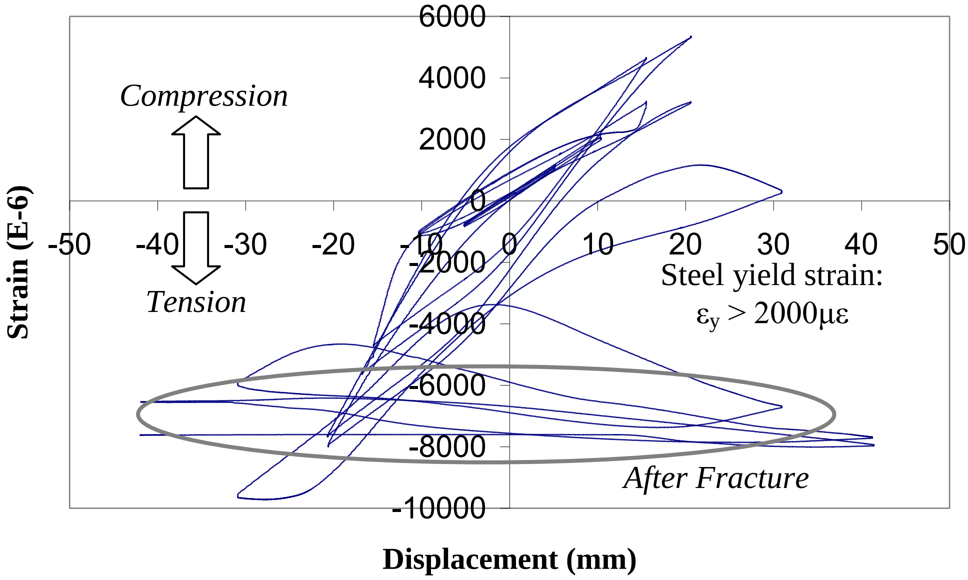

Figure 3.29 *Strain gage readings (SP5, bottom of the right column)*

In Figure 3.30, the RC column damages are demonstrated for SP5 specimen. It can be observed that employing steel I-beam foundation for the external steel frame did not affect the plastic hinge regions of the RC frame.

Figure 3.30 *Damage in SP5 Specimen RC columns*

3.6 Comparative Discussions on the Test Results

In Figure 3.31, the load-deformation envelopes of the cyclic curves of the specimens are presented. On these curves, the 85% of ultimate lateral load capacity line for each specimen is plotted in order to clarify the ductility levels and ultimate lateral load points. It was very clear on those curves that SP2 specimen exhibited the largest displacement ductility. Unlikely, SP5 specimen was contrarily had the lowest displacement ductility although they were strengthened with moment resisting steel frames. The reason explained in previous sections that the capacity of the steel frame could not be achieved in SP2 test. The substantial lateral stiffness enhancement of SP4 specimen was another striking observation that could be seen by visual inspection. It was very surprising that although the specimens SP3 and SP5 had the same lateral capacity and SP5 specimen exhibited the best energy dissipation capacity among the strengthened cases. For the two specimens, SP3 and SP5; the lateral stiffness difference between them was more than 30% besides similar lateral load capacity.

In Figure 3.32, the energy dissipation capacities of the specimens are given up to 4% drift ratio. In order to make an objective comparison among energy dissipation capacities, dissipated energy levels of each specimen at their first 15% lateral capacity drop were marked on the cumulative energy dissipation lines.

Considering the lateral load capacities of specimens, it can be concluded that the energy dissipated by SP5 was more efficient compared to other specimens. Although the lateral load capacity of the post-tensioned anchored system was less than 35% of the SP4 specimen, energy dissipation capacity was greater than that observed in specimen SP4. The increase of the cumulative energy dissipation of the SP5 specimen between 1% and 2% drift ratios can be observed in Figure 3.32. The stiffness of the specimen did not degregade in high drift demands leading the system to exhibit best level of dissipated energy.

Although SP3 specimen consisted of a steel member, the behavior was completely different. Steel plate did not resist any lateral force demand during unloading cycles due to thin plate’s post buckling action. Hence, the energy dissipation efficiency of the steel plate was the worst among the other retrofitted cases. Specimen SP3 had two times more lateral load carrying capacity compared to SP2 although, dissipated energy was less than the one SP2 dissipated at the 15% capacity drop point.

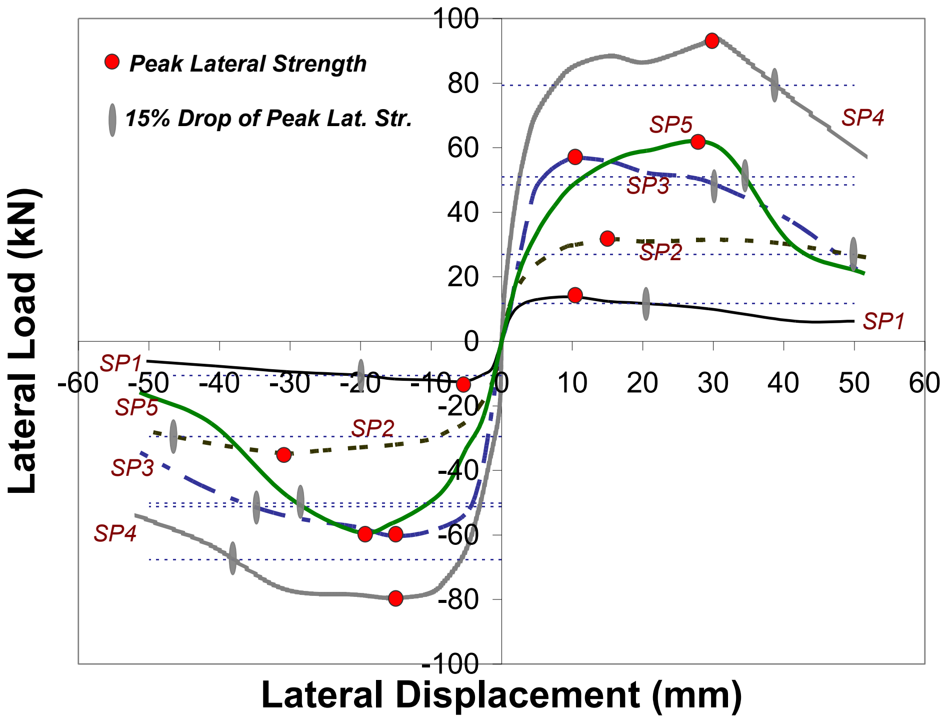

Figure 3.31 *Lateral load - displacement envelopes*

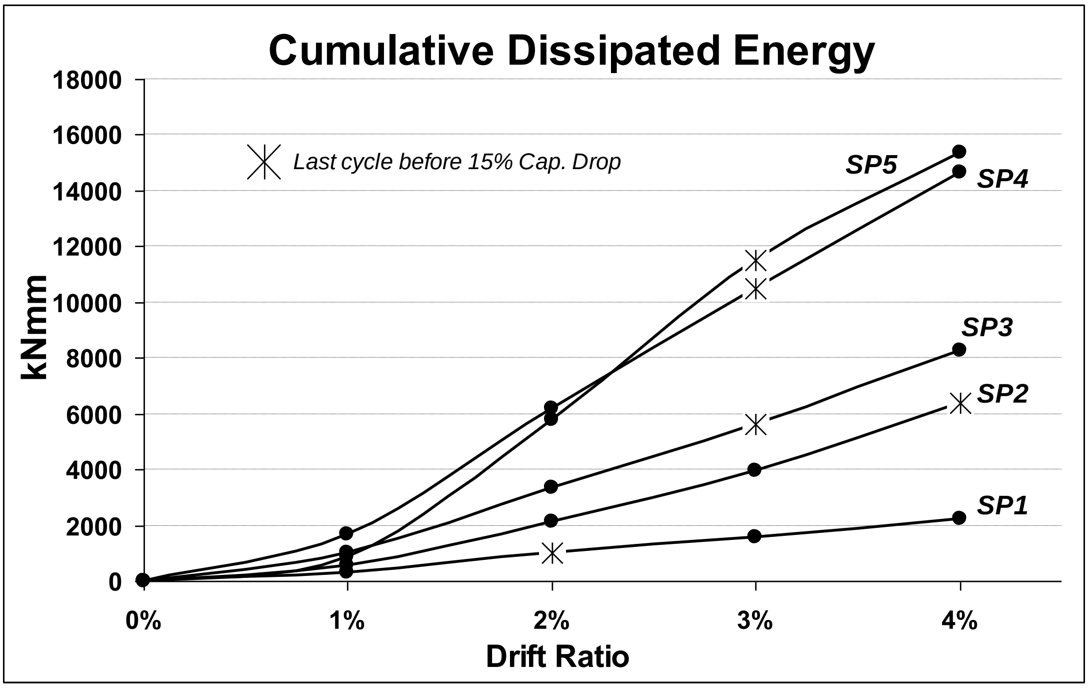

Figure 3.32
Cumulative dissipated energy of tested specimens

The total load carrying capacity of the SPSW system is estimated as 75 kN in the design. Considering bare frame's exact capacity from the test results the total capacity of the system is calculated as:

$$V_{SPSW} = 0.42 \times \sigma_{spy} \times L_{spc} \times t_w \times \sin 2\alpha$$
$$V_{SPSW} = 0.42 \times 340 \times 1250 \times 0.3 \times \sin(70) = 50.3 \text{ kN}$$
$$V = V_{br} + V_{SPSW} = 13.7 + 50.3 = 64 \text{ kN}$$

The angle of the tension field (α) was 45˚ in the very early loading stages. However, it became 35˚ (diagonal strip) after steel plate yielded. In the above capacity estimation it was employed as 35˚.

The difference between the lateral capacity estimation and the test result of the SPSW system may originate from two reasons. The employed expression for shear capacity of the SPSW system assumes that the plate is fully connected to the boundary elements (i.e. welded). However in this case, discrete anchor connections may avoid the complete formation of tension field strips. Furthermore, the plastic moment capacities of the RC columns may be affected due to the axial force alternation causing the bare frame to loose its lateral load carrying capacity rapidly which is also true for all specimens.

For the SP4 specimen, the RC member that was integrated to the RC frame enhances lateral load capacity as it upgrades the energy dissipation with the same ratio. This conclusion certainly can not be generalized for buildings where the number of strengthened bays and redistribution among them can be extremely influential on the expected energy dissipation capacity.

In Table 3.2, the calculated curvatures of the column ends are presented at which the specimens were at the end of the cycle that their load carrying capacity decreased under 85% of the ultimate capacity. Those curvatures are used to determine the plastic rotations at the column ends (Table 3.3).

Table 3.2 *Curvatures (Φ, 1/mm) of the column ends at 15% capacity drop*

Specimen	Left Bottom	Left Top	Right Bottom	Right Top
SP1	1.07E-04	2.60E-05	8.20E-05	3.80E-05
SP2	3.40E-05	3.58E-05	2.34E-04	3.96E-05
SP3	2.85E-05	-	1.24E-04	-
SP4	2.71E-04	2.88E-05	2.11E-04	4.10E-04
SP5	2.55E-04	2.08E-04	2.21E-04	2.11E-04

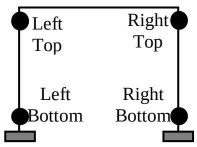

Yield curvature of the column section is estimated to be 25E-6 rad/mm for an axial load ratio of $0.2N_o$. Assuming a plastic hinge length (L_p) of h/2 (TEC 2007), plastic rotation demand at 15% capacity drop is calculated from: $\theta=(\Phi - \Phi_y)L_p$

Table 3.3
Plastic rotations (θ, rad.) of the plastic hinge regions of column sections at 15% capacity drop

Specimen	Left Bottom	Left Top	Right Bottom	Right Top
SP1	0.0062	0.0001	0.0043	0.0010
SP2	0.0007	0.0008	0.0157	0.0011
SP3	0.0003	-	0.0074	-
SP4	0.0185	0.0003	0.0140	0.0288
SP5	0.0173	0.0138	0.0147	0.0139

Calculated plastic rotation demands indicate that addition of external systems increased the damage on the RC columns. The highest plastic rotations were recorded for the specimens SP4 and SP5 due to sharp drop after achieving peak strength. It has to be also considered for these specimens that the load is transferred by the connections on the RC beam. Realizing the gradual strength decrease for SP3 specimen, there were no accumulated recorded plastic rotations on the top of the columns whereas slight damage was estimated on the column bases. SP3 specimen also exhibited plastic rotations on mid-height of columns observed by visual inspection at high deformation demands (4% D.R.). Moderate level of plastic rotations was seen on the hinge regions of SP2 specimen. Considering the rocking behavior of SP2 (relatively late strength decrease), the plastic rotations at the level of 15% capacity drop showed there was no significant damage seen on the RC columns.

Chapter 4

Analysis of Test Specimens and Seismic Performance

Previous chapters presented the experimental results of tests along with the physical properties of test specimens. The fundamental observed behavior was discussed for the specimens on the hysteretic load-displacement relationships. Upgraded specimens' performance enhancements were compared with respect to the behavior of the bare frame under hysteretic cyclic loading. This chapter covers numerical studies simulating the behavior of the specimens to investigate the mechanisms of force transfer and uncover possible retrofit design strategies.

4.1 Finite Element Analysis

Finite element analysis using the general purpose finite element platform DIANA (2003) was conducted for specimens SP1, SP3, SP4 and SP5. Specimen SP2 was excluded from the study due to unexpected foundation anchor failure during the tests. The models were generated for SP1, SP3, SP4 and SP5. The models were prepared in three dimensions in accordance with specimen dimensions. Monotonic static analysis was performed by imposing deformation demands at the slab level. The analysis was performed non-linearly using a standard Newton algorithm. 330MPa of steel yield stress was used for longitudinal bars and 8MPa of characteristic compressive strength was used for concrete. A parabolic unconfined stress-strain model was employed for concrete with a total strain rotating crack model. The axial load on the structure was distributed equally to the top two nodes. For SP3 model, RC columns and beam were modeled with Cl18b fiber elements that use Mindlin-Reissner Beam Theory whereas L13BE elements were used for the columns and beam in SP4 and SP5 that employ Bernoulli Beam Theory. Geometric nonlinearity was incorporated in all analysis. The steel plate in SP3 was modeled with the CQ40S, degenerated shell elements to simulate the buckling and tension-field action of the steel plate. The RC columns were split up to 20 elements whereas the beam was split up to 27 elements with 3 integration points for all models. The anchors were modeled with relatively stiff elements assuming that there was no slip between the end points of anchor elements. The points for anchor layout reflected the actual application locations. Steel materials employed with Von-Mises elastic - perfectly plastic model.

In the conducted analysis for SP3 model, steel plate was divided into 18 elements in vertical direction and 24 elements in horizontal direction. 432 curved shell elements were used for the SPSW model in order to introduce local buckling behavior completely. The foundation level was kept fixed. Although the pushover demand was 5cm at the top node, the analysis converged up to 3cm since the extreme deformations along the diagonal nodes leaded the system to diverge thereafter. The total analysis progress duration was about 70 hours due to extremely small step size.

The RC shear wall in SP4 model was to 20 parts in vertical direction and 10 parts in horizontal direction (200 shell elements in total). The steel columns and the beam in SP5 model were split into 16 and 27 parts, respectively. The analyses progress durations were approximately 60 minutes for SP4 model and 30 minutes for SP5 model. The generated models are presented in Figure 4.1.

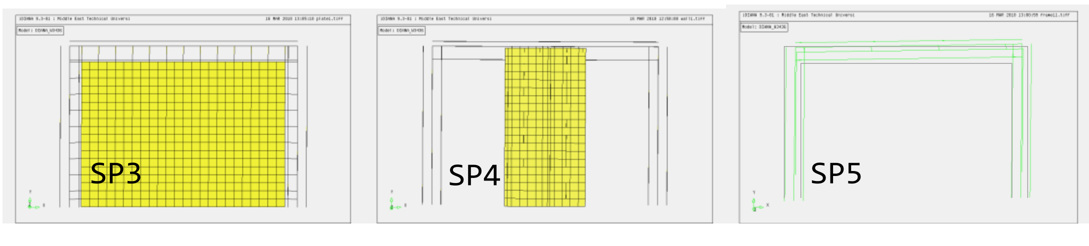

Figure 4.1 *Specimen models for Diana*

The FEA results were presented as lateral force – displacement envelopes in Figure 4.2 with the test data of specimens.

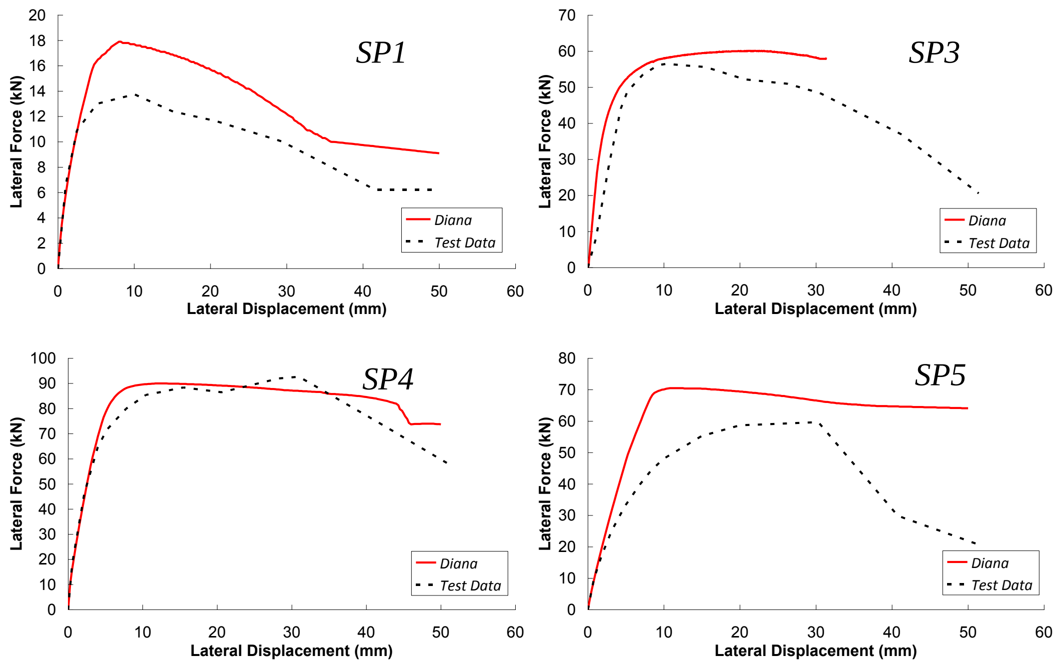

Figure 4.2 *Numerical and experimental pushover curves for specimen models*

The initial stiffness of the models corresponds well with the test data for SP1, SP4 and SP5 specimen models. The reason of the stiffness disparity in SP3 model can be the assumed constraints at the foundation connection (L-section connection did not exhibit perfect fixity in the tests).

The error in the lateral load capacities of the FEA models was less than 15% for the strengthened specimen models. The capacities of the models for SP1, SP3 and SP4 were achieved almost at the same displacement demands with the test results. However in the SP5 model, there was a slight difference between numerical simulations and test results. The major factor affecting this difference is believed to be the employed steel material model as discussed above.

In Figure 4.3, the force distribution in the anchors along the beam and columns of the specimens are presented. On the graphs, maximum shear capacity of the anchors is also demonstrated for number of anchors available at each location.

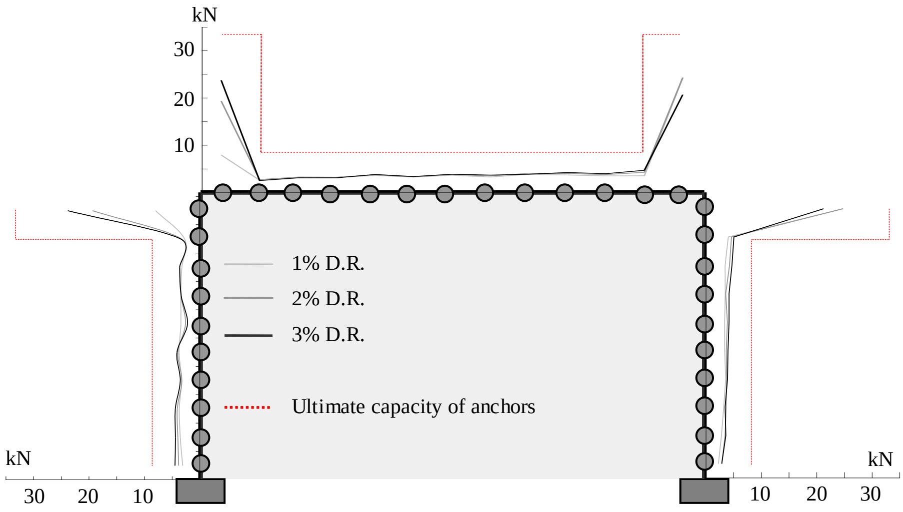

Figure 4.3a *The force distribution in the anchors of SP3*

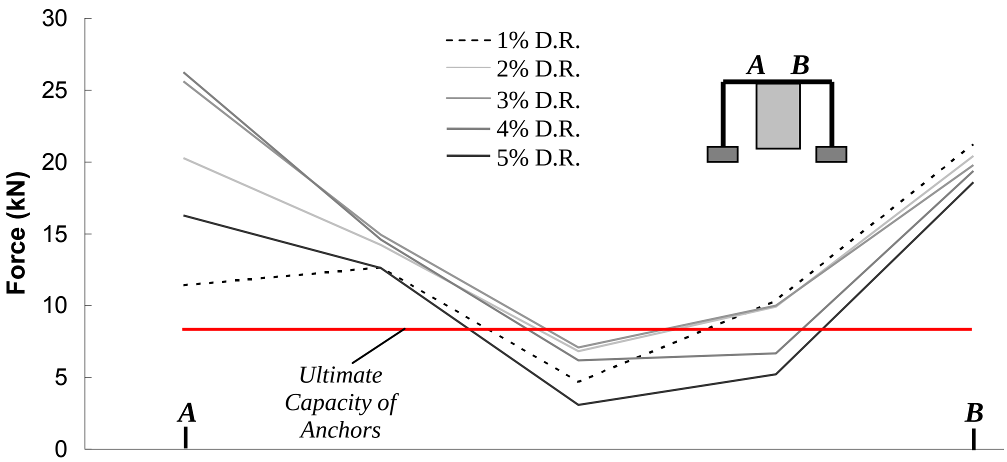

Figure 4.3b *The force distribution in the anchors of SP4*

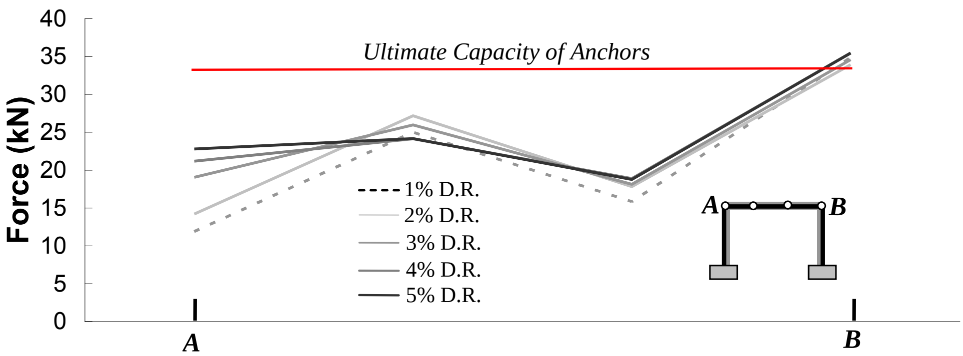

Figure 4.3c *The force distribution in the anchors of SP5*

The force distribution along the columns and beam of SP3 specimen model shows that the condensed anchor zones at the corners of the RC frame was an appropriate approach for design considering the stress concentrations. A relatively uniform distribution of anchor forces was observed. Assuming a single anchors (Φ6, Φ12) had a shear force capacity ($0.5 \times \sigma_u \times Anchor\ Section\ Area$ = 8.4kN and 33kN), the capacities of the anchor regions were sufficient for SP3 and SP5 specimens. However in SP4 specimen it was observed that the capacities of the anchor zones exhibited high force demands. This phenomenon is believed to be an evidence of the transverse reinforcement push-out as shown in Figure 3.21.

The moments at 4% D.R. resulting from the FEA along the nodes of RC wall of SP4 is presented in Figure 4.4 in order to show the consistency between design and analysis. The moment on the top end of the RC wall is increased as much as the moment capacity of the RC beam. The lateral capacity of the system is also shown below. The corresponding moment values and bare frame capacity are the results of FEA. It is definite that the total estimated capacity of the system is similar with the conducted FEA.

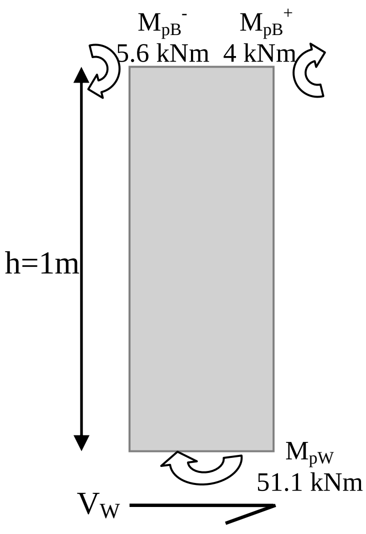

Figure 4.4
Resulting moments of the FEA in RC Wall, SP4

$$V_w = \frac{M_{pW} + M_{pB}^{+} + M_{pB}^{-}}{h}$$

$$V_w = \frac{51.1 + 5.6 + 4}{1}$$

$$V_w = 60.7kN$$

$$V = V_{br} + V_w$$

$$V = 13.7 + 60.7 = 74.4kN$$

The hinge patterns resulted from FEA of the strengthened models are presented in Figure 4.5. They are obtained by comparing the numerical longitudinal bar strains with the actual yield strain of the reinforcement (0.00165).

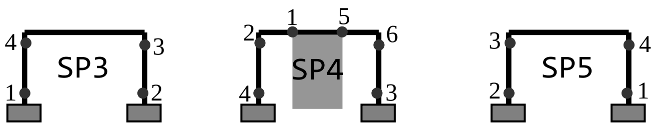

Figure 4.5 *Hinge patterns resulted from FEA*

In SP3 specimen, the first hinging of the columns is observed in the bottom of the columns followed by tops whereas in the estimated hinge patterns of the test results, the hinging at the column tops were not observed. In the FEA results, yielding is not observed for the mid-height of the columns in contrast to the actual behavior of SP3 specimen. The initial hinging in the columns of SP4 specimen is at the top of the left column resembling the negative loading cycle of actual behavior (the first column hinging was at the right column top end). In the FEA the system exhibited first hinging on the RC beam just at the upper left of RC wall indicating full moment transfer between RC beam and RC Wall at very early displacement demands. For SP5 specimen, the hinge pattern was similar to the actual observed pattern for the RC frame. The first hinges occurred at the column bottom ends followed by top of the columns.

In the Figure 4.6 below, the deformed shapes of the models for SP3 and SP4 are presented. The post buckled shape of the SP3 specimen model can be seen in Figure 4.6(b). The stress concentration on the RC shear wall is visible on the Figure 4.6(d). This indicates the reason of high moments achieved on the left top node of the wall.

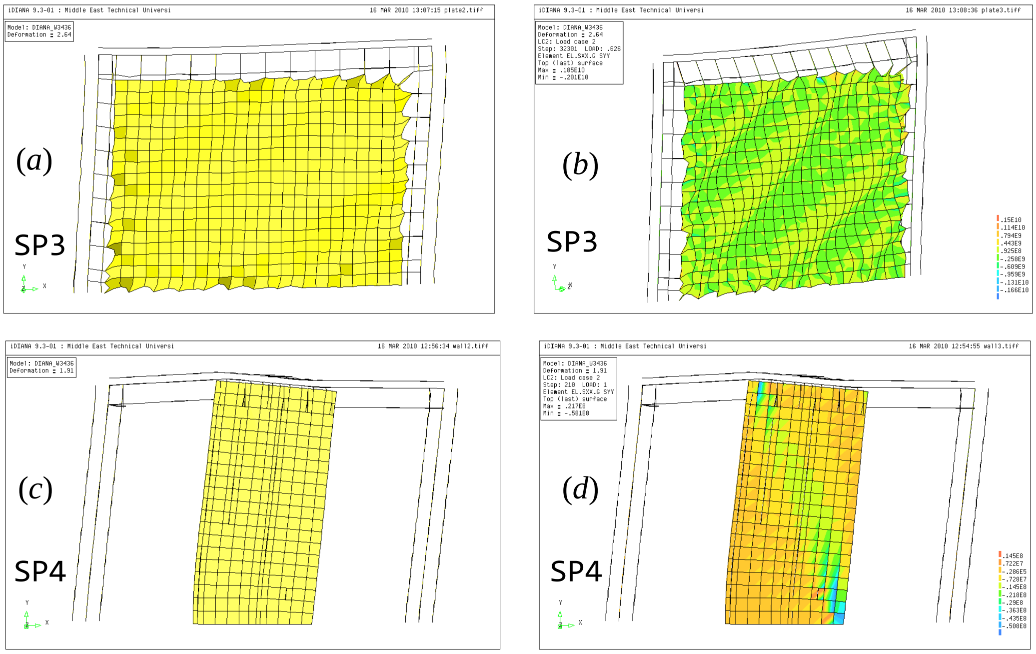

Figure 4.6 *Deformed shapes for models of specimens SP3 and SP4*

4.2 Parametric Study with the Strengthened Specimen Models

In order to have a better understanding on the behaviors of the specimen models, parametric study was conducted for SPSW and RC wall strengthened specimens. SPSW frame was investigated with two additional plate thickness values (0.6 and 0.9mm). The corresponding force-deformation responses of the analyses for SPSW system are presented in Figure 4.7.

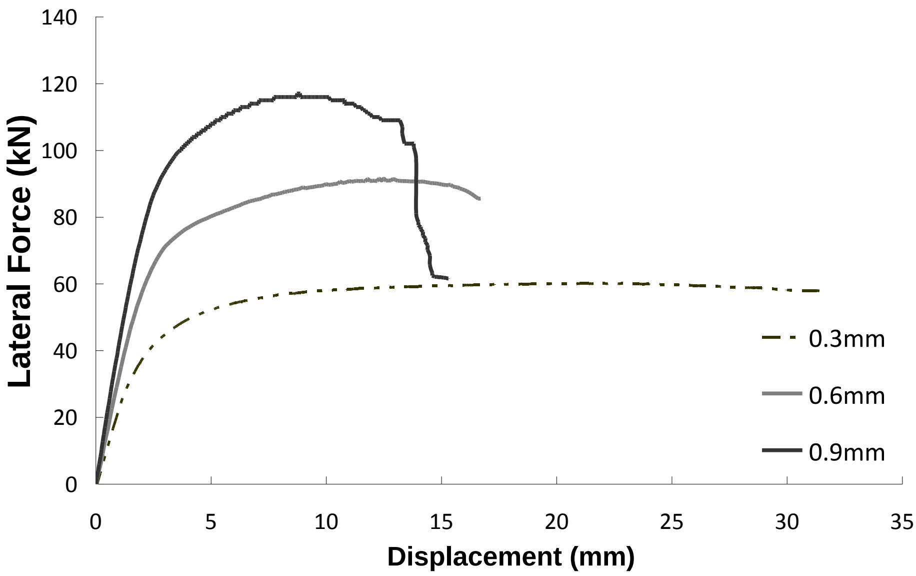

Figure 4.7 *Parametric FEA, load - displacement envelopes for SP3 model*

It can be justified from those envelopes that with the increasing thickness of steel plate, the integrated structure exhibits higher capacity with more brittle behavior. The reason for this behavior is the lack of rigidity in the boundary vertical elements showing excessive plastification along their length (Figure 4.8).

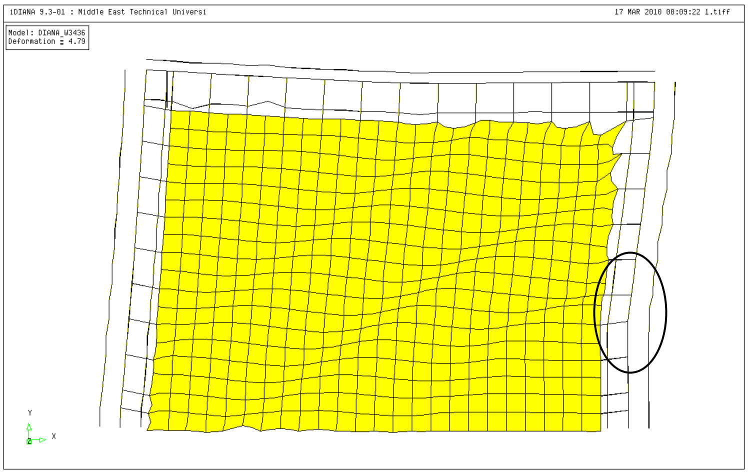

Figure 4.8 *Parametric study,*
SPSW (0.9mm) – plastic deformation along the boundary column

As it can be seen from Figure 4.8 the capacity of the SPSW system is limited by the vertical boundary elements (VBE) of the existing RC frame. Consequently, maximum plate thickness that can be employed in the existing structure depends on the capacity of VBEs provided that the steel plate yielded. In order to estimate the maximum plate thickness, internal force diagrams of the left RC column were investigated at 1% D.R. (peak strength was achieved) for the analyses for 0.3mm, 0.6mm and 0.9mm plate thickness values (Figure 4.9). In order to investigate shear force demands of applied SPSW systems the shear force capacity of the RC column section is calculated below:

$$V_r = V_{cr} + V_w$$

$$f_{ctk} = 0.35\sqrt{f_{ck}} \approx 1MPa$$

$$V_{cr} = 0.65\, f_{ctk} b_w d\,(\psi) = 8840N$$

$$V_w = \frac{A_{sw}}{s} f_{ywk} d = 9180N$$

$$V_r = 8840 + 9180 = 18020N \approx 18kN$$

where;
V_r : total shear capacity
V_{cr}: concrete cracking shear capacity
V_w: lateral reinforcement contribution
f_{ctk}: characteristic concrete tension str.
f_{ck}: characteristic concrete compressive str. (7.5 MPa)
b_w: column width (100mm)
d: column depth (136mm)
ψ: coefficient of axial load level (assumed as 1)
A_{sw}: area of total lateral reinforcement (25 mm^2)
s: lateral reinforcement spacing (100 mm)
f_{ywk}: lateral reinforcement yield stress (270 MPa)

For the 0.3 mm SPSW system the analyses results show that axial load was between 17 and 34 kN of compression. The axial load ratio was observed to influence shear capacity by about 15% at most according to TS500. Hence, the above calculations for shear strength can be thought as the acceptable shear capacity of the RC columns (ψ is assumed as 1).

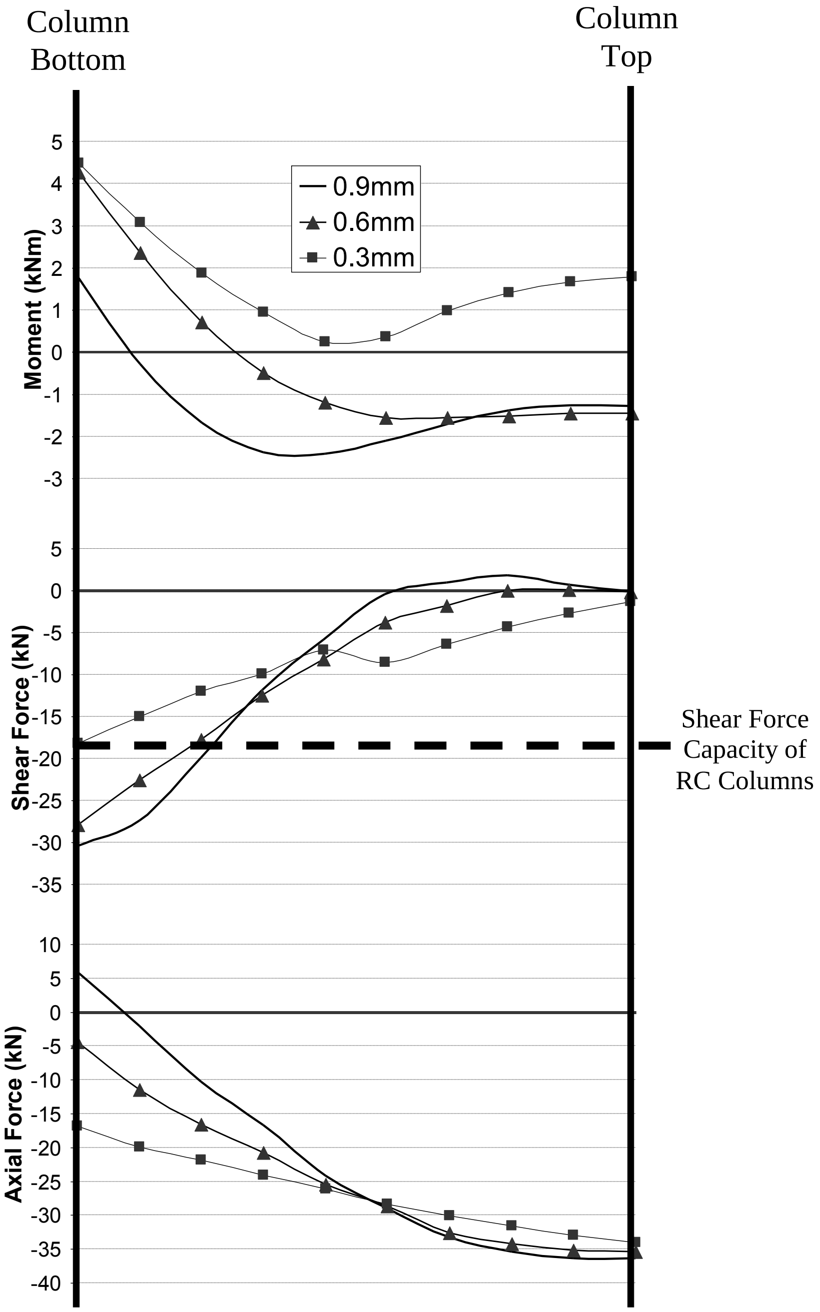

Figure 4.9 *Internal force diagrams of the left RC column, parametric FEA for SP3 (1% D.R)*

One can observe from the shear force diagram of the RC column that the VBEs can not bear shear forces for the plate thickness values approximately greater than 0.3 mm. Otherwise; thicker plates may be applied if shear strengthening the existing columns is provided. The free-body diagram of the 0.3 mm steel plate is given in Figure 4.10 to have a better understanding on the force demands. The forces were acquired with summing up the boundary forces along steel plate in 1% D.R. (in the same analysis step with above internal force diagrams). It must be noted that more than half of the lateral force is carried by horizontal boundary elements (HBE). Although the shear force demands of the HBE is almost the same with VBE, one need to realize that shear force capacity of the RC column is smaller than RC beam. Therefore, the VBEs are the critical elements that have to be checked due to excessive shear force demands. The same conclusion is also true if the moment demands became critical providing that it is about the same for VBE and HBE.

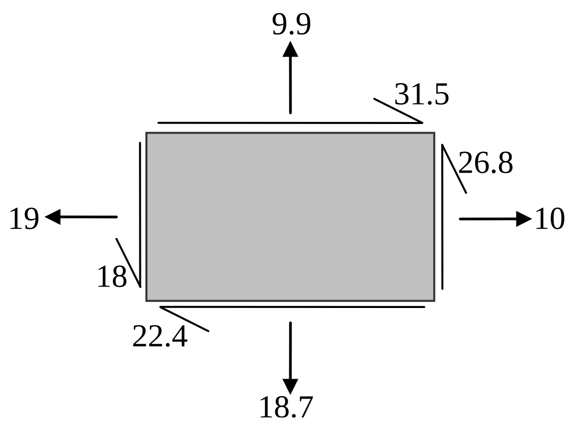

Figure 4.10 *Free-Body diagram of 0.3 mm steel plate (units in kN)*

Due to the limitations of the test setup external RC wall was not designed for full bay length. For the parametric study of RC wall strengthened specimen, RC wall was modeled having dimensions of 1550 x 1000 mm, covering the whole span. The reinforcement detail was formed accordingly with the same spacing and size. The investigation is aimed to see the total system capacity and excessive anchor forces along the RC beam. The load-deformation response fully and partially connected RC wall sections are shown in Figure 4.11.

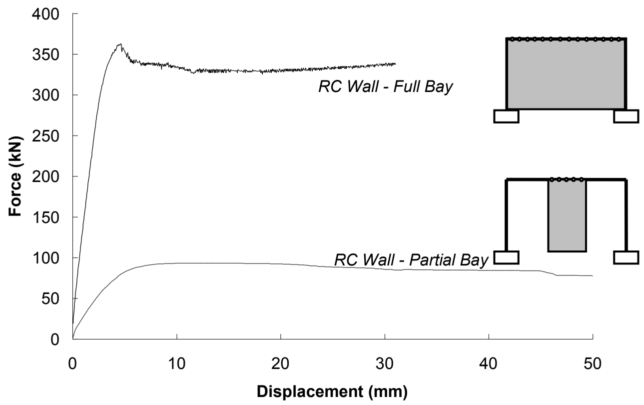

Figure 4.11 *Parametric FEA, load - displacement envelopes for SP4 Model*

The parametric analysis of the SP4 model showed the combined forces of the anchors along the RC beam were in the order of 60-70 kN. As long as detailing of the anchor rods are performed appropriately, it is observed that such use of external RC wall can be employed successfully. For such a retrofit the behavior of wall will be dominated by shear unlikely specimen SP4 which exhibited a flexural response which can not be generalized for the multi-story structures. Furthermore, one needs to consider the high force demands in the foundation level.

4.3 Single Degree of Freedom (SDOF) Models

In the literature, most of the seismic structural strengthening studies are based on the reversed cyclic static tests which can be questioned whether the loading cycles reflect the real dynamic effects. In order to discuss the seismic performance improvement comparisons, dynamic loading should be conducted such that actual loading history is simulated. Nevertheless, the experimental studies performed by static loading systems can give a general feeling about the corresponding strengthening techniques.

In order to support the experimental works conducted in this study, dynamic performance of the specimens were investigated with the SDOF models (Figure 4.12). For this purpose load-deformation response obtained from experiments were used to calibrate a simple hysteretic model. The behavior of the one storey frames can accurately be represented by single degree of freedom (SDOF) model for dynamic analysis purposes.

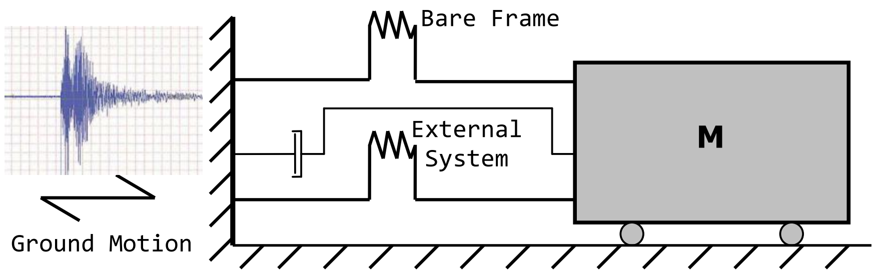

Figure 4.12 *SDOF Model*

For the models that were to be generated, open source analysis software, OpenSees 2.1.0 (1999) was used. It is a software framework for developing applications to simulate the performance of structural systems which is under continual development.

The material model employed in the SDOF model represented a hysteretic material behavior which allows building trilinear load-displacement responses. The hysteretic material model and resultant cyclic behavior of the SDOF system is presented in Figure 4.13.

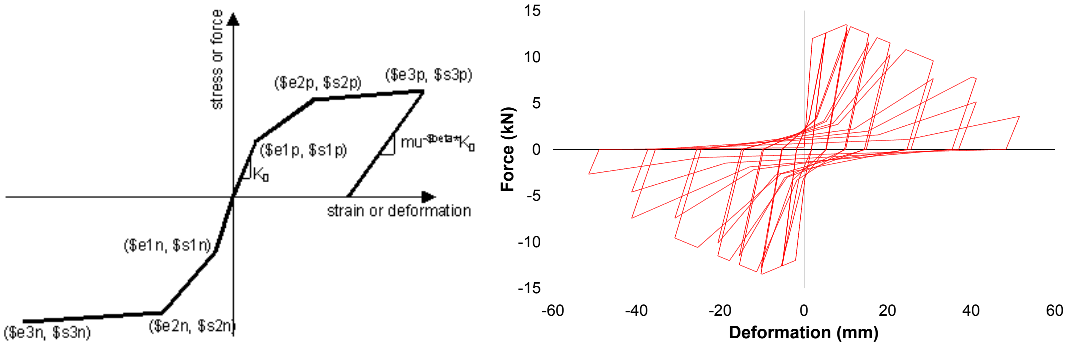

Figure 4.13 *Trilinear hysteretic material model (OpenSees command language manual) and cyclic behavior of SDOF model for SP1*

The model above consists of some major parameters labeled as force and deformation (ep, en used in the models refers to the force and sp, sn refers to the displacement levels at the same points with force excursions). In addition to those parameters in the hysteretic load-displacement model, some other parameters are available to incorporate stiffness, strength degradation and pinching. The pinching factors had two different types that represent the pinching for deformation and force demands. The factors for damage were also separated in two types representing the damage due to ductility and energy. The stiffness loss upon unloading was reflected to the model by a single parameter. Pinching and damage parameters used for each model are presented in Table 4.1.

Table 4.1 *Hysteretic model parameters used in Opensees*

Parameters	***SP1***	***SP2***	***SP3***	***SP4***	***SP5***
pinchX	0.665	0.660	0.650	0.600	0.500
pinchY	0.250	0.350	0.200	0.500	0.590
damage1	0.009	0.005	0.030	0.037	0.028
damage2	0.000	0.000	0.000	0.000	0.020
beta	0.500	0.400	0.400	0.600	0.220

The above parameters are defined as such:

pinchX : pinching factor for deformation during reloading

pinchY : pinching factor for force during reloading

damage1 : damage due to ductility

damage2 : damage due to energy

beta : power used to determine the degraded unloading stiffness

The matching of the models to the test data was performed by trial and error practice. The primary target was to match the load-displacement responses of specimens in the cycles that include 4% drift ratio (~40mm). In addition the energy dissipation capacities of the specimens and generated models were matched to be the same for the cycles imposed during the tests. The difference between the dissipated energy of models and the test response was less than 1%.

The SDOF model response of the SP1 specimen (bare frame) presented in Figure 4.14 along with the specimen's actual cyclic response.

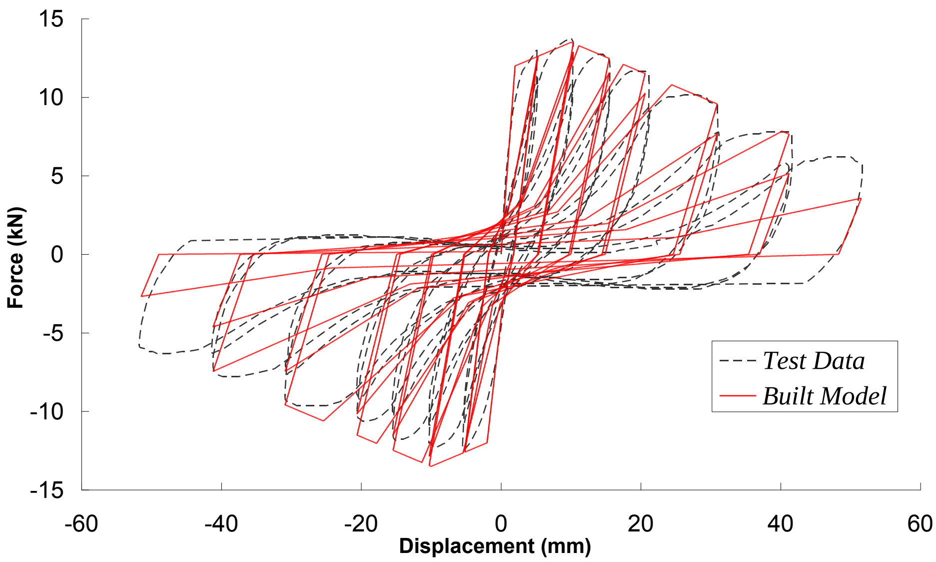

Figure 4.14 *The cyclic response of the generated model for SP1*

In the models that were generated for the strengthened specimens, the hysteretic model parameters of the bare frame were used based on the bare frame parameters. Another hysteretic material and member were formed that stands for the strengthening components (labeled as External System in Figure 4.12). In other words, two different member models formed a SDOF system that was linked to result in similar lateral displacements; one of them was representing the bare frame and the other one simulating the external strengthening member. The cyclic matches of the strengthened models are presented in Figure 4.15.

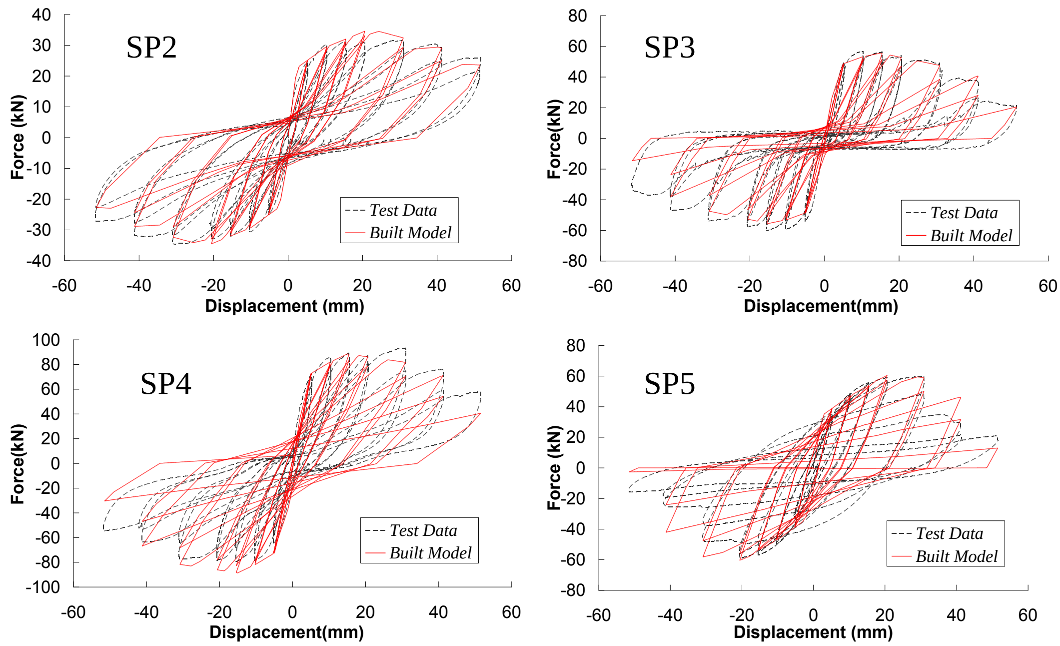

Figure 4.15 *The cyclic responses of the generated strengthened models*

4.4 Incremental Dynamic Analysis

After generating the SDOF models, incremental dynamic analysis were performed in order to demonstrate the dynamic performance improvements. Totally twenty-one ground motion acceleration data were used in a range of peak-ground acceleration (PGA) varying from 0.179g to 0.592g. The ground motion data were taken from PEER (Pacific Earthquake Engineering Research Center) database and was also used by Doruk (2006). The employed ground motions are given in Table 4.2 along with the recording location, PGA and available PEER ground motion number. In this way uncertainty in the ground motion was considered while maintaining all other system parameters as deterministic values.

Table 4.2 *Employed ground motions for IDA*

GM	Location	PGA	GM	Location	PGA
1	Coalinga (P0323)	0.281	12	Northridge (P0887)	0.344
2	Imperial Valley- el centro (P0177)	0.537	13	Northridge (P0893)	0.410
3	Landers (P0816)	0.284	14	Northridge (P0927)	0.583
4	Northridge (P0889)	0.444	15	Cape Mendocino(P0810)	0.385
5	Loma Prieta (P0733)	0.411	16	Duzce	0.427
6	Whitter Narrows (P0595)	0.414	17	Dinar	0.303
7	Northridge (P0899)	0.357	18	Erzincan	0.489
8	Northridge (P0925)	0.292	19	K.Cekmece	0.179
9	Imperial Valley (P0190)	0.287	20	Kocaeli	0.326
10	Coalinga (P0369)	0.592	21	Yarimca	0.349
11	Whitter Narrows (P0714)	0.374			

In the performed analysis 2% damping ratio was assigned using Rayleigh's method. Incremental dynamic analysis was performed for each acceleration data repeatedly to 20 increments. The analysis carried out starting from 10% scaled of the original data and ending up 200% of it with 10% scaling increments.

It is apparent that the major factor that affects the performance of external retrofit systems was the ultimate load capacities of the trilinear force-deformation behavior of the generated SDOF models. In order to compare the strengthened specimen models conveniently, the ultimate load capacities of the SDOF models should be similar. As it was discussed in Chapter 3, SP3 and SP5 specimens had their ultimate lateral load capacities about 60kN whereas SP2 and SP4 were under and over of that value respectively. Consequently, it is reasonable to scale the capacities of the SDOF models of SP2 and SP4 specimens to a level of the other two strengthened specimen models and keeping the capacities of the SP3 and SP5 at the same level.

The incremental dynamic analyses results of the SDOF models are presented in Figure 4.16. The results were plotted as PGAs vs. maximum tip displacements for each ground motion data set. Each of 21 envelopes represents the maximum displacements recorded for single ground motion with increasing scales starting from 10% and ends with 200% of the original data with 10% increments.

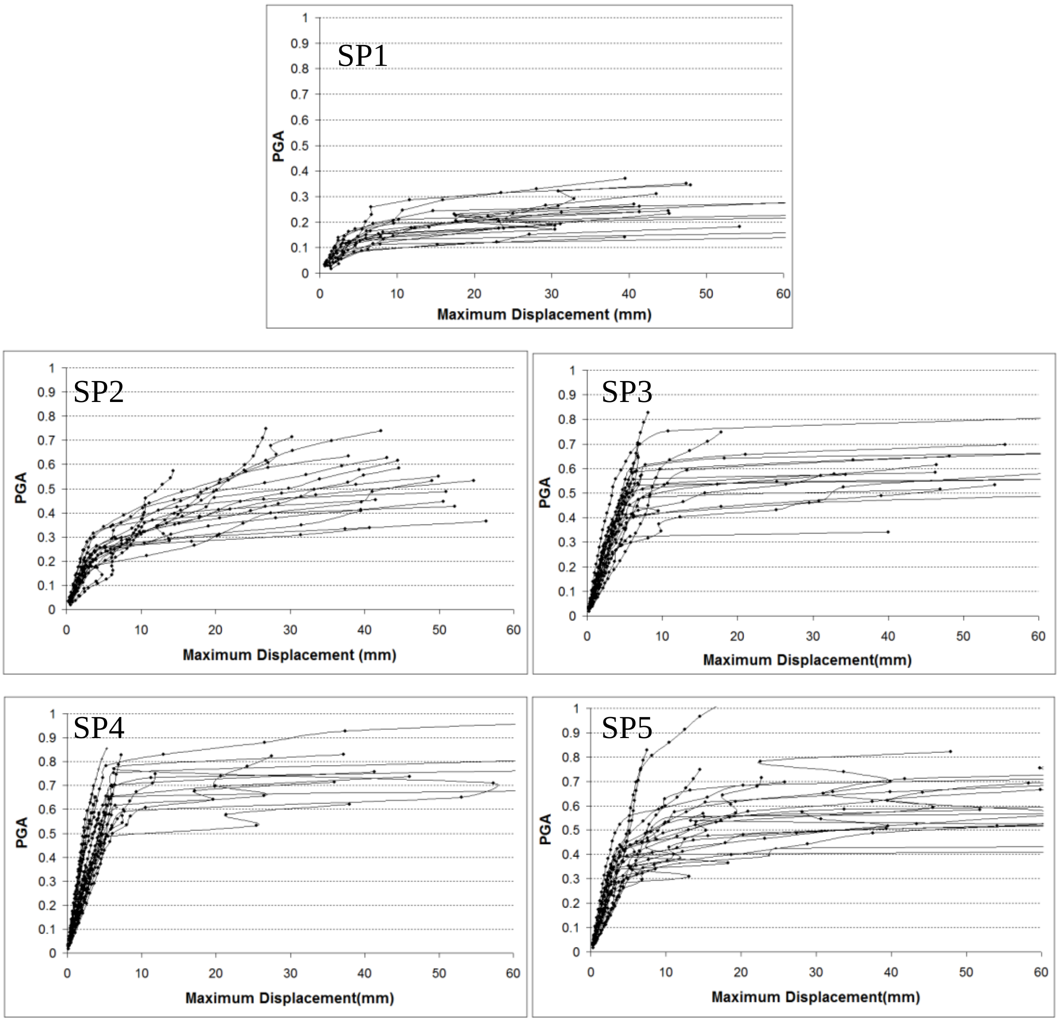

Figure 4.16 *IDA PGA – Max. displacement envelopes*

The incremental dynamic analyses results of the specimens' models gave a general idea about the dynamic capacity enhancement of upgraded cases compared to the bare specimen model. Upon investigation of those curves, it was seen that some of the ground motion data sets exhibited large scatter due to the variation in acceleration time-series characteristics. The sudden increase of displacements after a certain PGA level can be viewed as the collapse PGA level of structures. It can be observed that SP1 reached this collapse level around 0.2g, whereas this value was about three times on average of the bare frame for the strengthened specimens. This result is consistent with the static test results for bare shear capacity.

Although the IDA curves demonstrate the dynamic developments of the strengthened specimens, it is difficult to define the performance enhancements level. In order to have more distinctive conclusions of the related IDA results, the performance PGA points of are designated. In the procedure of determining a distribution for the life-safety level, it is needed to specify a drift or displacement limit to the specimen models which was taken as 3% drift ratio (See Table 3.1). It is a consistent drift ratio considering the deformations in the 15% capacity drops and TEC 2007 life safety level.

The means (μ) and standard deviations (σ) of the distributions of PGA points those bring the system to the life safety limit of 30 mm displacement are shown in Table 4.3.

Table 4.3 *Mean and standard deviations of the PGA points those bring the systems to 30 mm displacement*

	SP1	SP2	SP3	SP4	SP5
μ	0.241	0.609	0.562	0.558	0.559
σ	0.121	0.122	0.103	0.076	0.086

The major reason of the differences between the standard deviations of the strengthened models was the cyclic material properties of the SDOF systems. This means numerically that the employed parameters for matching each model can affect the scattering of IDA results. Once the IDA curves inspected visually the scattering of the data explains the relatively high standard deviation values of SP2 and SP3 among the strengthened cases. Besides, the mean of the distributions are almost the same for the strengthened specimen models. This means the importance of lateral capacity similarity of the strengthened models however SP2 exhibited the best response due to its rocking behavior that affects the employed parameters in the SDOF model.

CHAPTER 5

SUMMARY AND CONCLUSION

The building stock in Turkey has poor design and construction quality and this fact was observed in the recent heavy earthquakes poignantly. It is definite that so many structures are required rapid structural strengthening implementations for the expected earthquake scenarios. The scope of this study was to possibly offer effective strengthening techniques for the existing RC structures.

One-bay, one-storey 1/3 scale specimens were tested in this study. External strengthening methods include moment resisting steel frame, steel plate shear wall and RC shear wall.

It must be noted that all the experimental results and conclusions are only valid for this study. The loading history, scale of the RC frame specimens, the configuration of the reinforcing bars, physical properties of strengthening members and mechanical properties of materials employed in the tests are the major factors that could introduce bias to the results.

Test results showed that employed strengthening techniques enhanced the lateral load capacity and stiffness of the existing frame considerably. The remarks, conclusions and recommendations of the study are listed below:

- The retrofit methods applied externally with steel members are good alternatives of external wall system as long as they are detailed carefully.

- External steel frame systems have the best energy dissipation efficiency among other retrofitted specimens used in this study. The foundation connections have to satisfy end rigidity demand to the integrated structure's full capacity.
- For the external strengthening with SPSW, in order to avoid local tears on the stress concentrated regions of the plate or anchors, anchors have to be condensed on the corresponding zones and on the necessary regions plate has to be strengthened.

- External connected RC wall exhibited acceptable seismic performance as obtained in the previous studies. It is applicable to connect the wall to the outer plane of the frame if the forces on the employed anchors would not cause local failures on the RC members. It may be safer to connect the external walls to both beams and columns in the case of complete external RC wall installation.

- The foundation capacity design check should be the vital consideration especially for the shear wall retrofitted structures. High tension force in the practicing anchors in the foundation level results in the failure of foundation.

- The life safety deformation limit was 3% story drift for all systems which is similar to that proposed by TEC (2007) story drift limit.

- Finite element analyses point out the condensation of anchor forces near by joint zones. In the design and formation of anchors, that fact has to be considered seriously.

- For the SPSW retrofitted structures, the stiffness of the boundary elements has to be checked in order to allow SPSW to respond displacement demands by tension field action. Insufficient boundary elements lead to system to fail by boundary plastification. Furthermore, high anchor forces in the boundary elements can cause local failures if the corresponding element does not have sufficient capacity.

- The hysteretic behavior of retrofitted frames had an influence on the probability of failures under seismic demand. The fragility curves of the specimen models are similar to each other except for the SP2 specimen model. The reason for this can be stated as the high ductility of the hysteretic characteristics of the tested specimen. Ductility and damage parameters arranged for the specimen model lead the system to exhibit slightly better performance in IDA than other strengthened cases.

REFERENCES

1. Acun B. and Sucuoğlu H., “Strengthening of Masonry Infill Walls in Reinforced Concrete Frames with Wire Mesh Reinforcement”, In Proceeding of 8NCEE, 2006, San Francisco.

2. AISC, Seismic Provisions for Structural Steel Buildings, 2005, Chicago, Illinois.

3. Altın, S., Ersoy, U., Tankut, T., "Hysteretic Response of Reinforced Concrete Infilled Frames", Journal of Structural Engineering, 1992, Vol. 118, No. 8, pp. 2133-2150.

4. Anil, O., Altin S., “An Experimental Study on Reinforced Concrete Partially Infilled Frames”, Engineering Structures, 2007, Vol.29, pp.449-460.

5. Aoyama, H., Kato, D., Katsumata, H., Hosokawa, Y., “Strength and Behavior of Postcast Shear Walls for strengthening of existing R/C Buildings”, 8th World Conference on Earthquake Engineering, 1984 July, San Francisco CA, Vol. 1, pp.485-492.

6. Badoux, M. and Jirsa, J.O., “Steel Bracing of RC Frame for Seismic Retrofitting,”, Journal of Structural Engineering, 1990, Vol. 116, No. 1, pp. 55-74.

7. Baran, M., “Precast Concrete Panel Reinforced Iinfill Walls for Seismic Strengthening of Reinforced Concrete Framed Structures”, A Doctor of Philosophy Thesis in Civil Engineering, Middle East Technical University, 2005.

8. Caccese, V., Elgaaly, M. and Chen, R., “Experimental Study of Thin Steel-Plate Shear Walls Under Cyclic Load”, Journal of Structural Engineering, ASCE, 1993, Vol. 119, No. 2, pp.573-587.

9. Canbay, E., “Contribution of RC Infills to the Seismic Behavior of Structural Systems”, A Doctor of Philosophy Thesis in Civil Engineering, Middle East Technical University, 2001.

10. Choi, I-R., Park, H-G., “Ductility and Energy Dissipation Capacity of Shear-Dominated Steel Plate Walls”, Journal of Structural Engineering, ASCE, 2008, Vol. 134, No. 9, pp1495-1507.

11. Choi, I-R., Park, H-G., “Steel Plate Walls with Various Infill Plate Designs”, Journal of Structural Engineering, ASCE, 2009, Vol. 135, No. 7, pp785-796.

12. Doruk K., “Fiber Reinforced Polymer Confined RC Circular Columns Subjected to Axial Load and Bending Moment”, A Master of Science Thesis in Civil Engineering, Middle East Technical University, 2006.

13. Erdem, I, Akyuz, U., Ersoy, U., Ozcebe, G. (2006) “An experimental study on two different strengthening techniques for RC frames”, Engineering Structures, 2006, Vol. 28, No. 13, pp. 1843-1851.

14. Ersoy, U., Uzsoy, S., "The Behavior and Strength of Infilled Frames", Report No. MAG-205, 1971, TUBITAK, Ankara, Turkey.

15. Kaltakci, M. Y., Arslan, M. H., Ulku, S. Y., Arslan, H. D. (2007) “A New Approach on the Strengthening of Primary School Buildings in Turkey: An Application of External Shear Wall”, Building and Environment, 2007, Vol. 43, pp. 983-990.

16. Kara, M. E., Altin S.,”Behavior of Reinforced Concrete Frames with Reinforced Concrete Partial Infills”, ACI Structural Journal, 2006, Vol.103, pp. 701-709.

17. Kazunori I., Hayashida N., Norimitsu H., Kiyoshi S., Kei H., “Development of Seismic Strengthening Technology Using the Fitting Shear Wall Construction Method and the External Frame Method”, Kumagai Technical Research Report, 1999, Vol:58, Pages:61-67.

18. Kurban C.O., “A Numerical Study on Response Factors For Steel Plate Shear Wall Systems”, A Master of Science Thesis in Civil Engineering, Middle East Technical University, 2009.

19. Maheri M.R., Hadjipour A., (2003), “Experimental investigation and design of steel brace connection to RC frame”, Engineering Structures, 2003, Vol.25, pp.1707-1714.

20. Maheri, M., Sahebi, A., Use of steel bracing in reinforced concrete frames. Engineering Structures, 1997, Vol. 19, No. 12, pp.1018-1024.

21. Maheri, M.R., Kousari, R., and Razazan, M. (2003) “Pushover Tests on Steel X-Braced and Knee-Braced RC Frames”, Engineering Structures, 2003, Vol. 25(13), pp. 1697-1705.

22. Moehle, J.P., “State of Research on Seismic Retrofit of Concrete Building Structures in the US,” US-Japan Symposium and Workshop on Seismic Retrofit of Concrete Structures, 2000, Tokyo, Japan.

23. OpenSees, “Software Framework for Developing Applications to Simulate the Performance of Structural and Geotechnical Systems Subjected to Earthquakes”, University of California, 1999.

24. Ozcebe, G., Ersoy, U., Tankut, A. T., Erduran, E., Keskin, R. S., Mertol, C., "Strengthening of Brick-Infilled RC Frames with CFRP", Turkish Scientific and Technical Council, Project No. 2003/1 (SERU), 2003, Ankara, Turkey.

25. Ozcelik R. and Binici B., "Application of steel retrofit schemes for deficient buildings in Turkey. In Proceedings of the First European Conference on Earthquake Engineering and Seismology, 2006, Genewa, Switzerland. ID 1030.

26. Ozden, S., Akguzel, U., Ozturan, T., "Seismic Retrofit of R/C Frames with CFRP Overlays", Seismic Assessment and Rehabilitation of Existing Buildings Edited by S. Tanvir Wasti and Guney Ozcebe, Nato Science Series, IV. Earth and Environmental Series, Vol. 29, 2003, pp.357-382.

27. Park, H-G., Kwack, J-H., Jeon, S-W., Kim, W-K., Choi, I-R., "Framed Steel Plate Behavior under Cyclic Lateral Loading", Journal of Structural Engineering, ASCE, 2007, Vol. 133, No. 3, pp378-388.

28. Pincheira, J.A. and Jirsa, J.O., "Seismic Response of RC Frames Retrofitted with Steel Braces or Walls," Journal of Structural Engineering, 1995, Vol. 121, No. 8, pp.1225-1235.

29. Sonuvar, M. O., "Hysteretic Response of Reinforced Concrete Frames Repaired by Means of Reinforced Concrete Infills", A Doctor of Philosophy Thesis in Civil Engineering, Middle East Technical University, 2001.

30. TNO Diana, "Finite Element Analysis Software", TNO Company, 2003.

31. Tsunehisa M., Kazuyuki S., Tsuneaki I., "A study on seismic strength method using brace of outer-frame", Technical Research Report of Hazama Corporation, 1999, Vol:31, Pages: 17-25.

32. Turk, A. M., "Rehabilitation of Reinforced Concrete Infill Walls", A Doctor of Philosophy Thesis in Civil Engineering, Boğaziçi University, 1998.

33. Turkish Seismic Code, Ministry of Public Work, Ankara, 2007.

34. Yuzugullu, O., "Repair of Reinforced Concrete Specimens with Reinforced Concrete Precast Panels", Report No. MAG-494, TUBITAK, 1979, In Turkish.